A Role for Heat Shock Protein 90 (Hsp90) in Fibronectin Matrix Dynamics

A thesis submitted in the fulfillment of the requirements for the degree of

Master of Science in Biochemistry

of

Rhodes University

by

Kyle Leonard O'Hagan

March 2013

Abstract

To date, a significant portion of research has been devoted to understanding the biological role of the molecular chaperone, heat shock protein 90 (Hsp90), in cancer development and metastasis. Studies have alluded to over 300 clients for intracellular Hsp90, many of which are involved in oncogenic signaling pathways, making Hsp90 a *bone fide* drug target with several inhibitors already in clinical trials. In recent years, a limited number of extracellular Hsp90 clients have been elucidated with roles in cancer cell migration and invasion. Examples of such clients include matrix metalloproteinase-2 (MMP-2), LRP-1/CD91 and HER-2. Inhibition of extracellular Hsp90 using cell-impermeable inhibitors has been shown to reduce cancer cell migration and metastasis by a hitherto undefined mechanism.

Using surface biotinylation and an enzyme-linked immunosorbent assay, we provided evidence to support that Hsp90 was found extracellularly in cancers of different origin, cell type and malignancy. Next, we isolated extracellular Hsp90-containing complexes from MDA-MB-231 breast cancer cells using a cell impermeable crosslinker followed by immunoprecipitation and identified by mass spectrometry that the extracellular matrix protein, fibronectin, co-precipitated with Hsp90β. This interaction between Hsp90β and fibronectin was confirmed using pull down assays and surface plasmon resonance spectroscopy with the purified proteins. The ability of exogenous Hsp90β to increase the insoluble fibronectin matrix in Hs578T breast cancer cells indicated a role for Hsp90 in fibronectin matrix stability or fibrillogenesis.

Hsp90 knockdown by RNA interference or inhibition with the small molecule inhibitor, novobiocin, resulted in a dose and time-dependent reduction of the extracellular fibronectin matrix. Furthermore, novobiocin was shown to cause the internalization of a fluorescently-labeled exogenous fibronectin matrix incorporated into the extracellular matrix by Hs578T cells. This suggested endocytosis as a possible mechanism for fibronectin turnover. This was supported by the colocalization of fibronectin with key vesicular trafficking markers (Rab-5 and LAMP-1) in small, intracellular vesicles. Furthermore, treatment with the vesicular trafficking inhibitor, methyl-β-cyclodextrin,

resulted in a dose-dependent recovery in the extracellular fibronectin matrix following treatment with novobiocin. Taken together, these data provided the first evidence to suggest fibronectin as a new client of Hsp90 and that Hsp90 was involved in regulating extracellular fibronectin matrix dynamics.

Declaration

I declare that this thesis is my own, unaided work. It is being submitted for the degree of Master of Science of Rhodes University. It has not been submitted before for any degree or examination at any other university.

Mr Kyle O'Hagan, March 2013

Table of Contents

List of Figures

List of Tables

List of Abbreviations

ATP	Adenosine triphosphate
BSA	Bovine Serum Albumin
CFDA-SE	Carboxyfluorescein diacetate succinimidyl ester
CFDA-SE-FN	CFDA-SE-labeled fibronectin
CRC	Colorectal cancer
DMEM	Dulbecco's Modified Eagle Medium
DTSSP	3,3'-Dithiobis[sulfosuccinimidyl]propionate
DOC	Deoxycholate
ECM	Extracellular matrix
ECL	Enhanced chemiluminescence
EDTA	Ethylenediaminetetraacetic Acid
EGFR	Epidermal Growth Factor Receptor
ER	Endoplasmic Reticulum
ERK	Extracellular signal-regulated kinase
FAK	Focal Adhesion Kinase
FCS	Fetal Calf Serum
FN	Fibronectin
GA	Geldanamycin
GDF	Growth Differentiation Factor
GRP	Glucose Regulated Protein

HER-2	Human Epidermal Growth Factor Receptor-2
Hop	Hsp70/Hsp90 organising protein
HRG	Heregulin
Hsp	Heat shock protein
HKC	Human Keratinocyte
Ig	Immunoglobulin
JAK	Janus Kinase
LAP	Latency Associated Peptide
LPS	Lipopolysaccharide
LRP-1	Low density lipoprotein Receptor-related Protein-1
K/D	Knockdown
KSHV	Kaposi's Sarcoma-associated Herpes Virus
MβC	Methyl-β-cyclodextrin
MAPK	Mitogen Activated Protein Kinase
MEK	Mitogen-activated protein/Extracellular regulated Kinase
MMP-2	Matrix Metalloproteinase-2
MS/MS	Tandem Mass Spectrometry
NF-κB	Nuclear Factor-KappaB
NHS	N-Hydroxysuccinimide
NOV	Novobiocin
PBS	Phosphate Buffered Saline

PI3K	Phosphatidylinositol 3-kinase
PMSF	Phenylmethanesulfonylfluoride
RIPA	Radio-immunoprecipitation assay
RTK	Receptor Tyrosine Kinase
SDF-1	Stromal Derived Factor-1
SDS-PAGE	Sodium-Dodecyl-Sulphate Polyacrylamide Gel Electrophoresis
SHR	Steroid Hormone Receptor
siRNA	Short interfering Ribonucleic Acid
STAT	Signal Transducers and Activators of Transcription
TBS	Tris-Buffered Saline
TBST	Tris-Buffered Saline with Tween-20
TGF	Transforming Growth Factor
TLR	Toll-like receptor
TNF	Tumor Necrosis Factor
tPA	Tissue Plasminogen Activator
TPA	Tetradecanoylphorbol-13-acetate
TRAP1	Tumor necrosis factor type 1 Receptor Associated Protein

List of Symbols

α	Alpha
β	Beta
°C	Degree Celsius
M	Molar
mM	Millimolar
µM	Micromolar
nM	Nanomolar
g	Grams
mg	Milligrams
µg	Micrograms
L	Litres
ml	Millilitres
µl	Microlitres
kDa	Kilodaltons
Da	Daltons
min	Minutes
mol	Moles
%	Percent or g/100 ml
U	Units
x *g*	Relative centrifugal force to gravity

rpm	Revolutions per minute
v/v	Volume per volume
w/v	Weight per volume
V	Volts
nm	Nanometers
pH	Hydrogen ion concentration

Acknowledgements

If I were to write the full extent of my gratitude for each of you mentioned below, I'd be stuck with a few more theses to write. So while this appears to be a pretty excessive acknowledgements section, I couldn't leave a single one of you out. I wish I had the space to write more, but please find it within these few words my greatest appreciation and love.

To my supervisor, Dr Adrienne Edkins – there will come a day when I will look back on my career with great pride knowing full well that you were a big part in making it happen. Thank you for your endless enthusiasm, encouragement, support and input throughout my post-graduate career at Rhodes University. I would never have pushed myself this far if I hadn't caught onto a glimpse of the passion that you have for what you do. Thank you for an incredibly solid foundation in science that will set me up for a fruitful and happy future. It is going to be very difficult to find another supervisor like you.

To my closest friend, Craig Wynn – your section has proven to be the hardest to write; not because I have nothing to say, but simply too much. Even though it's been a short period of time, I feel like you have been there with me through it all; the countless frustrations and celebrations of love, life and work. Even after a hard day, you always managed to put a smile on my face and made me realize that I'm still somewhat smart. Thank you for allowing me to be myself and for teaching me that there is strength in vulnerability. The countless memories we have made I'll take with me to the grave. I will always treasure the time we had together and will miss you so much!

To my people: Pumelela Nquelenga, Jessica Harrison and Sifiso Sikhakhane – thank you all for pursuing me with an incredible amount of love and support, even when I felt I didn't deserve it. You are all wise beyond your years and I have appreciated every piece of advice that you have dished out. I am a better person today because of the example you have given me.

To my best friends, Judith and Garth Alistoun – friends for life… never has that saying been truer than in my friendship with you guys. Thank you for the endless laughter, advice, support and love that you have given me over the 16 years that I've

known you collectively. I will always hold you both close to my heart and can't wait to be reunited in the near future. I love you both so much!

To my labby, Tarryn Willmer – words cannot express how big a part you have played in my life here at Rhodes. Often, when work got tough, it was you who gave me a reason to wake up and come to the lab because I knew that spending time with you would put a smile on my face and instill fresh optimism. I guess we were destined to be lab soul mates. Thank you for always making me roll on the (lab) floor with laughter… literally. I'll never be able to watch a cat video again without thinking of you. I love you!

To my lab husband, Cindy Slater – I miss you already. Thank you for the endless laughter you have given me over these past 6 years. From dinners in Allan Webb Hall, to walking to lectures together, to updating our lab books with a bottle of wine (and a few strawpedos), we've literally gone through our time at Rhodes like an old married couple. Thank you for such incredible memories! You're irreplaceable! Loving you for days!

To my lab, BioBRU – what an incredible team of people! No matter where I end up in the world, I don't think any lab will come close to measuring up to you all. Don't ever take each other for granted! Thank you for all your support and encouragement and making my time at Rhodes a truly incredible and memorable one. I don't think I would have arrived at this point in my life without your major contributions!

To all the Mandalaysians of team 18 and team 20 – I couldn't think of a better bunch of people to spend my last few months with in Grahamstown. I wish I could take you all with me to America to continue the amazing friendships we've started. I hate that our time together was so short, but know that I hold all our memories together close to my heart. I love you all and can't wait to see you when I return!

To my incredible family: Sean, Maryann and Kerry-Lee O'Hagan – most of all, my gratitude and love goes to my parents (and sister) who willingly sacrificed their all to give me the opportunity to pursue my dreams. Never once have you questioned my intentions, but you have given me the freedom to hold my future in my own hands.

Thank you for loving me, supporting me on all levels and always believing that I can achieve my highest goals. I love you all so much and can't wait to make you proud!

To Rhodes University, the National Research Foundation and DAAD – I would like to thank Rhodes University as well as the National Research Foundation in conjunction with DAAD for funding my Masters research. Without your assistance, I would never have been able to take hold of this opportunity.

Chapter 1 :

Literature Review

1.1 Cancer and cancer metastasis

Cancer can be fundamentally defined as a population of cells that undergo aberrant, unregulated growth as a result of genetic mutations that cause either a loss or gain of function of important regulatory genes (Miller *et al.*, 1981). Following intensive research into cancers of different origin and genotype, investigators have identified six key hallmarks that can appropriately describe cancer cell physiology. These included self-sufficiency in growth signals, insensitivity to anti-growth signals, evading apoptosis, sustained angiogenesis, limitless replicative potential and tissue invasion and metastasis (Hanahan and Weinberg, 2000). Of these six key hallmarks, the process of tissue invasion and metastasis has received a considerable amount of attention. This is based on statistics which indicate that 90% of poor prognoses associated with cancer are seldom due to the primary tumor, but rather as a result of primary cancer cells invading secondary sites within the body (Gupta and Massagué, 2006; Steeg, 2006; Tsutsumi *et al.*, 2009). Cancer metastasis is a complex process mediated by several signaling pathways that have been exploited by cancerous cells (Steeg, 2006). The metastatic process involves the acquisition of an invasive phenotype comprising the detachment of cancer cells from the primary tumor, the degradation of the extracellular matrix (ECM) and the subsequent migration of the cells into the bloodstream (intravasation) to a secondary site where they exit the bloodstream (extravasation) and proliferate into a macrometastasis (Dowling *et al.*, 2008; Steeg, 2006; Theiry, 2002).

Since there is currently no standardized treatment for cancer metastasis, there is a heightened interest in determining the signaling proteins and pathways that facilitate metastatic progression. Steeg (2006) indicates that a number of proteins, when activated, are able to initiate tumor cell migration; an important component of metastasis. These include matrix metalloproteinases, integrins, urokinases, plasmin, plasminogen activator proteins, cathepsins and heparanases. A role in invasion has been elucidated for the majority of these proteins with additional roles including the release of growth factors and chemokines which result in signal-mediated cell migration and the activation of membrane proteins that promote the longevity of tumor cells (Steeg, 2006). Critical to the effective completion of the signaling pathways that regulate cancer metastasis is the maintenance of protein homeostasis within the cell (Bagatell

and Whitesell, 2004). Numerous environmental factors often experienced by cancer cells including nutrient starvation, hypoxia and acidosis compromise the integrity of the cells protein complement, directly affecting its ability to manage signal-mediated events. Consequently, this has initiated a heightened interest in cell stress proteins, particularly molecular chaperones, and the role they serve in assisting the cell during pressurized or jeopardizing conditions (Bagatell and Whitesell, 2004; Hartl *et al.*, 1994; Xu and Neckers, 2007).

1.2 Molecular Chaperones and Heat Shock Proteins

Heat shock proteins (Hsps), the largest family of molecular chaperones, were originally discovered in the early 1970s in *Drosophila* cells in response to heat shock (Tissiéres *et al.*, 1974). Numerous laboratories, over the next two decades, provided evidence to define molecular chaperones as proteins involved in the correct folding of nascent polypeptides and the prevention of protein aggregation and misfolding in response to cellular stress (Bukau *et al.*, 2006; Hartl and Hartl, 2002; Schlesinger, 1990).

Although different in prokaryotic and eukaryotic systems, Hsps form a fundamental component of the total protein complement and exhibit potent cytoprotective properties (Csermely *et al.*, 1998; Calderwood *et al.*, 2006). Various families of Hsps have been characterized based on their molecular weight (in kDa) and distinct functions have been allocated to each. Heat shock protein 70 (Hsp70) is required by the cell for the correct *de novo* folding of nascent polypeptides, refolding of denatured proteins after stress, translocation of proteins across cellular membranes as well as the proteolytic turnover of cell proteins (Michels *et al.*, 1997; Mayer and Bukao, 2004). Heat shock protein 60 (Hsp60) is involved in promoting correct protein folding of imported proteins and preventing aggregation of mitochondrial proteins (Hartl *et al.*, 1994). Heat shock protein 40 (Hsp40), also referred to as DnaJ, serves to assist the functions of Hsp70 through accelerating ATP hydrolysis, critical for its intracellular function. Some Hsp40 proteins also possess their own role, however, in preventing protein aggregation as has been reported by *in vitro* assays (Mayer and Bukao, 2004). While the majority of cells require the Hsp70/Hsp40 system to acquire their native state, studies indicate that a proportion of the substrate proteins are transferred from this Hsp70/Hsp40 complex to the heat

shock protein 90 (Hsp90) family of proteins for terminal folding. Hsp90 serves to maintain these proteins in a stable, inducible conformation (Hartl and Hartl, 2002). Recent studies also suggest additional roles for Hsp90 in modulating client protein maturation, expression or secretion (Tsutsumi *et al.*, 2009).

While Hsps are essential for normal cell function, there is increasing evidence to suggest that this group of molecular chaperones is essential for driving the proliferation of cancer cells. Hsps, in general, are overexpressed in all major cancer cell types including melanoma, breast, lymphoma, bladder and colon carcinomas (Becker *et al.*, 2004; Eustace *et al.*, 2004; Sidera *et al.*, 2008; Stellas *et al.*, 2008; Tsutsumi *et al.*, 2007). Since the uncontrolled growth associated with cancer is thought to cause cellular stress, it is predicted that high Hsp expression is exploited to counteract these stressful conditions. Through facilitating the correct folding of mutated and overexpressed client substrates, Hsps may consequently serve to assist in disease progression (Calderwood *et al.*, 2006; Cheng and Li, 2008).

1.3 Heat Shock Protein 90 (Hsp90)

Hsp90 is one of the most abundant intracellular proteins, constituting approximately 1-2% of the total cell protein complement under normal conditions (Cheng and Li, 2008). To date, this family of proteins is thought to consist of five distinct isoforms with different subcellular locations. Hsp90 isoforms have been observed and well-characterized in the cytosol (Hsp90α and Hsp90β), endoplasmic reticulum (Grp94) as well as the mitochondrial matrix (TRAP1/Hsp75) (Pearl and Prodromou, 2000; Sreedhar *et al.*, 2004). A more controversial finding was that of a truncated 75-kDa Hsp90 isoform observed on the plasma membrane of numerous cancerous cells, termed Hsp90N (Grammatikakis *et al.*, 2002).

Structurally, Hsp90 exists as a monomer in its inactive form, but under conditions of stress, Hsp90 monomers dimerize to form an active chaperone (Csermely *et al.*, 1998). The protein monomers constitute three highly conserved domains for the Hsp90 isoforms described (with the exception of Hsp90N), as illustrated in Figure 1.

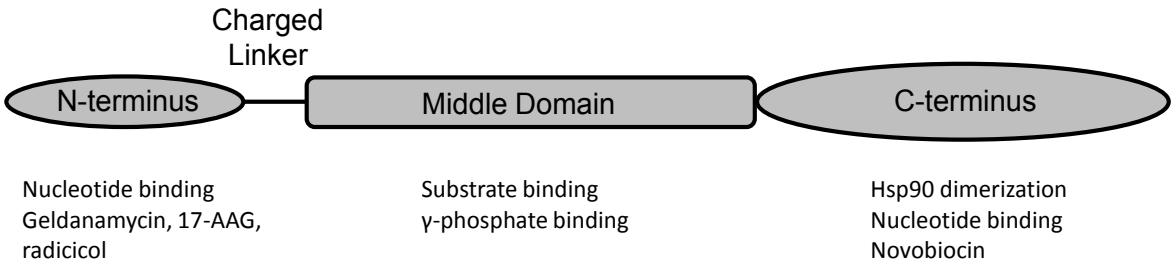

Figure 1: Schematic diagram illustrating the conserved domains for Hsp90.

Hsp90 consists of the 25 kDa N-terminal ATPase domain responsible for the ATP-dependent clamping mechanism associated with substrate binding, the 35 kDa middle domain responsible for binding Hsp90 client proteins as well as the γ -phosphate of ATP and the 12 kDa C-terminal domain responsible for Hsp90 dimerization and co-chaperone interactions via the conserved MEEVD motif (Adapted from Sreedhar et al., 2004).

It is well established that the ATPase activity associated with the N-terminus is critical for normal functioning of cytosolic Hsp90 and that mutants demonstrating hyper- or hypo-activity of this domain resulted in inhibition of normal functioning *in vivo* (Panaretou *et al.*, 1998; Jackson *et al.*, 2004; Soldano *et al.*, 2003). ATP binding alters the conformation of the chaperone from an “open” state to one of a “closed” state, creating a molecular clamp. It is within this pocket that specific client substrates bind, and with the assistance of co-chaperones, Hsp90 can perform its characteristic chaperone functions (Terasawa *et al.*, 2005). The middle substrate binding domain possesses a hydrophobic region that influences protein-protein interactions, critical for binding Hsp90 client substrates (Meyer *et al.*, 2003). Furthermore, the γ-adenine nucleotide of ATP is known to bind at this region and as a result contributes to the ATP-dependent chaperoning of Hsp90 (Meyer et al., 2003). Bagatell and Whitesell (2004) also indicate that the middle domain is the binding site for a co-chaperone, Aha-1, that stimulates the interaction between the middle and N-terminal domains, resulting in accelerated ATP hydrolysis (Meyer *et al.*, 2003). The Hsp90 carboxyl terminus (C-terminus) has shown critical importance in the dimerization of Hsp90 monomers as well as interaction with several co-chaperones, such as Hop, Cdc37 and p23 (Allan *et al.*, 2006). Due to the weak forces that bind the N-terminal domains of an Hsp90 homodimer, deletion of the C-terminus of Hsp90 resulted in the loss of ATP hydrolysis and overall function of the chaperone (Harris *et al.*, 2004). Additionally, the C-terminus contains the MEEVD motif

which represents the binding site for tetratricopeptide repeat (TPR)-containing proteins, such as the co-chaperones: p23 and Hop (Pearl and Prodromou, 2000).

There are five conserved sequences that serve as a signature for the Hsp90 family of proteins and are conserved in all Hsp90 isoforms (Chen *et al.*, 2005). Three of these sequences reside in the ATPase N-terminal domain (residues 38-59, 106-114 and 130-145) and often classify a protein within the Hsp90 family and the remaining two reside in the middle domain (residues 360-370 and 387-401). Apart from these conserved sequences, each Hsp90 isoform exhibits biochemical and functional differences (Chen *et al.*, 2005; Sreedhar *et al.*, 2004). It has been reported that the two cytosolic Hsp90 isoforms (α and β) are differentially induced and exhibit different functions (Csermely *et al.*, 1998; Sreedhar *et al.*, 2004; Pearl and Prodromou, 2000). The expression of Hsp90β is considerably higher in normal cells and is proposed to be involved in the evolution, adaptation and transformation of undifferentiated cells over a length of time. With its higher expression, Hsp90β is proposed to be the critical isoform for house-keeping functions including cell maintenance and differentiation (Sreedhar *et al.*, 2004). In contrast, Hsp90α is more sensitively induced by external stimuli or stresses even though it is expressed at lower levels. Induced expression of Hsp90α is often associated with processes such as cancer development, modulation of cell cycle events and the signaling of growth factors through certain kinases, indicating that this isoform is most likely associated with stress responses (Grammatikakis *et al.*, 2002; Felts *et al.*, 2000; Sreedhar *et al.*, 2004). TRAP1 was shown to be biochemically active in mitochondria through ATP-dependent binding of substrates, specifically related to apoptotic events. When placed in conditions similar to that of the cytosol, function was severely retarded (Felts *et al.*, 2000), suggesting that TRAP1 may require a specific microenvironment and accessory proteins to achieve its function. More interestingly, Grp94 shows 50% homology with cytosolic Hsp90 and controls similar functions to the α- and β-isoforms, including modulation of cell cycle events and cancer development, but also possesses distinct roles in apoptosis and antigen presentation (Argon and Simen, 1999; Chen *et al.*, 2005; Csermely *et al.*, 1998). The Grp94 protein is highly hydrophobic and tends to associate with the lipids of the ER and Golgi lumen. It has been shown that under conditions of cellular stress, Grp94 is transported via the classical secretory pathway

from the ER to the Golgi apparatus and may even translocate to the extracellular space or the extracellular leaflet of the plasma membrane (Schmitt *et al.*, 2006, Eletto *et al.*, 2010). It is therefore worth noting that even with homologous sequences or domains, the subcellular localization of the different Hsp90 isoforms alludes to a variety of specialized functions.

In the cytosol, Hsp90 is responsible for maintaining the active conformation of over 300 client proteins, the majority of which appear to be signaling proteins involved in different signal transduction pathways. In addition to this, Hsp90 has been shown to modulate the activity and stability of numerous mutated and overexpressed proteins associated with the development and survival of cancer (Chen *et al.*, 2010; Sidera *et al.*, 2008; Tsutsumi and Neckers, 2007; Tsutsumi *et al.*, 2009). Some examples include the Src-kinases, Raf-1, receptor tyrosine kinases (HER-2), mutated p53, steroid hormone receptors and telomerase (Holzbeierlein *et al.*, 2010). As a consequence, extensive research has been invested in deriving inhibitors of Hsp90 that can be used as a cancer therapeutic. To date, numerous inhibitors have been described that target Hsp90 at either the N-terminus or C-terminus of the protein. The earliest N-terminal Hsp90 inhibitors discovered were geldanamycin (a benzoquinone ansamycin antibiotic) and radicicol (a macrolactone antibiotic) which both compete with ATP binding and retard Hsp90 function (Holzbeierlein *et al.*, 2010; Smith and Workman, 2008). However, as a result of liver toxicity and poor stability, more effective derivatives were synthesized and include the geldanamycin derivatives, 17-allylamino geldanamycin (17-AAG) and 17-dimethylamino-17-demethoxygeldanamycin (17-DMAG), and radicicol oxime derivatives (Smith and Workman, 2008). The earliest C-terminal Hsp90 inhibitor described was novobiocin, a coumarin analogue that binds and inhibits the bacterial DNA gyrase II ATP site (Yu *et al.*, 2005). Novobiocin was shown to prevent the dimerization of Hsp90 into an active conformation and competed with co-chaperone binding, affecting functions such as protein client transfer and stimulation of Hsp90 activity (Blagg and Kerr, 2005; Holzbeierlein *et al.*, 2010).

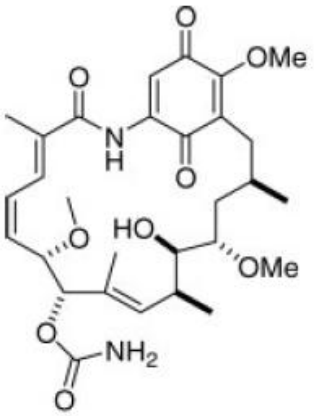

Geldanamycin (GA)

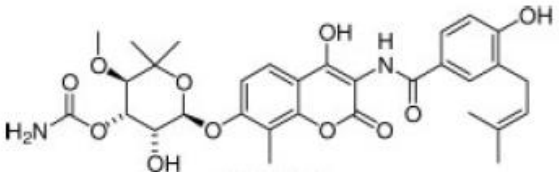

Novobiocin (NOV)

Figure 2: Chemical structure of Hsp90 inhibitors.

Geldanamycin (left) and novobiocin (right) bind the N- and C-terminal domains of Hsp90 respectively (Blagg and Kerr, 2005).

Other C-terminal Hsp90 inhibitors discovered include cisplatin (which showed activity against nucleotide binding) and the active ingredient in green tea extract, epigallocatechin-3-gallate (Palermo *et al.*, 2005). The chemical structure of the two most commonly used published Hsp90 inhibitors, geldanamycin and novobiocin, are illustrated in Figure 2.

1.4 Hsp90 multi-protein complexes

1.4.1 Hsp90 interaction with co-chaperones

In the late 1970s, researchers studying steroid hormone receptors (SHR) discovered a multi-protein complex whose formation was critical for the effective binding of steroid ligands to their respective receptors. Through co-immunoprecipitation studies, it was concluded that Hsp90 was an essential component of these complexes and facilitated the stability of the SHR prior to ligand binding (Richter and Buchner, 2001; Pratt, 1998). Initially, it was thought that Hsp90 was the principal component within these complexes. *In vitro* studies in rabbit reticulocyte lysates, however, reported that Hsp90 was accompanied by several other accessory proteins, including Hsp70, the Hsp70/Hsp90 organizing protein (Hop), p23 and immunophilins, which were shown to collectively regulate the folding, activity or stability of Hsp90 client proteins or substrates (Richter

and Buchner, 2001; Pratt, 1998). Using glucocorticoid receptors as a model, researchers proposed a mechanism by which the Hsp90 multi-chaperone complexes facilitated the active conformation of various client proteins (Figure 3).

Initially, Hsp70 binds to the client protein (glucocorticoid receptor) which exists in an inactive conformation. This binding is an ATP-dependent process stimulated by the chaperone activity of Hsp40. The initial complex is then formed when Hsp40 is released and replaced by binding of Hop to Hsp70. Hsp90 is subsequently recruited to the complex and binds through a co-chaperone interaction with Hop, forming the intermediate complex. Hsp70 and Hop are competitively exchanged for p23 and immunophilins (critical for stabilizing the interaction between Hsp90 and the substrate), forming the final complex (Richter and Buchner, 2001; Pratt, 1998). Hsp90 is then able to maintain its substrate (glucocorticoid receptor) in a stable, open conformation allowing the appropriate ligand (in this case, a steroid hormone) to bind. Ligand binding induces a change in the conformation of the substrate and its affinity to Hsp90, allowing Hsp90 and its accessory proteins to be released from the complex (Richter and Buchner, 2001).

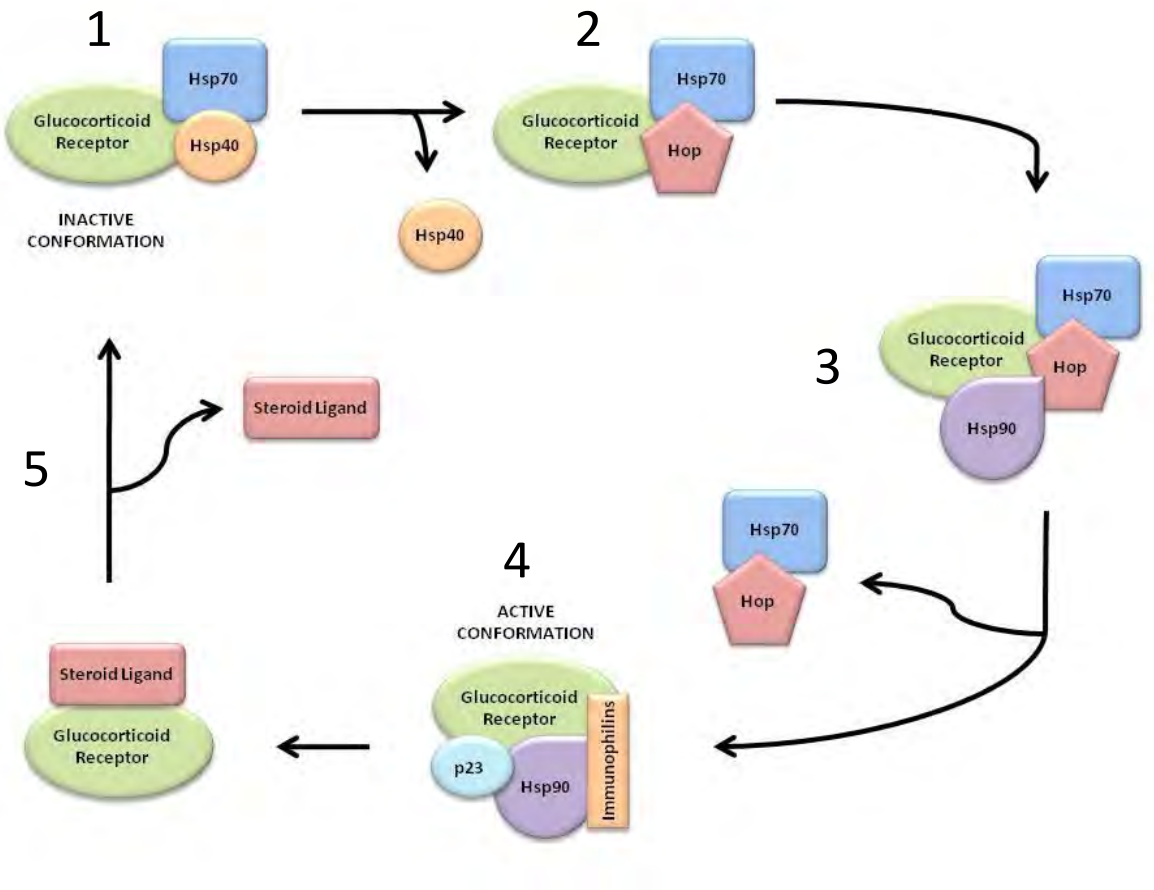

Figure 3: Proposed mechanism for the activation of a glucocorticoid receptor by the Hsp90 multi-chaperone complex.

For Hsp70 to bind the inactive client protein (glucocorticoid receptor), Hsp40 is required to stimulate its ATPase activity (1). Once bound to the client, Hsp40 can be released and replaced with the adaptor protein, Hop, forming the initial complex (2). The client protein is loaded onto Hsp90 through an interaction with Hop, forming the intermediate complex (3). Co-chaperones, such as p23 and immunophilins, compete with Hop and Hsp70 for binding to Hsp90, forming the final complex (4). Hsp90 activates the client protein by altering its conformation such that the appropriate ligand (steroid hormone) can bind. Binding of the ligand to the receptor causes a conformational change that decreases the affinity of Hsp90 (and the co-chaperones) for the client protein and the complex is disassembled (5).

Based on these initial studies, investigators began to appreciate that Hsp90 function was regulated by numerous proteins, termed co-chaperones. The earliest discovered included p23 and immunophilins. The co-chaperone, p23, has shown an ability to bind Hsp90 as well as the inactive client protein to which Hsp90 is bound. Deletion mutants lacking the p23 gene have shown an increased sensitivity to ansamycin antibiotics, such as geldanamycin, suggesting that p23 plays an important role in stabilizing the Hsp90-client complex (Weikl *et al.*, 1999). Immunophilins (FKBP52, FKBP51 and CyP-40)

possess quite a distinct role in binding microtubules (specifically dynein) for shuttling of the Hsp90-client complex from the cytoplasm to the nucleus where the activated client protein can regulate gene transcription in response to a signal stimulus (Pratt *et al.*, 2004). While these two co-chaperones were the earliest discovered, the list of Hsp90 co-chaperones has been revised to include the proteins: Activator of Hsp90 ATPase 1 (Aha1), Cdc37, TPR1 and TPR2 (Panaretou *et al.*, 2002). Aha1 was shown to activate the ATPase activity of Hsp90 not by affecting the loading of ATP, but rather increasing the efficiency of N-terminal dimerization (Panaretou *et al.*, 2002). Cdc37, a kinase-binding protein, has been reported to recruit protein kinases to the Hsp90 multi-chaperone complex for activation. Since a considerable number of Hsp90 clients are in fact kinases, Cdc37 is an essential component that confers substrate specificity (Pearl, 2005). TPR1 and TPR2 have shown specific roles in regulating Rab recycling to the plasma membrane and regulating the binding and release of substrate proteins from Hsp70 to Hsp90 respectively (Brychzy *et al.*, 2003; Liu *et al.*, 2009).

1.4.2 Hsp90 interaction with client proteins

It has been reported that intracellular Hsp90 is responsible for chaperoning approximately 10% of the yeast protein complement, indicating its versatility in chaperoning a diverse range of client proteins. While some would label such proteins “sticky”, inhibition of Hsp90 function has shown a change in cellular function as well as increased degradation of client proteins in cells treated with geldanamycin, an established and highly selective Hsp90 inhibitor (Basso *et al.*, 2002; Pratt *et al.*, 2010; Schnaider *et al.*, 2000; Theodoraki and Caplan, 2012). This would suggest that Hsp90 exhibits some form of selectivity towards its clients.

The fact that Hsp90 has been described in all the major subcellular compartments of the cell would suggest functions specific to its location. In the cytosol, Hsp90 has shown great importance in regulating different signaling pathways through chaperoning various kinase proteins. Collectively, results have reported that Hsp90 binds the αC-helix and the β4-loop situated in the amino-terminus of tyrosine kinases (Citri *et al.*, 2006; Prince and Matts, 2004). Citri *et al.* (2006) reported that 40 of the 43 tyrosine and tyrosine-like kinases that were examined contained the αC-β4 loop and were expected to be clients

of Hsp90. By comparison, only 29 of the 51 serine/threonine kinases showed a similar outcome. Regardless of the kinase family, there is evidence that intracellular Hsp90 has a high affinity for these signaling proteins, supporting the role of Hsp90 in chaperoning signal-mediated events. While Hsp90 exhibits functions in the cytosol, numerous reports have shown that Hsp90 can be translocated to the nucleus, either with the help of immunophilins, protein kinases or steroid hormone receptors (Csermely *et al.*, 1998). Furthermore, Nardai *et al.*, (1996) have suggested that Hsp90 possesses its own nuclear localization sequence within the highly charged region of the middle substrate binding domain, reserving an ability to reach the nucleus independent of other proteins. Nonetheless, Hsp90 has shown an ability to activate numerous transcription factors that regulate the expression of important regulatory genes. These include heat shock factor-1 (HSF-1) which regulates the transcription of heat shock genes and hypoxia inducible factor-1 (HIF-1) which regulates the transcription of genes encoding vascular endothelial growth factor and erythropoietin in response to reduced oxygen levels (Hu and Mivechi, 2003; Minet *et al.*, 1999). Furthermore, Hsp90 has been shown to bind both DNA and RNA directly and has demonstrated topoisomerase-like activity, suggestive of a role in DNA and RNA processing during stress (Szántó *et al.*, 1996). The function of Hsp90 has also in recent years been extended to the extracellular space where it interacted with a limited number of extracellular client proteins involved in cell migration and invasion. Examples include matrix metalloproteinase-2, HER-2 and tissue plasminogen activator (Eustace *et al.*, 2004; McCready *et al.*, 2010; Sidera *et al.*, 2008) and are discussed in more detail later. Collectively, Hsp90 interacts with over 300 client proteins in the cell with the list increasing rapidly, pointing to the fact that this molecular chaperone is essential for protein quality control and cell survival. A list of the most extensively studied Hsp90 client proteins is provided in Table 1.

Table 1: Hsp90 interacting proteins

Protein	Function	Reference
HSF-1	Activates the RalGTP signal transduction pathway to regulate transcription of heat shock genes	Hu and Mivechi (2003)
p53 (mutated)	Stabilizes the mutated p53 conformation	Blagosklonny *et al.* (1996)
Stat3	Stabilizes STAT3 and promotes interleukin-6 (IL-6)-mediated signaling	Sato *et al.* (2003)
BCL-6	Stabilizes BCL-6 and represses expression of BCL-6 apoptotic genes, promoting cell survival	Cerchietti *et al.* (2009)
Protein Kinase B (Akt)	Maintains Akt kinase activity through preventing dephosphorylation by PP2A	Sato *et al.* (2000)
EphA2	Responsible for EphA2 receptor stability and signaling	Annamalai *et al.* (2009)
GSK3β	Required for stability and kinase activity in complex with NDRG1	Banz *et al.* (2009)
ErbB2 (HER-2)	Modulates the stability and trafficking of nascent ErbB2	Xu *et al.* (2002)
Glucocorticoid Receptor (GCR)	Regulates proper folding of GCR allowing cortisol-based hormones to bind and regulate gene transcription	Dittmar *et al.*, 1997
Wee-1	Regulates kinase activity to facilitate the G2 phase of the cell cycle	Aligue *et al.* (1994)

*A more comprehensive list of Hsp90 interacting partners can be accessed using the following reference: http://www.picard.ch/downloads/Hsp90facts.pdf

1.5 Extracellular and Membrane-Associated Hsp90

Hsp90 was originally thought to function predominantly within the cell. Recent reports, however, have indicated that Hsp90 function is not limited to intracellular compartments, but extends to the extracellular space and plasma membrane (Eustace and Jay, 2004; Multhoff and Hightower, 1996; Tsutsumi *et al.*, 2009). Only recently has the biological role of this extracellular pool of Hsp90 been appreciated.

Due to the lack of a conventional signal sequence targeting intracellular Hsp90 to the cell surface or extracellular space, the mechanism by which it is secreted or associates with the membrane remains unknown (Cheng and Li, 2008; Multhoff and Hightower, 1996). Some have proposed that Hsp90 is secreted through an unconventional exosomal pathway and is loosely bound to the extracellular region of the plasma membrane where it interacts with membrane clients (Cheng *et al.*, 2008; McCready *et al.*, 2010). Alternatively, Hsp90 may be proteolytically cleaved from the surface of the

cell releasing the protein into the extracellular space as is demonstrated for the ectodomain proteins TNFα, TGFα and L-selectin (Althoff *et al.*, 2001). Given that Hsp90 has been detected on the surface of numerous cells (Cheng *et al.*, 2008; Eustace *et al.*, 2004; Sidera *et al.*, 2004; Tsutsumi *et al.*, 2009) as well as in the extracellular space (Li *et al.*, 2007; Liao *et al.*, 2000; Wang *et al.*, 2009), it may be reasonable to hypothesize that two distinct extracellular pools of Hsp90 exist: extracellular soluble Hsp90 and extracellular membrane-associated Hsp90. Based on reports by Eustace *et al.* (2004), Hsp90 was detected in association with the matrix metalloproteinase-2 (MMP-2) on the membrane surface as well as in the conditioned media of HT-1080 fibrosarcoma cells. This suggested that both membrane and soluble Hsp90 complexes were present extracellularly, supporting the hypothesis that two distinct extracellular Hsp90 pools are present. The majority of studies, however, are exceptionally vague in distinguishing between the two extracellular species resulting in confusion as to what differentiates extracellular soluble from extracellular membrane-associated Hsp90.

Evidence suggests that extracellular Hsp90 is derived from the cytosolic isoforms, Hsp90α and Hsp90β (Cheng *et al.*, 2008; Eustace *et al.*, 2004; Sidera *et al.*, 2008). Some have shown that both Hsp90α and Hsp90β were secreted to the cell exterior via exosomes (Hegmans *et al.*, 2004). Others have shown the presence of Hsp90α on the surface of cancer cells coupled with the secretion of Hsp90α, and not Hsp90β, into the extracellular space (Eustace and Jay, 2004; Li *et al.*, 2007; Liao *et al.*, 2000). While it is appreciated that the cytosolic Hsp90 isoforms can be found extracellularly, one cannot ignore the discovery of an extracellular, membrane-bound Hsp90 isoform discovered to be highly expressed in pancreatic carcinoma cells. It was termed Hsp90N due to its high similarity with Hsp90α with the exception of an N-terminal truncation that appeared to be replaced with a short hydrophobic peptide sequence distinct from all other isoforms (Grammatikakis *et al.*, 2002). Classification within the Hsp90 family of heat shock proteins is fundamentally based on the presence and function of this ATPase domain, therefore explaining the controversy associated with its discovery (Pearl and Prodromou, 2000; Sreedhar *et al.*, 2004).

Studies have shown that the activation of an important signal transducer, Raf-1, occurs through the chaperoning activity of Hsp90 in association with a co-factor, Cdc37. This co-factor binds the N-terminus of Hsp90 and its association was thought to be indispensable for Raf activation (Grammatikakis *et al.*, 1999). Results, however, indicated that the activation of Raf could be performed in association with Hsp90N, independent of the N-terminal ATPase domain (Grammatikakis *et al.*, 2002), suggesting that the ATPase domain may not be an appropriate classification for this family of Hsps. The rationale behind these contradictory results can possibly be explained by the discovery of C-terminal Hsp90 chaperoning activity that is independent of the N-terminal ATPase domain. With the absence of the N-terminus and the conserved C-terminus fully present and functional, Hsp90N may therefore still retain the ability to bind and activate client proteins (Grammatikakis *et al.*, 2002).

However, a comprehensive study by Zurawska *et al.* (2008) demonstrated that many of the results described to substantiate the existence of Hsp90N as a separate gene were not reproducible. The authors also put forward convincing evidence to suggest that the discovery of Hsp90N may have been a result of accidental gene rearrangements and template switching during reverse-transcription of the mRNA into cDNA within the carcinoma cells from which it was discovered. Additionally, since PCR-amplification of Hsp90N from many primate species and cancer cell lines (which were implicated to express this isoform) produced negative results, the authors concluded that it is unlikely that Hsp90N is a protein of evolutionary origin, but rather a result of post-translational modifications (Zurawska *et al.*, 2008).

Regardless of isoform specificity, the mechanism of extracellular Hsp90 function in the extracellular environment is not well elucidated. It is well established in literature that intracellular Hsp90 function is dependent on the formation of a multi-chaperone complex that is driven by the availability of ATP (Goes and Martin, 2001; Pearl and Prodromou, 2000; Pratt and Toft, 2003; Zhang and Burrows, 2004). Protein clients are delivered and loaded onto Hsp90 with the assistance of accessory factors such as Hsp40, Hsp70 and Hop followed by ATP hydrolysis which drives the conformational change required for Hsp90 to bind and capture substrates (Pratt and Toft, 2003). Given the vast difference

between the intracellular and extracellular environments, further studies are required to characterize the chaperone function of extracellular Hsp90 and whether this function is analogous to that of intracellular Hsp90.

1.6 Extracellular Hsp90 protein clients

In an attempt to better understand the mechanism of chaperone function in the extracellular space, several studies have adopted an interest in identifying and characterizing protein clients for extracellular soluble and extracellular membrane-associated Hsp90. A list of these extracellular clients is provided in Table 2. Eustace *et al.* (2004) stated that extracellular Hsp90 was essential for the proteolytic maturation of MMP-2, a surface enzyme implicated in cancer cell invasion. Binding of a cell impermeable inhibitor to cell surface Hsp90 significantly retarded the processing and maturation of MMP-2, subsequently reducing the observed invasion (Eustace *et al.*, 2004). Furthermore, extracellular soluble Hsp90α has been shown to interact with the cell surface receptor, LRP-1/CD91. LRP-1/CD91 appears to demonstrate multiple functions including endocytosis and the association with several focal adhesion complex proteins involved with cell morphology, adhesion and migration (Chen *et al.*, 2010). The authors reported that secreted Hsp90α physically interacted with the receptor, CD91, and induced significant cell invasion in human HCT-8 colon cancer cells. In the same study, it was shown that the serum levels of Hsp90α in colorectal cancer (CRC) patients was significantly greater compared to the control patients; a possible indication that extracellular Hsp90 may chaperone both extracellular soluble and extracellular membrane-associated proteins (Chen *et al.*, 2010).

Table 2: Extracellular Hsp90 interacting proteins

Year	Protein	Function	Membrane or Secreted Hsp90?	Reference
2004	Annexin	Indirectly increases plasmin activity in diabetic patients	Membrane	Lei *et al.* (2004)
2004	TLR-1/CD14, CXCR4, GDF-5	Multi-protein complex involved in innate immune recognition of bacterial lipopolysaccahrides	Membrane	Triantafilou *et al.* (2004)
2004	Matrix Metalloproteinase-2 (MMP-2)	Stability of MMP-2; promotes matrix catabolism and invasion of cancer cells	Both	Eustace *et al.* (2004)
2005	Heat shock protein 70 (Hsp70)	Creates receptor complex for Dengue virus entry in monocytes/macrophages	Membrane	Reyes-del Valle *et al.* (2005)
2008	HER-2/ErbB-2	Promotes cancer cell invasion	Membrane	Sidera *et al.* (2008)
2010	Latency-associated peptide (LAP)	Inactivation of TGF-β1 signaling pathway in cancer	Both	Suzuki and Kulkarni (2010)
2010	Tissue Plasminogen Activator (TPA)	Promotes cancer cell motility	Secreted	McCready *et al.* (2010)
2011	Low density lipoprotein-like receptor (LRP-1)/CD91	Promotes invasion of glioblastoma cells via Akt-EphA2 signaling	Undefined	Gopal *et al.* (2011)

HER-2 is another membrane protein implicated in cancer cell invasion. Its activation is commonly induced through the binding of heregulin (HRG) resulting in the cytoskeletal rearrangements often observed in invasive tumors (Yfanti *et al.*, 2004). Sidera *et al.* (2008) demonstrated that the addition of an Hsp90-inhibiting antibody, mAb 4C5, to HRG-enriched media impaired the activation of HER-2 and the subsequent invasion in breast cancer cells. Furthermore, it was shown through GST pull down assays that cell surface Hsp90 directly interacted with the extracellular domain of HER-2 (Sidera *et al.*, 2008). The authors concluded that extracellular Hsp90, whether soluble or membrane-associated, is essential for the activation of the HRG-induced HER-2 receptor and, therefore, directly contributes to cancer cell invasion.

Extracellular Hsp90 has also demonstrated an indirect role in activating cell migration and invasion. Thuringer *et al*. (2010) reported that recombinant Hsp90α applied to

glioblastoma U87 cells resulted in cross communication between toll-like receptor 4 (TLR-4) and the epidermal growth factor receptor (EGFR). Activation of a TLR-4 signal pathway was induced by Hsp90α and resulted in the transactivation of EGFR and a change in cytosolic calcium concentration patterns. Both outcomes were predicted to facilitate the cell migration observed (Thuringer *et al.*, 2010).

Extracellular Hsp90 possesses additional roles in the pathogenicity of bacterial and viral infections. Reyes-Del Valle *et al.* (2005) reported that Hsp90, along with Hsp70, form a receptor complex at the surface of human monocytes/macrophages and facilitate the entry of the Dengue virus through interacting with the viral E-protein. Cell surface Hsp90 has also been implicated in recognizing lipopolysaccharides (LPS) on the surface of Gram-negative bacteria and facilitates the inflammatory immune response (Triantafilou and Triantafilou, 2004). Hsp90 was shown to form a signaling complex constituting other membrane proteins including Hsp70, growth differentiation factor-5 (GDF-5) and CXCR4, which is coincidently an important chemokine receptor for the migration of breast cancer cells in response to stromal derived factor-1 (SDF-1) (Fernandis *et al.*, 2004). Altogether, this signaling complex is implicated in the potentially fatal sepsis that results from LPS-induced signaling pathways (Triantafilou and Triantafilou, 2004). The function of Hsp90 within this complex, however, was not specified, but may serve to stabilize or activate other proteins within the complex to achieve the innate response.

1.7 The Role of Extracellular Hsp90 in Cell Migration

The majority of the aforementioned studies suggested that extracellular Hsp90 was primarily involved in promoting cancer cell migration and invasion, a critical contributor to metastatic progression. If cancer cells were unable to detach from the surrounding environment and migrate to a distal site, the disease would certainly have a better prognosis. For this reason, researchers have flagged extracellular Hsp90 as a potentially revolutionary therapeutic target for cancer treatment.

Cell migration within normal cells involves the regulated and coordinated events of adhesion coupled with the degradation and remodeling of the extracellular matrix (ECM) (Sottile and Chandler, 2005). Cells react to a particular chemo-attractant and polarize

toward the source, forming either large protrusions, termed lamellipodia, or thin filamentous protrusions, termed filopodia (Ridley *et al.*, 2003). Of particular importance during cell migration, is the signaling events induced by the large family of integrin adhesion molecules which bind the ECM. Constituting at least 18 α- and 8 β-subunits, integrins are able to form at least 24 different heterodimers on the surface of the cell, each combination exhibiting some form of specificity for its particular ligand/s. Examples include the binding of the $\alpha_1\beta_1$ integrin to collagens and laminins and the $\alpha_5\beta_1$ integrin which binds only to fibronectin and fibrin (Mizejewski, 1999; Takada *et al.*, 2007).

Of particular relevance is the matrix protein, fibronectin. Fibronectin is a large, multimeric protein (400 – 450 kDa) that exists as a soluble protein intracellularly where it is synthesized. This soluble form of fibronectin is secreted as a dimer bonded together by disulfide linkages. Each dimer subunit comprises three repeating functional domains (type I, II and III) which allow interaction of fibronectin with cell surface receptors and other extracellular matrix proteins, such as heparin, collagen and fibrin (Mao and Schwarzbauer, 2005). Upon secretion, soluble fibronectin is polymerized into an insoluble matrix that forms a component of connective tissues and allows cells to adhere to the substratum (Baneyx *et al.*, 2001; Christopher *et al.*, 1997). Polymerization of the matrix is directly regulated by binding of the β1-integrin to an Arg-Gly-Asp (RGD) motif on the type III module of fibronectin (Maity *et al.*, 2010). This binding initiates a two-fold response: firstly, the soluble fibronectin molecule unfolds, exposing motifs and residues that allow adjacent fibronectin molecules to bind to each other, forming a dense, insoluble network. Secondly, a signaling cascade is initiated intracellularly that is responsible for regulating processes such as cell adhesion, morphology or migration The model put forward states that upon integrin binding, focal adhesion kinase (FAK) becomes phosphorylated, initiating fibronectin assembly. This is followed by clustering of integrins at focal adhesion points along the membrane and the recruitment of cytosolic signaling and cytoskeletal proteins. In particular, fibronectin matrix assembly is regulated along the Ras-MAPK and Rho GTPase signaling pathways (Brenner *et al.*, 2000; Maity *et al.*, 2010; Ridley *et al.*, 2003; Wierzbicka-Patynowski and Schwarzbauer, 2003). While both responses have been extensively studied in literature, an increasing number of questions are being raised as we begin to understand the mechanisms associated with

fibronectin unfolding, organization, assembly and turnover (Sottile and Hocking, 2002; Wierzbicka-Patynowski and Schwarzbauer, 2003). While it was initially thought that the fibronectin matrix was predominantly assembled for cell adherence, there is increasing evidence to suggest that the function of fibronectin is multifaceted and includes the regulation of embryogenesis, mesoderm formation, tissue repair, cell migration, differentiation, cell growth as well as certain pathological disorders such as fibrosis, tumor development and atherosclerosis (Crawford *et al.*, 1994; George *et al.*, 1993; Mao and Schwarzbauer, 2005; Prescott *et al.*, 1999; Schwarzbauer and Sechler, 1999). Furthermore, Sottle and Hocking (2002) have reported that the presence of an intact fibronectin matrix is essential for the deposition and assembly of other ECM proteins, including collagen-I and thrombospondin-1. This points to the fact that fibronectin plays a major role in ECM dynamics and possibly an important role in facilitating cell migration associated with cancer metastasis. Interestingly, studies have suggested that Hsp90 may possess roles in the formation of the ECM as well as in the signaling pathways that regulate its assembly. Liu and colleagues (2011) showed that when Hsp90 was inhibited in the PC3 prostate cancer line, a reduced adhesion was reported between fibronectin and the β_1-integrin. Furthermore, Luo and colleagues (2011) reported that α_4-integrin expression and adhesion to fibronectin was reduced when the ER Hsp90 isoform, Grp94, was transiently silenced.

1.8 Research Motivation and Knowledge gap

Only a handful of extracellular clients have been elucidated for secreted or extracellular membrane-associated Hsp90 in comparison to the varied list determined for intracellular Hsp90 (Chen *et al.*, 2010; Sidera *et al.*, 2008; Tsutsumi and Neckers, 2007). This presents a potential problem in that extracellular Hsp90, both membrane-associated and secreted Hsp90, are potentially involved in the stabilization, activation or maturation of important proteins at the membrane surface and in the extracellular space. Since these proteins might promote oncogenic transformation, extracellular Hsp90 may contribute to driving the development of cancer and cancer metastasis. To date, a significant portion of research has been devoted to understanding intracellular Hsp90 and its role in cancer development, making it a *bone fide* drug target with several inhibitors already facing clinical trials. There are no studies, however, that have taken a focused approach on

identifying and assessing the clientele for extracellular membrane-associated or secreted Hsp90. This is the first study to provide evidence that suggested an interaction between extracellular Hsp90 and the extracellular matrix protein, fibronectin. As a consequence, we have attempted to characterize the putative role of Hsp90 in fibronectin matrix dynamics; a role previously not defined in literature.

1.9 Research hypothesis

Fibronectin is a novel client protein for extracellular Hsp90 and Hsp90 is involved in regulating fibronectin matrix dynamics.

1.10 Project objectives

The broad aim of the project was the identification of novel client proteins, and hence potentially novel therapeutic targets, of extracellular Hsp90. The following objectives were assessed in the Hs578T breast carcinoma cell line:

1. Characterization of the expression of extracellular Hsp90
2. Identification of novel client proteins of extracellular Hsp90
3. Confirmation and characterization of any identified interactions between Hsp90 and putative extracellular client proteins identified in (2)

Chapter 2 : Materials and Methods

2.1 Materials

MCF-7 (HTB-22) and MDA-MB-231 (HTB-26) breast cancer cell lines were a generous gift from Dr Sharon Prince (University of Cape Town, South Africa). Hs578T (HTB-126, American Type Culture Collection [ATCC]) breast cancer cell line and the paired SW480/SW620 (87092801/87051203, European Collection of Cell Cultures [ECACC]) colon cancer cell lines were purchased from ATCC and ECACC respectively. THP-1 (TIB-202) and U937 (CRL-1593.2) leukemic cell lines were from lab stocks. General reagents were purchased from Sigma-Aldrich (Germany) or Saarchem (Merck, South Africa). Tissue culture reagents (Dulbecco's Modified Eagle Medium [DMEM] with GlutaMAX™-I, fetal calf serum [FCS], 10 x Trypsin-Ethylenediaminetetraacetic acid [EDTA] and Penicillin/Streptomycin) were from Gibco, Invitrogen (Paisley, United Kingdom) and Biowhittaker (United Kingdom). Tissue culture plasticware was from Corning Incorporated (United States of America). Hybond nitrocellulose membrane was from Bio-Rad (United Kingdom). Hsp90α ELISA kit (cat no.: SKT-107) was from StressMarq Biosciences Inc. (Canada). Mouse anti-Hsp90α/β [F-8] (cat no.: sc-13119), goat anti-Hsp90α/β [N-17] (cat no: sc-1055), rabbit anti-Rab 5 [D11] (cat no.: sc46692), rabbit anti-Rab 7 [H-50] (cat no.: sc-10767) and mouse anti-LAMP-1 [E-5] (cat no.: sc17768) antibodies were from Santa Cruz Biotechnology (United States of America). Mouse anti-human fibronectin (cat no.: F0916), rabbit anti-human fibronectin (cat no.: F3648), rabbit anti-actin (cat no.: A2103), colchicine (cat no.: C9754), methyl-β-cyclodextrin (cat no.: C4555), genistein (cat no.: G6649) and Exo 1 (cat no.: C6637) were from Sigma Aldrich (Germany). Rabbit anti-Extracellular Regulated Kinase 1/2 [ERK1/2] (cat no.: MAB1576) and rabbit anti-Phospho-ERK1/2 (cat no.: AF1018) were purchased from R&D Systems (United States of America). Mitogen-induced Extracellular Kinase 1/2 [MEK1/2] inhibitor (U0126; cat no.: 9903) was from Cell Signaling Technology (United States of America). Alexa-Fluor-488 donkey anti-mouse (cat no.: A21202), Alexa-Fluor-633 donkey anti-goat (cat no.: A21082), Alexa-Fluor-555 donkey anti-rabbit (cat no.: A31572) were from Invitrogen (Paisley, United Kingdom). 3,3'-dithiobis[sulfosuccinimidyl]propionate [DTSSP] (cat no.: 21578) was purchased from Thermo Scientific (United States of America). Manufacturers or suppliers of any other specialized reagents are referenced in-text.

2.2 Methods

2.2.1 Routine culture maintenance of cancer cell lines

MDA-MB-231 and MCF-7 breast cancer cells and HeLa cervical cancer cells were maintained in Dulbecco's Modified Eagle Medium (DMEM) supplemented with GlutaMAX™-I, 5% (v/v) fetal calf serum (FCS) and penicillin/streptomycin (100 units/ml). Hs578T breast cancer cells were maintained in DMEM supplemented with GlutaMAX™-I, 10% (v/v) FCS, penicillin/streptomycin (100 U/ml) and 2 mM human insulin (Novorapid). SW480 and SW620 colon cancer cell lines were maintained in L-15 medium supplemented with GlutaMAX™-I, 5% (v/v) FCS and penicillin/streptomycin (100 U/ml). Leukemic cell lines, THP1 and U937, were maintained in Roswell Park Memorial Institute (RPMI) medium containing 10% (v/v) FCS, 1% (v/v) glutamine and penicillin/streptomycin solution (100 U/ml). All mammalian cancer cell lines were maintained at 37°C with 9% CO_2.

2.2.2 Sodium Dodecyl Sulphate-Polyacrylamide Gel Electrophoresis (SDS-PAGE)

Proteins were separated by SDS-PAGE using the method described by Laemmli (1970). Protein concentration was determined using the NanoDrop 2000™ (Thermo Scientific) at an absorbance of 280 nm and equal amounts of total protein were loaded. Proteins were resolved using a 4% stacking gel in 0.5 M Tris-HCl (pH 6.8) and a range of percentage resolving gels prepared in 1.5 M Tris-HCl (pH 8.8) in SDS-PAGE running buffer (0.25 mM Tris, 192 mM glycine, 1% [w/v] SDS) at 120 V for 90 minutes. Prior to loading, 5 x SDS-PAGE sample buffer (0.05 M Tris-HCl, 10% [v/v] glycerol, 2% [w/w] SDS, 1% [w/v] bromophenol blue, 5% [v/v] 2-mercaptoethanol) was added to each sample and boiled for 8 minutes. For estimating the approximate molecular weight of sample proteins, PeqGOLD Protein Marker II and Protein Marker IV (Optima Scientific) were used.

2.2.3 Western blotting and chemiluminescent detection of proteins

The Western blot method described by Towbin and colleagues (1979) was used for the detection of proteins. Resolved proteins were transferred from the SDS-PAGE gel onto

nitrocellulose membrane in transfer buffer (13 mM Tris-HCl, 100 mM glycine, 20% [v/v] methanol) at 120 V for 2 hours at 4°C, with continual stirring. Transfer efficiency and protein levels were observed on the nitrocellulose membrane using Ponceau S staining (0.5% [w/v] Ponceau S, 1% [v/v] glacial acetic acid). Destaining of the membrane was achieved with Tris-Buffered Saline [TBS] (50 mM Tris, 150 mM NaCl, pH 7.5). Nitrocellulose membrane was blocked with 5% BLOTTO (5% [w/v] non-fat milk powder in TBS) for at least 1 hour at room temperature, followed by incubation with primary antibody against the protein of interest (using the dilution recommended by the manufacturer in 5% [w/v] BLOTTO) at 4°C overnight, with gentle rocking. The membrane was washed twice with TBS containing Tween-20 (TBST; 1% [v/v] Tween-20 in TBS) for 20 minutes each wash to remove unbound primary antibody. The membrane was incubated with species matched secondary antibody (conjugated to horseradish peroxidase [HRP]) at a dilution of 1:5000 in 5% (w/v) BLOTTO for 1 hour at room temperature. The membrane was washed at intervals of 15 minutes for 1 hour using TBST and the proteins detected using a combination of prepared and commercial chemiluminescence reagents (Enhanced Chemiluminescence [ECL], GE Healthcare, United Kingdom) in the Chemidoc™ EQ system (Bio-Rad, United Kingdom).

2.2.4 Cell Surface biotinylation and streptavidin-agarose affinity chromatography

Breast cancer (MDA-MB-231, MCF-7 and Hs578T) and colon cancer cell lines (SW480 and SW620) were grown to confluency in a T75 culture flask. The cells were washed with phosphate-buffered saline (PBS, pH 7.4; 137 mM NaCl, 27 mM KCl, 4.3 mM Na_2HPO_4, 4 mM KH_2PO_4) and subsequently incubated in 1 mg/ml solution of N-hydroxysuccinimide (NHS)-Biotin (Sigma-Aldrich) prepared in PBS (pH 8.0) for 1 hour at 4°C, with gentle rocking. The NHS-Biotin was quenched for 5 minutes with 1 M Tris-HCl (pH 7.5) and the cells washed twice with PBS (pH 7.4). One biotinylated flask of cells was lifted using a cell scraper and lysed in 600 µl Radio-Immunoprecipitation assay (RIPA) buffer (50 mM Tris-HCl [pH 7.4], 150 mM NaCl, 1 mM ethyleneglycol-bis(beta-aminoethylether)N'N'N'N-tetraacetic acid/ethylenediaminetetraacetic acid [EGTA/EDTA], 1 mM Na_3VO_4, 1% [v/v] NP40, 1 mM sodium deoxycholate (DOC), 1 mM phenylmethanesulfonylfluoride (PMSF) and 0.05% [v/v] protease inhibitor cocktail). A

second biotinylated flask was lifted with 1 x trypsin/EDTA and the trypsin/EDTA was removed from the cells by centrifugation at 2000 rpm in a microcentrifuge for 2 minutes. The cells were resuspended in 600 µl RIPA buffer and allowed to lyse for 30 minutes at 4°C, with gentle rocking. Complete cell lysis was ensured by gently pipetting the samples. Centrifugation at 13000 rpm in a microcentrifuge at 4°C for 5 minutes was used to clear the cell lysates. A total of 100 µl of the cleared lysate (pre-agarose supernatant) was removed and added to 5 x SDS-PAGE sample buffer for Western analysis. The remaining 500 µl was added to 100 µl streptavidin-agarose beads (Thermo Scientific, United States of America), following equilibration of the beads with PBS. The supernatant-bead mixture was incubated at 4°C for 1 hour with gentle rocking to prevent sedimentation of the beads. The post-agarose supernatant was cleared by centrifugation at 13000 rpm in a microcentrifuge for 1 minute at 4°C. A volume of 100 µl of the supernatant was removed and added to 5 x SDS-PAGE sample buffer for Western analysis. The remaining supernatant was discarded and the beads resuspended in 100 µl SDS buffer (25 mM Tris-HCl, pH 8.0, 1% [w/v] SDS, 2 mM PMSF, 2 mM EDTA and 0.05% [v/v] protease inhibitor cocktail). Purified proteins were released from the beads by boiling for 8 minutes. Proteins were subsequently resolved by SDS-PAGE and analysed by Western analysis with chemiluminescence detection (Section 2.2.3).

2.2.5 Indirect Immunofluorescence Assay (IFA) and confocal microscopy

Cells were seeded at a density of 2 x 10^4 cells/ml and incubated overnight at 37°C with 9% CO_2 to allow cells to adhere. In certain instances, the culture dish was pre-treated with fibronectin (5 µg/ml) overnight at 4°C and washed with 1 x PBS prior to seeding cells. Following each treatment, the culture media was removed and the cells washed in 0.1% [w/v] bovine serum albumin in TBS (BSA/TBS) for 5 minutes, flash-treated (5 seconds) with ice-cold methanol/ethanol and allowed to air-dry. The cells were subsequently blocked with 1% [w/v] BSA/TBS for 60 minutes at room temperature and then incubated with the appropriate primary antibodies in 1% [w/v] BSA/TBS overnight at 4°C. Cells were washed twice with 0.1% [w/v] BSA/TBS for 5 minutes each wash followed by incubation with the respective secondary antibodies at 4°C for 1 hour in the dark. Detailed descriptions of the dilutions and treatments used are presented in the

figure legends. The coverslips were washed twice with 0.1% [w/v] BSA/TBS for 5 minutes each wash followed by nuclear DNA staining with Hoechst-33342 dye (1 µg/ml). The coverslips were mounted onto microscope slides with fluorescent mounting medium (Dako Mounting Medium, United States of America). Immunofluorescence was detected using a Zeiss LSM 510 Meta laser scanning confocal microscope and the images analysed using AxiovisionLE 4.7.1 software (Zeiss, Germany). Images were captured using either 40x or 63x oil objective as indicated in the figure legends.

2.2.6 Hsp90α Enzyme-linked Immunosorbent Assay (ELISA)

To analyse the concentration of Hsp90α in the cell culture supernatant of a panel of cancer cell lines, an Hsp90α ELISA kit was used. Briefly, cells were seeded at a density of 1 x 10^5 cells/ml in a 4-well culture dish and allowed to adhere overnight at 37°C, 9% CO_2. The following day, one well for each cell line was left untreated while a second was treated with 100 ng/ml stromal derived factor-1α (SDF-1α) for 5 hours at 37°C, 9% CO_2. The cell culture supernatant was removed and stored at -20°C prior to analysis with the ELISA kit. Both the Hsp90α standard and assay protocol were performed as indicated in the manufacturer's instructions. The levels of Hsp90α in each sample were detected by absorbance at 450 nm and the concentration calculated using the linear equation associated with the Hsp90α standard curve.

2.2.7 3,3'-dithiobis[sulfosuccinimidyl]propionate (DTSSP) crosslinking, co-immunoprecipitation and identification of extracellular Hsp90 complexes

Cells were grown to confluency in a T75 culture flask, washed with PBS and lifted with 1% (w/v) EDTA. The EDTA was removed by centrifugation at 2000 rpm in a microcentrifuge for 2 minutes and the cell pellet resuspended in the DTSSP crosslinker (2 mM) constituted in PBS (pH 7.5). The cells were incubated at 4°C for 2 hours with gentle rocking. The crosslinker was quenched with Tris-buffer (20 mM, pH 7.5) for 15 minutes at room temperature and cleared by centrifugation at 2000 rpm in a microcentrifuge for 2 minutes. The cell pellet was washed twice in 2 ml PBS (pH 7.5) and a co-immunoprecipitation was performed using the Dynabeads® Co-Immunoprecipitation kit (Invitrogen, Paisley, United Kingdom) following all

manufacturers' instructions. Briefly, 50 µg mouse anti-Hsp90α/β antibody was covalently coupled to 5 mg magnetic Dynabeads® and incubated with the cleared cell lysate of crosslinked cells for 2 hours at 4°C with gentle rocking. Eluted protein was stored at -20°C. Immunoprecipitated protein complexes were resolved on an 8% non-reducing SDS-PAGE gel and detected by colloidal Coomassie staining (Candiano *et al.*, 2004). Putative Hsp90 protein complexes were analysed by tandem mass spectrometry (MS/MS) by Dr. Gabre Kemp in the Department of Microbial, Biochemical and Food Biotechnology at the University of the Free State, South Africa. Protein bands were excised from the gel and subjected to trypsin digestion (Ngubo *et al*., 2011). Five microliters of each digest was injected and concentrated on a C18 reverse phase trapping column (Agilent) and then eluted onto and separated by a custom packed 15cm C18 reverse phase column. The peptides were separated and eluted off the column at 350 nl/min using an Agilent Nano HPLC with a 10 to 25% Actetonitrile/0.1% formic acid gradient over 60 minutes. The eluting peptides were analyzed on an AB SCIEX 4000QTRAP hybrid triple quadrupole ion trap mass spectrometer with a nanospray source. The instrument was set up to perform a survey scan between 400 and 1200 Da on the eluting peptides, followed by an enhanced resolution scan to determine the charge state of each peptide before fragmenting the peptides in the collision cell. The peptide sequence information obtained from this MS/MS experiment was analyzed by an in-house Mascot (Matrix Science) server using the Swissprot database. MS/MS results were validated by Western analysis whereby both the uncleaved and cleaved (5% [v/v] 2-mercaptoethanol) samples were probed with antibodies against Hsp90α/β and putative interaction proteins.

2.2.8 *In vitro* pull down assay

Soluble Hsp90β (1 µg) and soluble fibronectin (1 µg) were incubated in a microcentrifuge tube for 15 minutes at room temperature. Hsp90 complexes were immunoprecipitated using anti-Hsp90α/β antibody-coupled Dynabeads®, prepared as previously described (Section 2.2.7). Beads incubated with Hsp90 alone served as a positive control and BSA-coupled Dynabeads® served as a negative control. Relative protein sizes were compared to the Hsp90β (1 µg) and fibronectin (1 µg) input controls. Immunoprecipitated proteins were analysed by Western analysis and silver staining

using the PageSilver™ Silver Staining Kit (Fermentas) where all manufacturers' instructions were followed.

2.2.9 Surface Plasmon Resonance with BIAcore X

Recombinant human fibronectin was immobilized on flow cell 1 (Fc1) of a CM5 sensor chip (GE Healthcare Life Sciences) by amine-coupling. Qualitative real-time interaction analyses were achieved using the Biacore X (GE Healthcare, Sweden) at a flow rate of 5 µl/minute following 10 µl injections of recombinant Hsp90β (20 mM Tris, pH 7.5, 175 mM NaCl, 0.1 mM EDTA, 1 mM DTT). Unmodified flow cell 2 (Fc2) was used as an internal control. In between injections, the flow cells were regenerated using 1.5 M glycine solution. Sensograms were analysed using BIAevaluation 4.1 software (GE Healthcare Life Sciences).

2.2.10 Deoxycholate (DOC) biochemical assay for fibronectin fractionation

Hs578T cells were seeded in complete medium at a density of 3 x 10^5 cells/ml in a 6-well culture dish such that 9 x 10^5 cells were aliquoted into each well. A sterile coverslip was placed into each well for indirect immunofluorescence analysis. Cells were incubated overnight at 37°C, 9% CO_2. Fresh DMEM (10% [v/v] FCS, 100 U/ml penicillin/streptomycin) was added to the cells the following day. Details of specific treatments are explained in figure legends. Cells were harvested by scraping into deoxycholate (DOC) buffer (2% [w/v] deoxycholate, 20 mM Tris-HCl, pH 8.8, 2 mM PMSF, 2 mM EDTA and 0.05% [v/v] protease inhibitor cocktail) and vortexed for 2 minutes. The soluble and insoluble fractions were separated by centrifugation at 13000 rpm in a microcentrifuge for 20 minutes. The supernatant (soluble fraction) was removed and the cell pellet (insoluble fraction) was resuspended by vortexing in SDS buffer (1% [w/v] SDS, 25 mM Tris-HCl, pH 8.0, 2 mM PMSF, 2 mM EDTA and 0.05% [v/v] protease inhibitor cocktail). Protein concentrations were determined using the NanoDrop 2000™ (Thermo Scientific).

2.2.11 Effect of treatment with exogenous Hsp90β on soluble and insoluble fibronectin

Hs578T cells were seeded at a density of 9 x 10^5 cells per well in a 6-well culture dish and allowed to adhere overnight at 37°C, 9% CO_2. Sterile, glass coverslips were placed into each well for analysis by confocal microscopy. The following day, the culture media was replaced with fresh media (DMEM, GlutaMAX™-I, 10% [v/v] FCS, 100 U/ml penicillin/streptomycin, 2 mM human insulin) supplemented with increasing concentrations of Hsp90β (50 ng/ml, 500 ng/ml and 1000 ng/ml). Culture media supplemented with the same range of concentrations of BSA and soluble fibronectin served as the negative and positive controls respectively. Cells were incubated with the respective treatments for a period of 16 hours prior to harvesting as per the DOC assay described in section 2.2.10. The coverslips were harvested and prepared for immunofluorescence as described in section 2.2.5.

2.2.12 Effect of chemical inhibition of Hsp90 on soluble and insoluble fibronectin

Hs578T cells were seeded at a density of 9 x 10^5 cells per well in a 6-well culture dish and allowed to adhere overnight at 37°C, 9% CO_2. Sterile, glass coverslips were placed into each well for analysis by confocal microscopy. The following day, the culture media was replaced with fresh medium (DMEM, GlutaMAX™-I, 10% [v/v] FCS, 100 U/ml penicillin/streptomycin, 2 mM human insulin) supplemented with increasing concentrations of either geldanamycin (500 nM, 2000 nM and 4000 nM) or novobiocin (250 µM, 750 µM and 1500 µM) and incubated for a period of 16 hours prior to harvesting as per the DOC assay described in section 2.2.10. Cells treated with 5 µg/ml of either a RGD peptide or the RAD mutant analogue served as controls. The coverslips were harvested and prepared for immunofluorescence as described in section 2.2.5.

2.2.13 Transient siRNA knockdown of Hsp90

Hs578T cells were seeded at 90% confluency into T25 culture flasks and serum-starved in antibiotic-free media (DMEM, 2 mM human insulin) for 8 hours on the day prior to siRNA transfection. As a negative control, cells were transfected with a scrambled, non-

targeting pool (25 nM) of siRNA oligonucleotides (cat no.: D-001206-13-05, Dharmacon). Knockdown of Hsp90β or Hsp90α was achieved by transfection with 25 nM isoform specific siRNA (cat no.: M-005187-02 and M-005186-02 respectively, Dharmacon) for 48 hours. To analyse the effect of Hsp90 knockdown on soluble and insoluble fibronectin, cells were transferred to a 6-well culture dish for 24 hours in normal growth media (DMEM, GlutaMAX™-I, 10% [v/v] FCS, 100 U/ml penicillin/streptomycin, 2 mM human insulin) and processed as per the DOC assay described in section 2.2.10. Co-transfection of Hsp90β and Hsp90α siRNA was optimized at 12 nM for each isoform.

2.2.14 Effect of exogenous Hsp90β treatment following knockdown of Hsp90 or inhibition with novobiocin

Hs578T cells were seeded at a density of 9 x 10^5 cells per well in a 6-well culture dish and allowed to adhere overnight at 37°C, 9% CO_2. Sterile, glass coverslips were placed into each well for analysis by confocal microscopy. The following day, the culture medium was replaced with fresh medium (DMEM, GlutaMAX™-I, 10% [v/v] FCS, 100 U/ml penicillin/streptomycin, 2 mM human insulin) supplemented with novobiocin (1 mM) and incubated for 1 hour before adding Hsp90β (100 ng/ml) to the cells for a period of 16 hours. Cells treated with novobiocin (1 mM) or Hsp90β (100 ng/ml) alone served as controls. For the knockdown of Hsp90, confluent Hs578T cells were treated with a combination of siRNA oligonucleotides against Hsp90α (12 nM) and Hsp90β (12 nM) as described in section 2.2.13. Following a 24 hour incubation period, exogenous Hsp90β (100 ng/ml) was added to the cells and incubated for a further 24 hours. Transfection of cells with a pool of non-targeting siRNA oligonucleotides (25 nM) was used as a negative control. For both sets of experiments, cells were harvested as per the DOC assay described in section 2.2.10. The coverslips were prepared for immunofluorescence as described in section 2.2.5.

2.2.15 Fluorescent Labeling of Purified Fibronectin with DyLight® 550 Reagent

Lyophilized fibronectin (1 mg) was reconstituted in a borate buffer (0.67 M) to a final concentration of 2 mg/ml. The total volume of fibronectin was transferred to a vial of

DyLight reagent, vortexed and incubated for 60 minutes at room temperature in the dark. Excess DyLight reagent was removed by centrifugation through a Zeba spin desalting column (7K molecular weight cutoff; Thermo Scientific) at 1000 x *g* for 1 minute. The concentration of labeled fibronectin as well as the moles of dye per moles protein was determined using the following calculations:

Protein concentration (M) = $[A_{280} – (A_{max} \times 0.081)] \div \varepsilon_{protein}$ x dilution factor

Moles dye per mole protein = (A_{max} of the labeled protein x dilution factor) ÷ (ε_{dye} x protein concentration [M])

2.2.16 Fluorescent Labeling of Purified Fibronectin with Carboxyfluorescein Diacetate Succinimidyl Ester (CFDA-SE)

Lyophilized fibronectin (1 mg) was reconstituted in 0.1 M sodium bicarbonate buffer to reach a final concentration of 2 mg/ml. The CFDA-SE reagent was solubilized in DMSO at a concentration of 10 mg/ml and added to the dissolved fibronectin with gentle agitation. The reaction was incubated for 1 hour at room temperature with continuous agitation followed by the addition of stop reagent (1.5 M hydroxylamine, pH 8.5) for 1 hour at room temperature. Excess CFDA-SE reagent was removed from the labeled fibronectin through a Zeba spin desalting column (7K molecular weight cutoff; Thermo Scientific) at 1000 x *g* for 1 minute and the eluted protein was stored at -20°C. Protein concentration was determined at 280 nm using the NanoDrop 2000™ (Thermo Scientific) and equal amounts of total labeled fibronectin were added to cells as indicated in the figure legends.

2.2.17 Live Cell Imaging of the fibronectin matrix

Cells were seeded into a sterile glass-bottomed cell culture dish and allowed to adhere overnight at 37°C in normal medium supplemented with 50 nM DyLight® 550-labeled fibronectin. The following day, the medium was removed and replaced with normal medium (DMEM, GlutaMAX™-I, 10% [v/v] FCS, 100 U/ml penicillin/streptomycin, 2 mM human insulin) lacking phenol red. The Zeiss LSM 510 Meta laser scanning confocal microscope was used for live cell imaging. Prior to treating cells, the microscope unit and stage was pre-warmed to 37°C and a regulated concentration of 10% CO_2 was

maintained. Cells were either untreated or treated with novobiocin (1 mM) and mounted onto the microscope stage using the 63x oil objective. A time series experiment was prepared such that 36 images were captured at 15 minute intervals, with a total incubation period of 9 hours. Images were analysed using AxiovisionLE 4.7.1 software and live cell video clips edited using Windows Movie Maker.

Chapter 3 : Results

3.1 Results

3.1.1 Expression of Hsp90 in five human cancer cell lines

To compare the constitutive expression of cytosolic Hsp90 in a range of human cancer cell lines, equal amounts of total protein from three breast and two colon cancer whole cell lysates were probed for the levels of Hsp90α/β by Western analysis (Figure 4A). Two triple negative, metastatic breast cancer cell types (MDA-MB-231 and Hs578T) were compared to the non-metastatic MCF-7 breast cancer cell type. The genetically paired colon cancer cell lines, SW480 (primary tumor) and SW620 (secondary metastasis), were also compared.

Western analysis revealed a band for each sample at approximately 90 kDa, the predicted subunit molecular weight of Hsp90 (Figure 4A). The densitometry for each signal was analysed using ImageJ and would suggest that the metastatic cancer cell types (MDA-MB-231, Hs578T and SW620) constitutively expressed higher levels of Hsp90 relative to the non-metastatic counterparts (MCF-7 and SW480), with the MDA-MB-231 and MCF-7 cell lines showing the highest and lowest levels of Hsp90 expression respectively (Figure 4A). The relative expression of the two cytosolic Hsp90 isoforms, Hsp90α and Hsp90β, were also compared separately by Western analysis (Figure 4B). Equal amounts of total protein from whole cell lysates were probed with antibodies specific for either Hsp90α or Hsp90β. Recombinant Hsp90α and Hsp90β protein were used as input controls to ensure the specificity of the antibodies. In agreement with the levels of total Hsp90α/β (Figure 4A), isoform expression showed a pattern similar to that of Hsp90α/β, with the levels of Hsp90α and Hsp90β highest in the MDA-MB-231 cell line and lowest in the MCF-7 cell line (Figure 4B).

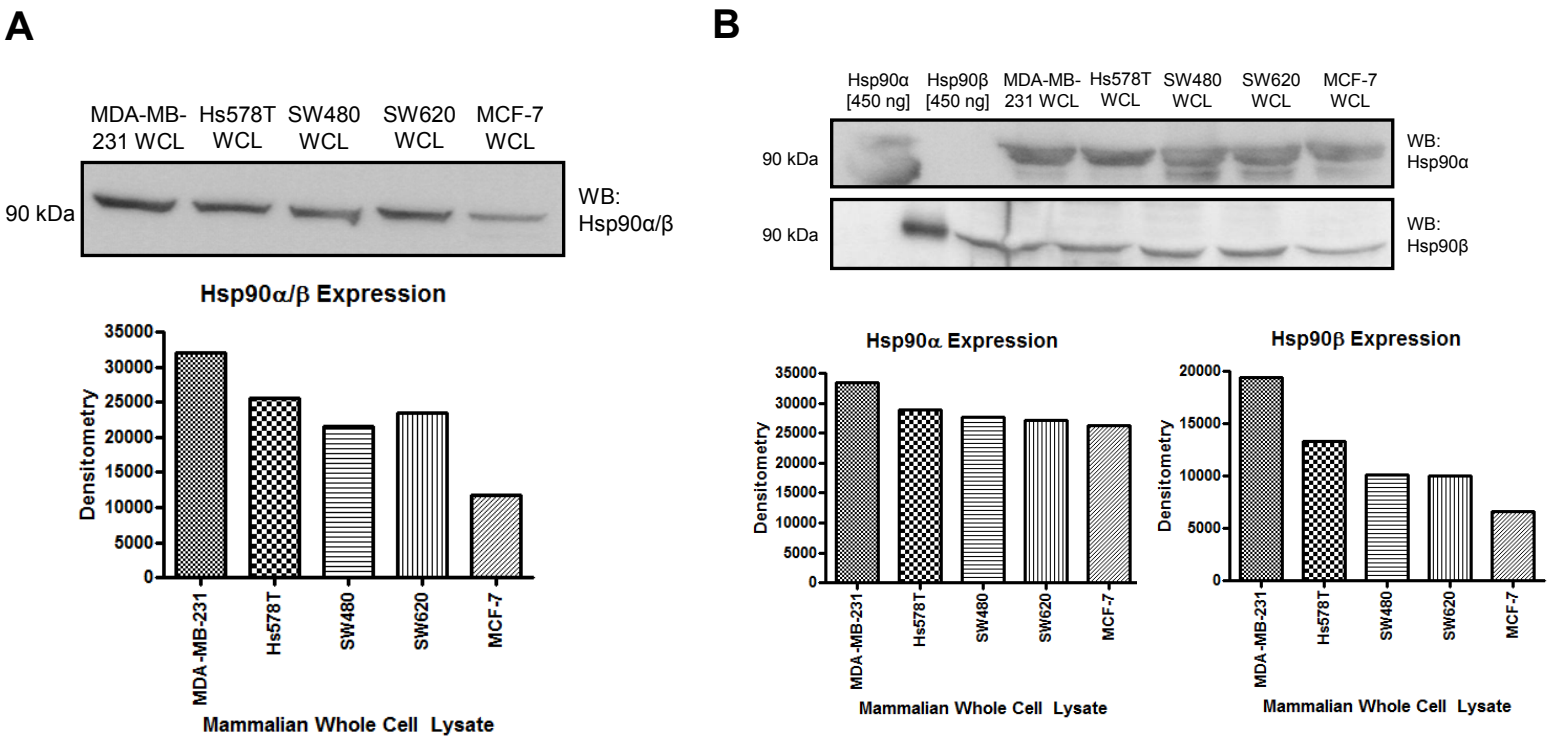

Figure 4 : Comparative expression of Hsp90 in 5 different cancer cell lines.

(**A**) Equal amounts of total protein (50 µg) from whole cell lysates of three breast (MCF-7, MDA-MB-231 and Hs578T) and two colon (SW480 and SW620) cancer cell lines were probed for the presence of Hsp90α/β by Western analysis. The graph (below) illustrates the relative densitometry for each sample determined using ImageJ software. (**B**) Equal amounts of total protein (50 µg) of the same samples were probed for the presence of Hsp90α or Hsp90β. Recombinant Hsp90α (450 ng) and recombinant Hsp90β (450 ng) were loaded as input controls to ensure the specificity of the isoform specific antibodies. Densitometric analysis for each Hsp90 isoform was determined using ImageJ software and is illustrated in the respective graphs.

3.1.2 Subcellular localization of Hsp90α and Hsp90β in a panel of five different cancer cell lines

We next investigated the subcellular distribution of Hsp90α and Hsp90β within the cell by indirect immunofluorescence and confocal microscopy using antibodies specific for each cytosolic Hsp90 isoform (Figure 5). Hsp90α was localized predominantly in the cytoplasm of all the cell lines studied, but was also found at the periphery of membrane protrusions in MDA-MB-231, MCF-7 and Hs578T breast cancer cells (Figure 5A – C, white arrows). Due to the small size of the SW480 and SW620 colon cancer cells, it was not possible to determine whether Hsp90α was localized at the cell periphery. Hsp90β showed a diffuse cytoplasmic staining pattern, was concentrated within punctate structures in the nucleus of all the cell lines, but also appeared to localize at the cell periphery in MDA-MB-231 and Hs578T breast cancer cells, indicated by white arrows (Figure 5A, C). An interesting phenotype was observed in Hs578T cells whereby Hsp90α was localized at the cell periphery and Hsp90β was directly adjacent, indicated by white arrows (Figure 5C). The Hsp90β staining pattern within these cells was also unique in that it appeared to resemble stress fibers that were reminiscent of an actin cytoskeleton staining pattern (Pellegrin and Mellor, 2007) (Figure 5C). These data indicated that the localization of Hsp90α and Hsp90β was distinct for each isoform and varied between cell lines.

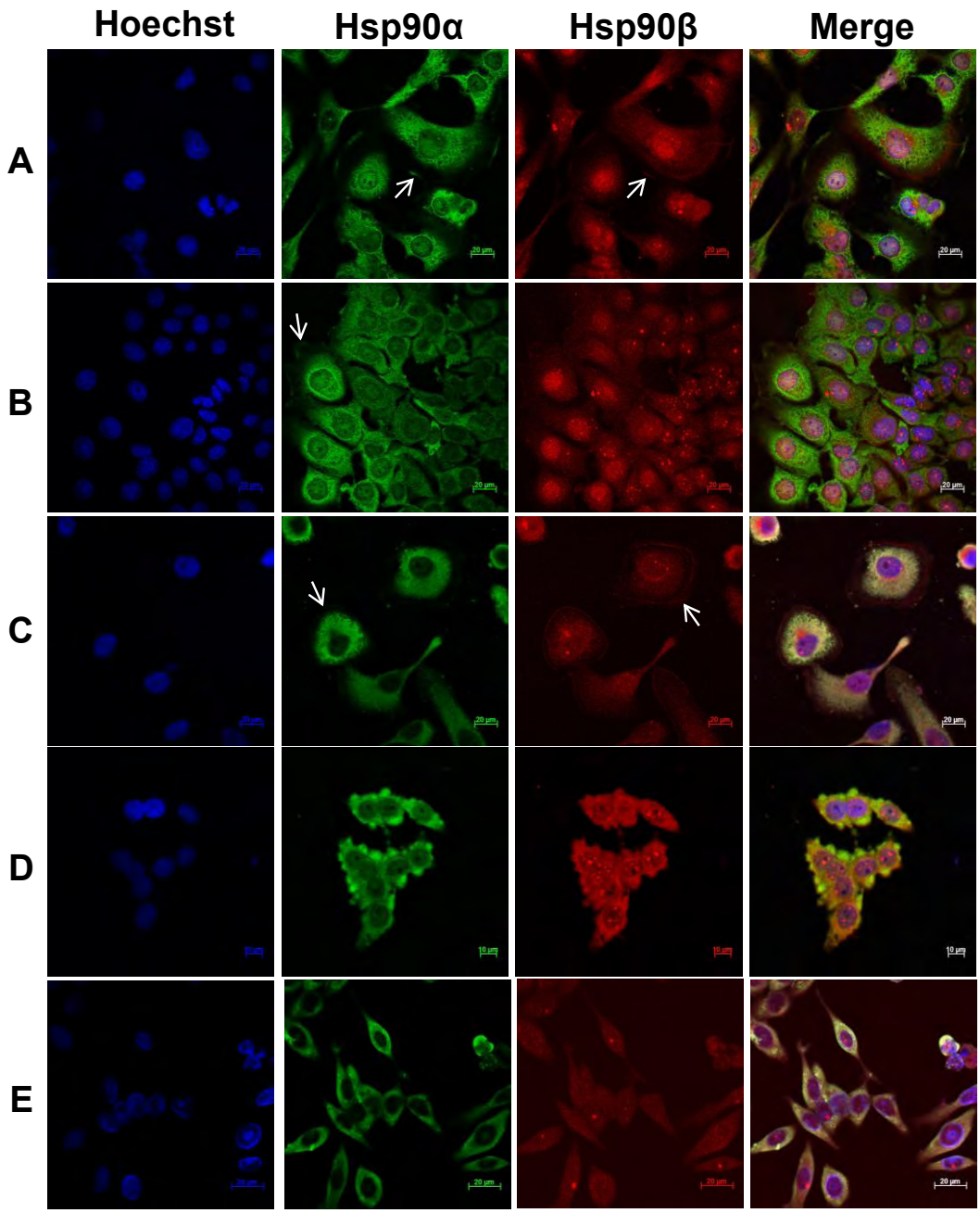

Figure 5: Subcellular localization of Hsp90α and Hsp90β in 5 different cancer cell lines suggested the presence of Hsp90 on the plasma membrane surface.

MDA-MB-231 (**A**), MCF-7 (**B**), Hs578T (**C**), SW480 (**D**) and SW620 (**E**) cells were seeded on fibronectin (5 µg/ml) overnight, fixed with methanol and incubated with mouse anti-Hsp90α and rabbit anti-Hsp90β primary antibodies followed by donkey anti-mouse Alexa-Fluor-488 (green) and donkey anti-rabbit Alexa-Fluor-555 (red) secondary antibodies. Nuclei were stained with 1 µg/ml Hoechst 33342 (blue). Images were captured using the Zeiss LSM 510 Meta laser scanning confocal microscope 40x oil objective and analysed using AxiovisionLE 4.7.1 (Zeiss, Germany). Scale bars represent 20 µm. White arrows illustrate points of putative plasma membrane localization. Data are representative of triplicate images obtained from three independent experiments showing similar results.

3.1.3 Isolation of extracellular Hsp90 by cell surface biotinylation and streptavidin affinity chromatography

Indirect immunofluorescence suggested that Hsp90 was localized at the cell periphery, particularly at regions of membrane protrusion. To investigate whether Hsp90 was extracellular, we used a combination of biotin-labeling followed by biotin-streptavidin affinity chromatography to purify the extracellular Hsp90 species. This method takes advantage of the highly selective and strong association exhibited between biotin and streptavidin; one of the strongest specific interactions known to date (Weber *et al.*, 1989). The biotin molecule contains a cell-impermeable NHS-moiety which is capable of covalently binding lysine residues of any protein within interacting range. This feature was exploited to label the lysine residues of Hsp90, such that only the extracellular species would appear in the affinity purified fractions. To prevent the NHS-biotin from being internalized by the cell which would result in biotinylation of intracellular proteins, incubation with biotin was limited to 30 minutes at 4°C (Sottile and Chandler, 2005).

Western analysis revealed that extracellular Hsp90 was observed in the affinity purified fractions of all five cell lines (Figure 6A). These fractions were compared to their respective whole cell lysates where equal amounts of total protein were loaded. In all samples, the amount of Hsp90 isolated in the biotinylated fraction was lower than compared to the whole cell lysates (Figure 6A), suggesting that only a portion of the total Hsp90 complement exists on the extracellular surface of the membrane.

To confirm that the biotinylated Hsp90 was extracellular, we attempted to cleave surface-bound Hsp90 using trypsin, a serine protease that digests proteins at the carboxyl end of lysines and arginines (Huber and Bode, 1978). Trypsin digestion should have theoretically cleaved the biotin-labeled Hsp90 from the surface of the membrane, reducing the levels of Hsp90 observed in the affinity purified fractions. On comparison with the untreated fractions, the samples exposed to trypsin resulted in an almost complete loss in biotinylated Hsp90 (Figure 6A). Interestingly, the affinity purified Hsp90 in MCF-7 cells appeared to be more resistant to trypsin digestion when compared to the

remaining cell lines studied (Figure 6A). To ensure the specificity of the streptavidin-affinity purifications, non-biotinylated cells were processed in the same manner and probed for Hsp90 by Western analysis (Figure 6B). Hsp90 was not observed in affinity purified fractions of non-biotinylated cells, indicating that the streptavidin-agarose beads were highly selective for biotin and did not interact non-specifically with Hsp90 (Figure 6B). Collectively, these data confirmed that at least a portion of the cytosolic Hsp90 complement was extracellular in the five cancer cell lines studied.

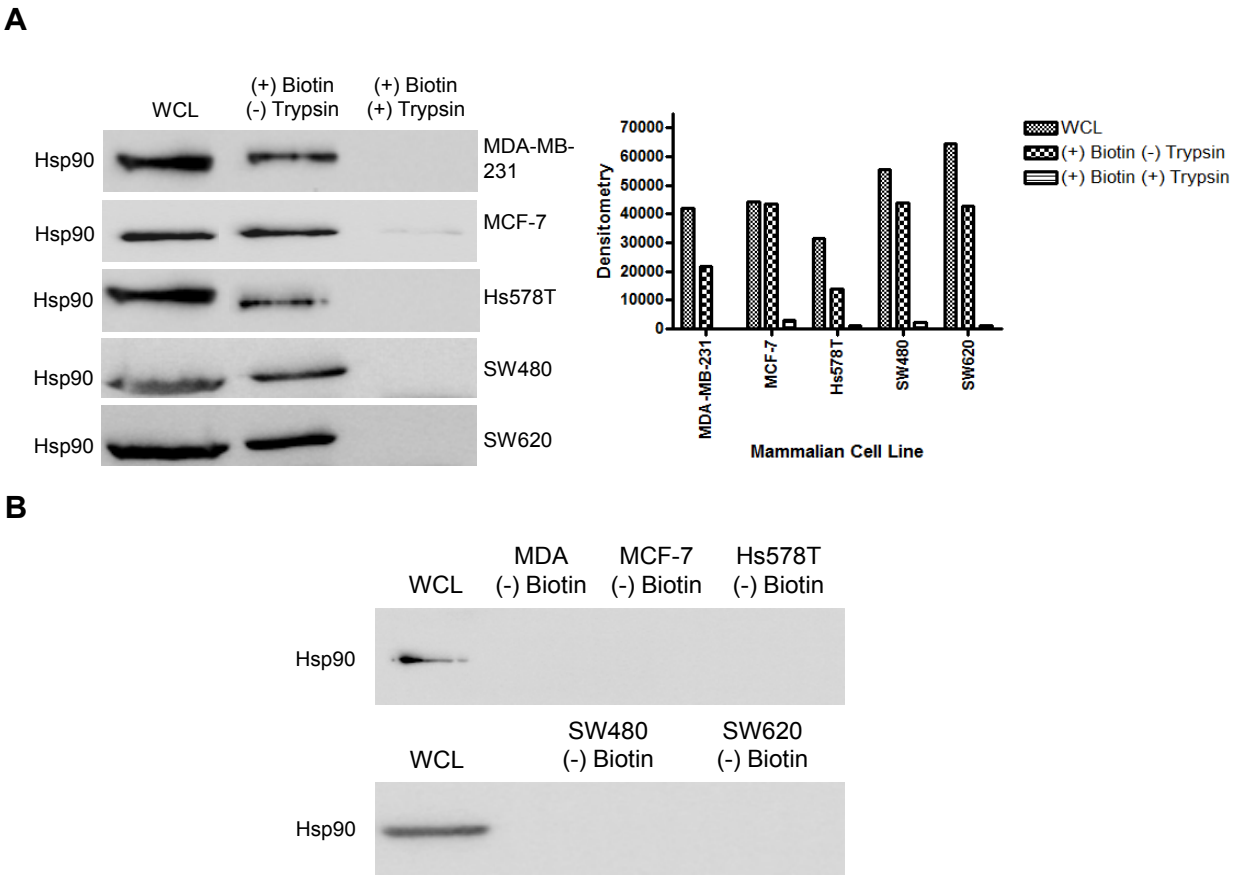

Figure 6: Surface biotinylation showed the presence of Hsp90 on the surface of cancer cell lines.

(**A**) Two confluent flasks of each cell line were incubated with NHS-biotin (1 mg/ml) for 30 minutes at 4°C. Unbound NHS-biotin was removed by washing twice with PBS. Cells in one flask were lysed directly into RIPA buffer while the cells in the remaining flask were lifted by trypsin digestion and washed twice in PBS before lysis in RIPA buffer. The cell supernatants were incubated with streptavidin-agarose beads for 1 hour at 4°C with gentle agitation. The beads were harvested by centrifugation and bound protein denatured from the beads by boiling each sample in 100 µl SDS-PAGE lysis buffer. Equal amounts of protein for each sample were probed for the presence of Hsp90α/β by Western analysis. Whole cell lysates (WCL) were run alongside each sample as a reference. The graph (right) represents the associated densitometry determined using ImageJ software. (**B**) Confluent flasks of each cell line were incubated at 4°C for 30 minutes in the absence of NHS-biotin, washed twice with 1 x PBS and lysed in RIPA buffer. The cell supernatants were subjected to the same treatments as previously described and each sample analysed for the presence of Hsp90α/β by western analysis. A whole cell lysate (WCL) was run alongside as a reference. Data are representative of three independent experiments with similar results.

3.1.4 Detection of extracellular soluble Hsp90α by an enzyme-linked immunosorbent assay (ELISA)

To determine whether an extracellular soluble Hsp90 pool existed, we measured the levels of secreted Hsp90 using a sandwich ELISA against Hsp90α (Figure 7). The ELISA kit used consisted of a 96-well immunoassay plate to which an anti-Hsp90α antibody was bound. This allowed any Hsp90α to be isolated from the cell culture supernatant of the cell lines studied. Following vigorous washing to remove unbound proteins, the Hsp90α bound to the immunoassay plate was detected with a biotinylated anti-Hsp90α antibody. The biotinylated antibody was subsequently detected with streptavidin conjugated horseradish peroxidase (HRP) and a colour change was quantified following the addition of TMB substrate.

The absorbance values at 450 nm were compared to the Hsp90α standard curve, which consisted of an assay range of 0.5 – 32 ng/ml (0, 0.5, 1, 2, 4, 8, 16 and 32 ng/ml). The standard curve obtained was considered acceptable with a correlation coefficient of 0.99 (Figure 7A). Using the linear equation calculated for the standard curve, we determined that all four cell lines secreted Hsp90α into the cell culture supernatant. More specifically, the colon cancer cell lines (SW480 and SW620) secreted the highest levels of Hsp90α of approximately 2 – 2.5 ng/ml. MDA-MB-231 and MCF-7 breast cancer cells appeared to secret moderate levels of Hsp90α ranging from 1 – 1.5 ng/ml. With an established role for extracellular Hsp90 in cell migration, we attempted to investigate the effect of untreated cells against those treated with SDF-1α, a pro-motility chemokine, on the levels of Hsp90α secreted. The effect of the SDF-1α treatment did not have any significant effect ($p > 0.05$) on the levels of extracellular Hsp90α in any of the cell lines studied (Figure 7B).

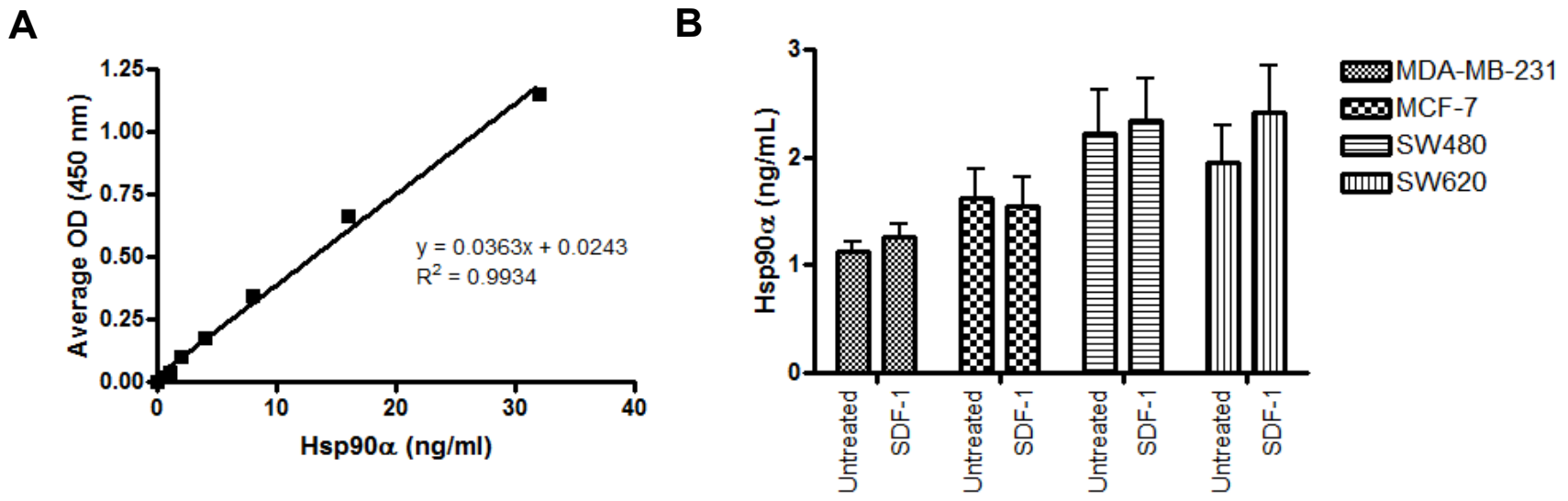

Figure 7: Hsp90α enzyme-linked immunosorbent assay (ELISA) showed the presence of Hsp90α in the cell culture supernatant of cancer cell lines.

(**A**) Purified Hsp90α was diluted to include an assay range of 0.5 – 32 ng/ml (0, 0.5, 1, 2, 4, 8, 16 and 32 ng/ml). The absorbance at 450 nm was determined and a linear curve (with the associated linear equation) was generated as a standard to compare all treatments. (**B**) Cells were seeded at a density of 1 x 10^5 cells/ml and allowed to adhere overnight at 37°C. The following day, the cells either remained untreated or were treated with SDF-1α (100 ng/ml) for 5 hours at 37°C after which the cell culture supernatant was cleared by centrifugation and analysed using the Hsp90α ELISA kit at an absorbance of 450 nm. Statistical significance was determined using a one-way ANOVA. Data are representative of three independent experiments performed in duplicate.

3.1.5 Crosslinking and identification of extracellular Hsp90 complexes in MDA-MB-231 breast cancer cells

Based on the data obtained from the prior experiments, we decided to investigate the extracellular Hsp90 client proteome of MDA-MB-231 breast cancer cells. The rationale for this decision was based on the high Hsp90 expression levels (Figure 4), distinct membrane localization of both Hsp90α and Hsp90β (Figure 5A), the isolation of extracellular Hsp90 by surface biotinylation (Figure 6A) and the moderate Hsp90 concentrations present in the cell culture supernatant (Figure 7B), all of which suggested that a portion of Hsp90 was extracellular in these cell lines.

The cell-impermeable, homo-bifunctional, cleavable crosslinker, DTSSP (3,3'-dithiobis[sulfosuccinimidyl]propionate) was used to covalently crosslink proteins in the plasma membrane. This crosslinker possesses an NHS-moiety on either end capable of covalently binding the lysine residues of any proteins within 12Å of each other (Keselowsky and García, 2004). Once covalently crosslinked, any complexes containing Hsp90 were purified by immunoprecipitation using an anti-Hsp90α/β antibody and subsequently identified using tandem mass spectrometry analysis.

Immunoprecipitated Hsp90-containing complexes were resolved on an 8% non-reducing SDS-PAGE gel and detected by colloidal Coomassie staining (Figure 8). Four putative Hsp90 complexes were identified: three higher molecular weight complexes (labeled B – D) and one band (labeled A) at the subunit molecular weight of Hsp90 (Figure 8A). The four bands (labeled A – D) were excised from the gel and analysed by tandem mass spectrometry (MS/MS) at the University of the Free State. Hsp90 was detected in all four samples, suggesting that the crosslinking and immunoprecipitation were successful in isolating Hsp90-containing complexes. Band D showed the presence of the human extracellular matrix protein, fibronectin, with a total of 19 query matches and a relative abundance index (emPAI) of 0.23 (Figure 8B). Both Hsp90α and Hsp90β were reported in the MS/MS analysis for band D, but Hsp90β showed a more favourable number of query matches (19) and possessed a higher relative abundance

index (0.8) as opposed to the 10 query matches and emPAI score of 0.34 reported for Hsp90α (Figure 8B). According to the MASCOT software used to analyse the MS/MS data, any protein score above 35 showed a significant association. All the hits listed were above this threshold value.

The crosslinker, DTSSP, consists of a disulphide linkage that can be cleaved in the presence of a reducing agent such as β-mercaptoethanol or DTT. Theoretically, this should release the proteins from the complex and allow detection of each protein at its subunit molecular weight. Consequently, a fraction of the immunoprecipitated complexes were treated with 5% β-mercaptoethanol (cleaved) while the remainder was left untreated (uncleaved). To verify the presence of fibronectin and Hsp90 in Hsp90-containing complexes isolated from MDA-MB-231 cells, the immunoprecipitated protein complexes were probed with antibodies against fibronectin and Hsp90α/β by Western analysis both in the uncleaved and cleaved forms (Figure 9). Results indicated the presence of Hsp90 in both the uncleaved and cleaved samples (Figure 9A). The uncleaved sample showed Hsp90 at its subunit molecular weight (~90 kDa) and in higher molecular weight complexes. An MDA-MB-231 whole cell lysate was loaded alongside both samples as a reference. Following cleavage of the crosslinker, Hsp90 was no longer observed in higher molecular weight bands, but rather as a single intense band at 90 kDa (Figure 9A), suggesting that the Hsp90 was successfully released from the complexes. A similar result was observed for fibronectin after probing the uncleaved and cleaved samples with an antibody against fibronectin (Figure 9B). In the uncleaved sample, fibronectin was detected in a higher molecular weight complex as well as in a few lower molecular weight bands. However, following cleavage of the crosslinker, fibronectin was only observed as a single band at approximately 220 kDa, the predicted subunit molecular weight of fibronectin. This single band correlated with the recombinant fibronectin input control loaded alongside the cleaved sample (Figure 9B).

A

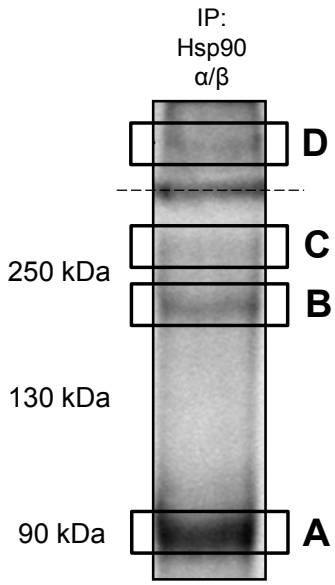

B

Mass Spectrometry Data Summary

Protein	Mass	Protein Score	Queries Matched	emPAI
SAMPLE A				
Human HSP90AB1	83212	728	42	2.09
Human HSP90AA1	84607	399	42	0.62
Human HSP90AB3P	68282	328	40	0.93
SAMPLE B				
Human HSP90AB1	83212	111	10	0.22
Human HSP90AA4P	47682	48	2	0.09
SAMPLE C				
Human HSP90AB1	83212	230	13	0.41
Human HSP90AA1	84607	149	5	0.16
SAMPLE D				
Human HSP90AB1	83212	298	19	0.8
Human FN1	262460	285	21	0.23
Human HSP90AA1	84607	153	10	0.34

Figure 8: Crosslinking of extracellular Hsp90 complexes in MDA-MB-231 breast cancer cells identified the presence of Hsp90β and the extracellular matrix protein, fibronectin.

(**A**) The extracellular proteins of MDA-MB-231 breast cancer cells were crosslinked using a cell-impermeable, cleavable crosslinker, DTSSP (2 mM) for 2 hours at 4°C. The crosslinker was subsequently quenched with 20 mM Tris-HCl (pH 7.5). Cells were lysed in RIPA buffer and complexes containing Hsp90 were isolated by co-immunoprecipitation using an antibody against Hsp90α/β. Crosslinked samples were resolved by non-reducing SDS-PAGE followed by colloidal Coomassie staining. Four bands (labeled A – D) were observed and subsequently analysed by tandem mass spectrometry (MS/MS). The dotted line represents the stacking and resolving gel interface. (**B**) Data summary from the MS/MS analysis indicated the presence of Hsp90α/β (Sample A – D) and human fibronectin (Sample D). The mass refers to the molecular weight of the respective proteins (in Daltons). The queries matched refer to the number of sequences with a direct match to the query protein. The emPAI (exponentially modified protein abundance index) refers to the relative abundance of the query protein in each sample.

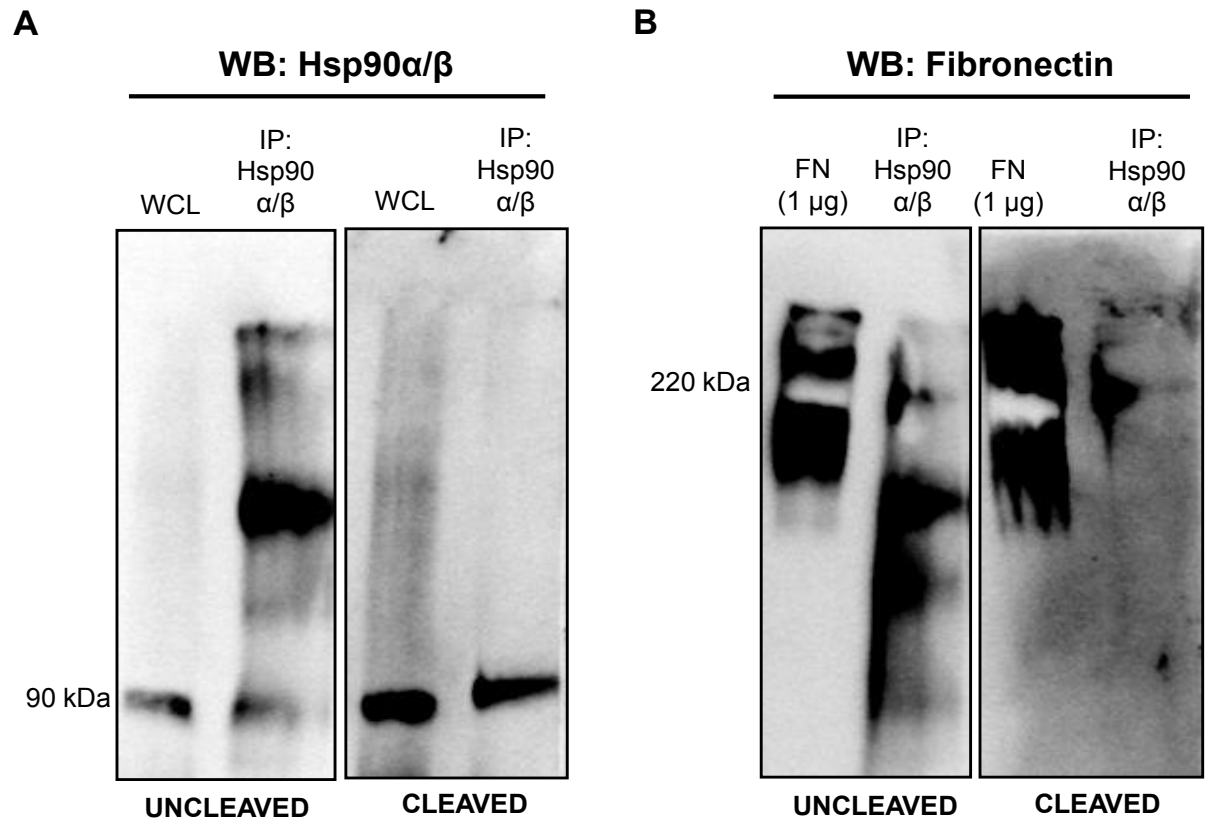

Figure 9: The presence of Hsp90 and fibronectin in an extracellular complex isolated from MDA-MB-231 breast cancer cells.

(A) The immunoprecipitated complexes (IP: Hsp90α/β) were left untreated (uncleaved) or treated with 5% (v/v) β-mercaptoethanol (cleaved) and probed for the presence of Hsp90α/β by Western analysis. An MDA-MB-231 whole cell lysate (WCL) was used as a reference. (B) Both uncleaved and cleaved samples were probed for the presence of fibronectin by Western analysis. Recombinant fibronectin (1 µg) was loaded alongside each sample as a reference.

3.1.6 *In vitro* verification of the putative interaction between Hsp90β and fibronectin

Since the crosslinked Hsp90 immunoprecipitates from MDA-MB-231 cells indicated a putative interaction between Hsp90β and fibronectin, we decided to analyse the interaction both in solution and on a solid surface *in vitro* (Figure 10). Hsp90β was used in subsequent experiments due to the high abundance of this isoform in band D (Figure 8B) as well as the availability of endotoxin-free commercial preparations of the protein.

The interaction between Hsp90β and fibronectin was tested using a pull down assay using the purified proteins. Recombinant Hsp90β (1 µg) was incubated with purified soluble human fibronectin (1 µg) and was allowed to interact for 15 minutes at room temperature. Co-precipitated proteins were isolated using the Dynabeads® Co-Immunoprecipitation Kit which employs a magnetic M-270 Epoxy resin to which any protein or antibody can be covalently coupled. Captured proteins or complexes present on the beads can be isolated by magnetic separation and eluted into a purified fraction. For our purposes, the magnetic Dynabeads® were coupled to an antibody against Hsp90α/β. BSA-coupled Dynabeads® incubated with Hsp90β (1 µg) or fibronectin (1 µg) served as the necessary controls. Recombinant Hsp90β (1 µg) and fibronectin (1 µg) served as input controls for sizing immunoprecipitates. Eluted complexes were separated by SDS-PAGE and analysed by silver staining (Figure 10A) or Western analysis (Figure 10B). When Hsp90β alone was incubated with anti-Hsp90α/β-coupled Dynabeads®, a single band at approximately 90 kDa was observed (Figure 10), suggesting that the immunoprecipitation was successful and specific for Hsp90. When Hsp90β was incubated with fibronectin, a band at the predicted molecular weight of fibronectin (~220 kDa) co-precipitated with Hsp90. This was verified by silver staining (Figure 10A) and Western analysis (Figure 10B). Interestingly, the silver stained SDS-PAGE gel showed, in addition to a 220 kDa band, higher molecular weight bands that did not correlate with the fibronectin input control (Figure 10A). No protein was detected in the immunoprecipitated sample when BSA-coupled Dynabeads® were incubated with Hsp90β or fibronectin. As a further control, we confirmed that anti-Hsp90α/β coupled Dynabeads® incubated with fibronectin did not pull down any protein (*data not shown*).

The interaction was further confirmed using surface plasmon resonance (SPR) spectroscopy. Recombinant fibronectin was immobilized to a CM5 sensor chip using combination of 1-ethyl-3-(3 dimethyl-aminopropyl)carbodiimide hydrochloride (EDC) and N-hydroxysuccinimide (NHS). Hsp90β (1 μM) was passed over the surface of the chip in the presence and absence of excess ATP (1 mM) at a standard flow rate of 5 μl/min. In the presence of ATP, a gradual on-rate was observed followed by a significant drop and gradual dissociation during the post-injection delay (Figure 10C). This interaction was not observed in the absence of ATP and the sensogram dipped below the baseline. ATP (1 mM) alone showed no binding to the chip and was subtracted from all treatments indicated (Figure 10C).

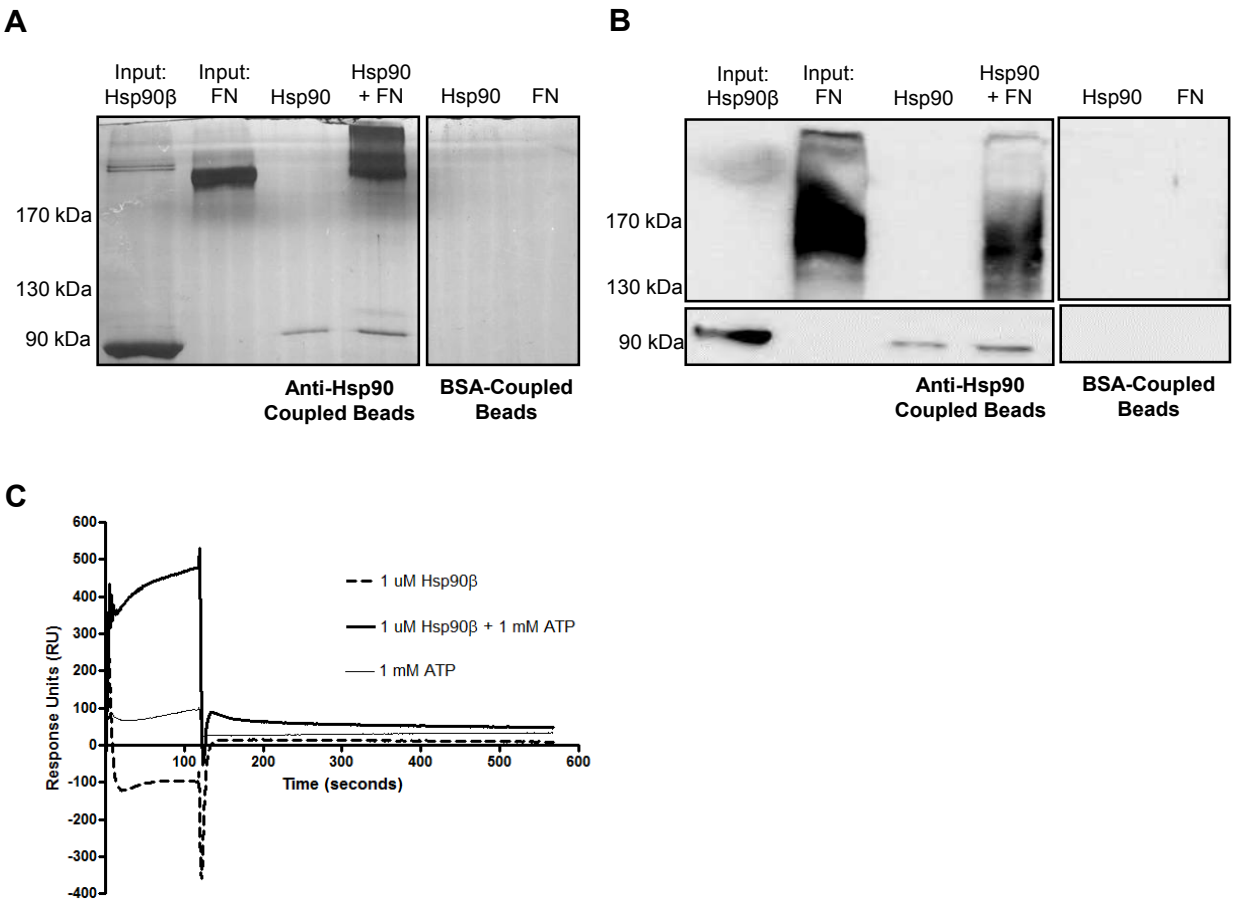

Figure 10: In vitro studies of the putative interaction between Hsp90β and fibronectin in solution and on a solid surface.

(**A**) Mouse anti-Hsp90α/β was covalently coupled to magnetic Dynabeads and incubated with 1 µg recombinant Hsp90β for 15 minutes to allow binding. The bound beads were incubated with 1 µg soluble fibronectin for 15 minutes, washed and immunoprecipitates eluted. BSA-coupled Dynabeads incubated with 1 µg recombinant Hsp90β or 1 µg fibronectin served as negative controls. Recombinant Hsp90β (1 µg) and fibronectin (1 µg) were loaded as input controls. Co-immunoprecipitated samples were separated by SDS-PAGE and analysed by silver staining. (**B**) The same samples were probed for the presence of fibronectin (upper panel) and Hsp90α/β (lower panel) by Western analysis. These data are representative of 2 independent experiments with similar results. (**C**) The Hsp90-fibronectin interaction was analysed by surface plasmon resonance spectroscopy (SPR). Recombinant human fibronectin was immobilized to a primed CM5 sensor chip (GE Healthcare, Sweden) and recombinant Hsp90β (1 µM) was passed over the surface in the presence and absence of 1 mM ATP. A standard flow rate of 5 µl/min with a 200 second post-injection delay was employed. Data are representative of three independent experiments with similar results.

3.1.7 Screening cancer cell lines for endogenous fibronectin expression

Six cancer cell lines, including MDA-MB-231, MCF-7, Hs578T, HeLa, THP1 and U937 cells, were screened for levels of endogenous fibronectin expression (Figure 11). Equal amounts of total protein from whole cell lysates were probed with an antibody against human fibronectin by Western analysis. The greatest proportion of endogenous fibronectin was detected in Hs578T breast cancer cells, which are epithelial cells that have been characterized as fibroblast-like (Sørlie *et al.*, 2001). Lower levels of fibronectin were detected in the remaining whole cell lysates compared to the Hs578T cell line (Figure 11A). In addition to the Western analysis, the morphology of fibronectin within MDA-MB-231, MCF-7 and Hs578T breast cancer cells was determined by confocal microscopy (Figure 11B). In support of the results from the Western analysis, Hs578T cells expressed high levels of endogenous fibronectin that was incorporated into an extracellular mesh or network. MDA-MB-231 and MCF-7 cells expressed considerably lower levels of fibronectin, with no extracellular fibronectin observed in MCF-7 cells. Although considerably lower, MDA-MB-231 cells still contained a portion of fibronectin that was incorporated into extracellular fibrils. The morphology, however, was different to that observed in Hs578T cells with the extracellular fibronectin being observed as single, separated fibrils as opposed to a fibrous network (Figure 11B). Based on these data, we decided to conduct further experiments using the Hs578T breast cancer cell line as opposed to MDA-MB-231 cells.

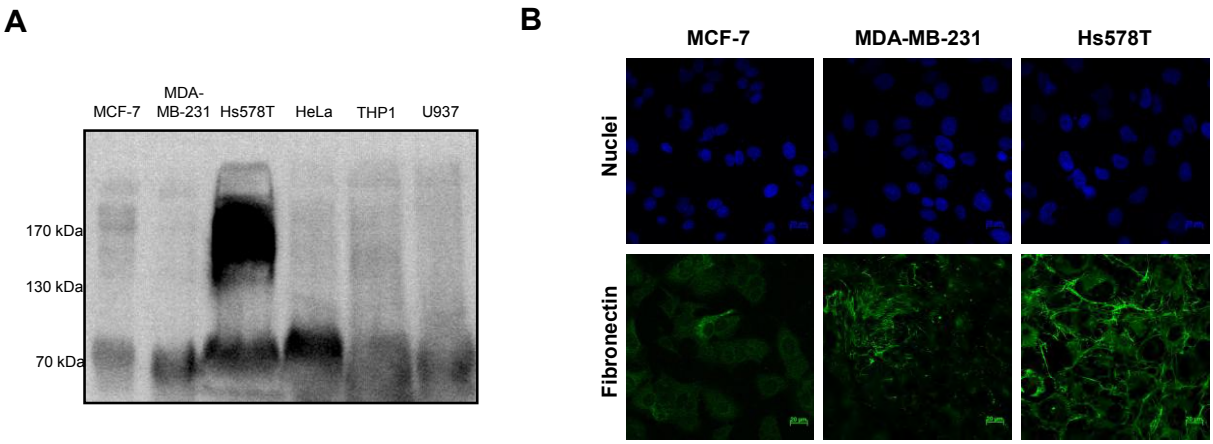

Figure 11: Hs578T breast cancer cells express the highest level of endogenous fibronectin in comparison to other cancerous cell lines.

(A) Equal amounts of total protein from whole cell lysates of three breast (MCF-7, MDA-MB-231, Hs578T), one cervical (HeLa) and two leukemic (THP1, U937) cancer cell lines were probed for the levels of endogenous fibronectin by Western analysis using a primary antibody against human fibronectin. (B) The relative proportion and morphology of endogenous fibronectin was also analysed by confocal microscopy. Cells were seeded onto sterile glass coverslips and fibronectin detected using a mouse anti-fibronectin primary antibody (1:100) followed by an anti-mouse Alexa-Fluor-488 secondary antibody (1:500, green). Nuclei were stained with 1 µg/ml Hoechst 33342 (blue). Images were captured using the Zeiss LSM 510 Meta laser scanning confocal microscope 40x oil objective and analysed using AxiovisionLE 4.7.1 (Zeiss, Germany). Scale bars represent 20 µm.

3.1.8 Determining whether fibronectin stability was dependent on Hsp90 activity in Hs578T cells

We next investigated whether the levels of fibronectin in Hs578T cells were sensitive to Hsp90 inhibition, suggestive of a dependency on Hsp90 activity. We determined the half maximal inhibitory concentration (IC_{50}) values in Hs578T cells of two commonly used Hsp90 inhibitors, geldanamycin and novobiocin, using the WST-1 cytotoxicity assay. Cells were incubated with each inhibitor at a range of concentrations for a period of 72 hours prior to assessing cell viability using WST-1 reagent. This assay determines cell viability by measuring the metabolic reduction of WST-1 to a soluble formazan salt that can be measured colorimetrically at 450 nm. Untreated cells were used as a reference for 100% cell viability and the IC_{50} values were determined using a non-linear regression equation determined for each kill curve using GraphPad Prism 4 software. The IC_{50} values in Hs578T cells were determined as 6200 nM and 1750 μM for geldanamycin and novobiocin respectively (Figure 12A and B). Based on these values, Hs578T cells were treated with increasing doses below the calculated IC_{50} values of geldanamycin (500 nM, 2000 nM, and 4000 nM) or novobiocin (250 μM, 750 μM and 1500 μM) for 16 hours. The effect of Hsp90 inhibition on fibronectin levels was quantified by Western analysis using histone H3 as a loading control. A dose-dependent decrease in fibronectin levels was observed for both geldanamycin and novobiocin treatments. Fibronectin, however, appeared to be more sensitive to novobiocin with a more significant decrease ($p < 0.01$) in total fibronectin relative to untreated cells (Figure 12C). Collectively, these data suggested that fibronectin stability in Hs578T cells was dependent on Hsp90 activity.

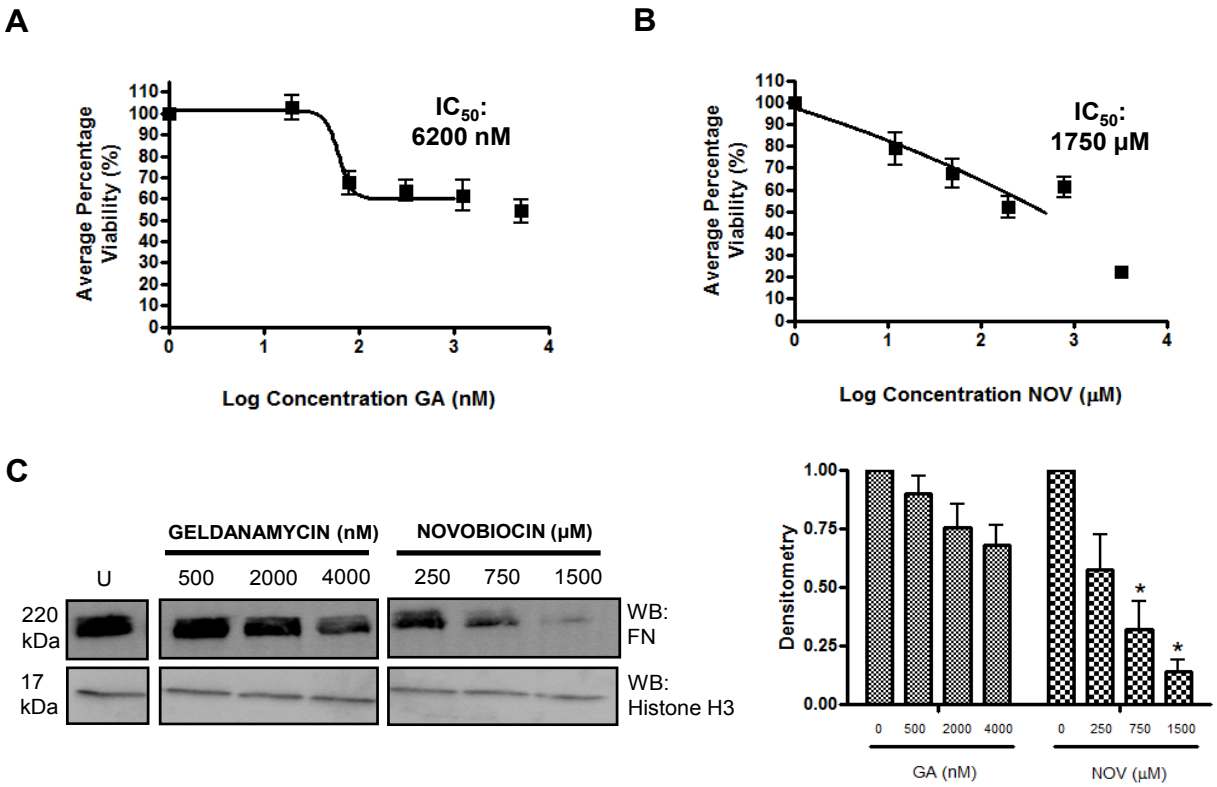

Figure 12: Fibronectin levels were reduced upon Hsp90 inhibition in Hs578T breast cancer cells.

The cytotoxicity of the Hsp90 small-molecule inhibitors, geldanamycin (**A**) and novobiocin (**B**), was determined for Hs578T cells using WST-1 cell proliferation reagent. Cells were seeded into a 96-well plate and incubated with increasing doses of geldanamycin (GA: 0 nM – 5000 nM) or novobiocin (NOV: 0 µM – 3125 µM) for 72 hours. Treated cells were incubated with WST-1 reagent for 4 hours and the reading at 440 nm was recorded. Data was averaged over 5 independent experiments and the half maximal inhibitory concentration (IC_{50}) was determined for each experiment using GraphPad Prism 4 software. (**C**) To test the effect of Hsp90 inhibition on the proportion of total fibronectin, cells were treated with increasing doses of geldanamycin (500 nM, 2000 nM, 4000 nM) or novobiocin (250 µM, 750 µM, 1500 µM). Cells were lysed and equal amounts of total cell protein were detected with mouse anti-fibronectin by Western analysis. The same blots were probed for Histone H3 to serve as a loading control. The graph (alongside) illustrates the average densitometry for triplicate experiments determined using ImageJ software. Statistical significance was determined using a one-way ANOVA (* = $p < 0.01$). Data are representative of three independent experiments with similar results.

3.1.9 Validation of the deoxycholate (DOC) biochemical assay for quantifying fibronectin matrix assembly

Brenner and colleagues (2000) have demonstrated a method that used deoxycholate to fractionate the soluble and insoluble fibronectin of cells. Deoxycholate is an ionic detergent in which the extracellular, insoluble fibronectin remains insoluble as a pellet and the intracellular, soluble fibronectin is separated in solution. The same authors exploited this assay to report that fibronectin matrix formation was dependent on Ras-signaling (Brenner *et al.*, 2000). As a means to validate this assay in our cell line, we treated Hs578T cells with an increasing dose of the MEK1/2 inhibitor, U1026. MEK1/2 is a signaling molecule downstream of Ras (Seger and Krebs, 1995) and should theoretically affect the levels of soluble and insoluble fibronectin.

Western analysis to detect fibronectin in untreated or U1026-treated Hs578T cells revealed a dose-dependent decrease in the proportion of soluble and insoluble fibronectin with increasing doses of U1026 (5 μM, 50 μM and 100 μM). While there was an initial increase in fibronectin levels after treatment with 5 μM U1026, there was a dose-dependent decrease in the insoluble/soluble fibronectin ratio in treated cells (Figure 13A). To ensure that there was no cross-contamination between the soluble and insoluble fibronectin fractions, the levels of GAPDH in the same samples were determined by Western analysis. Results showed that GAPDH was only present in the soluble fraction (Figure 13A). Changes in the morphology of fibronectin after treatment with U1026 were also analysed by confocal microscopy and showed a less dense matrix with a reduction in the mesh-like phenotype compared to untreated cells (Figure 13B). In order to quantify any changes observed, ImageJ was used to calculate the mean gray value for each field of view (depicted as the number at the bottom of each frame).

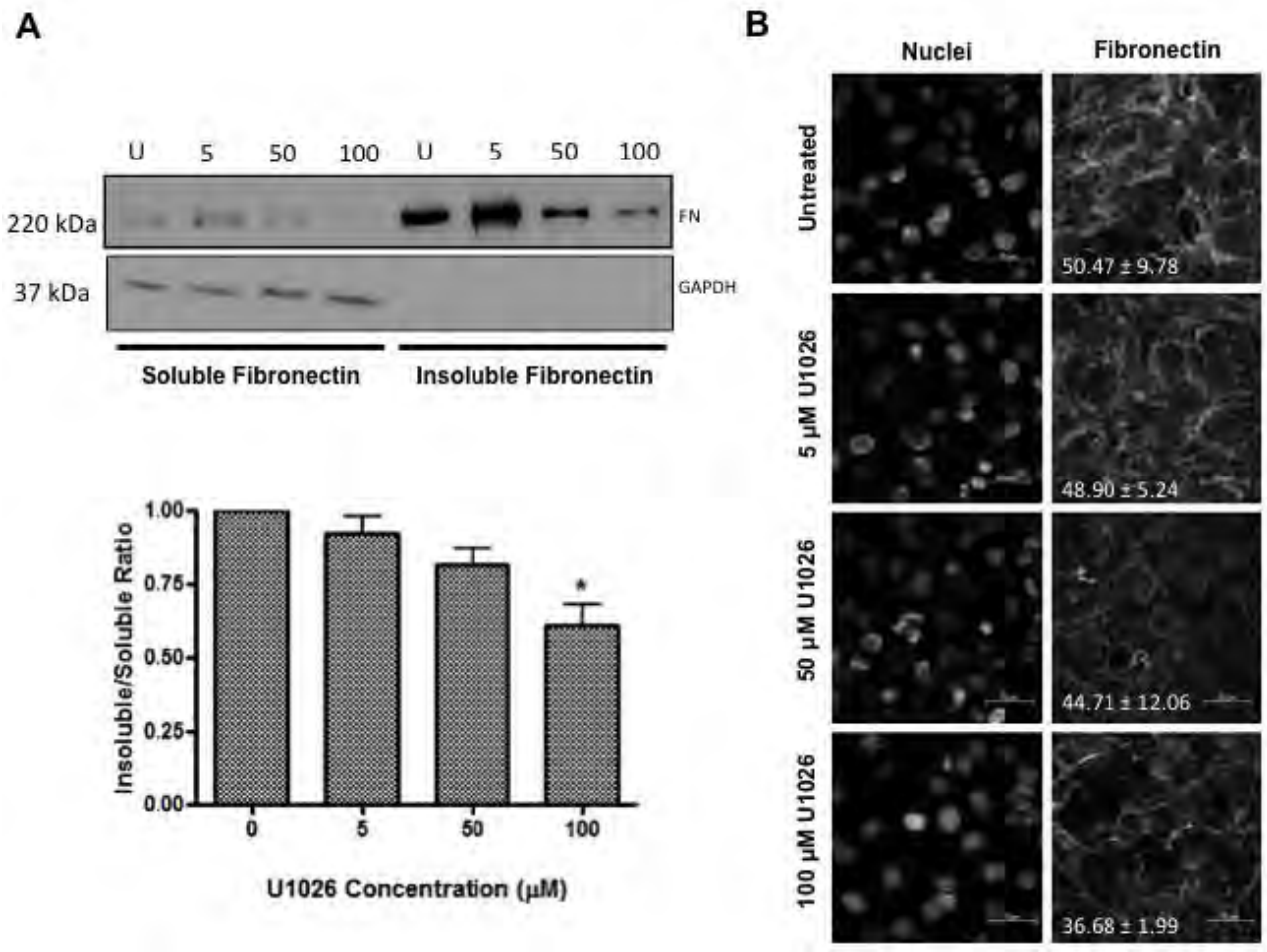

Figure 13: Validation of the deoxycholate (DOC) assay to quantitate fibronectin matrix assembly in Hs578T breast cancer cells.

(**A**) Confluent Hs578T cells were incubated with increasing doses of the MEK1/2 inhibitor, U1026 (5 μM, 50 μM and 100 μM), for 16 hours at 37°C. Cells were lysed and the soluble and insoluble fibronectin fractions were separated using the DOC assay described in the methodology (Brenner *et al.*, 2000). The levels of soluble and insoluble fibronectin (FN) for each treatment were determined by Western analysis using an antibody against fibronectin. To ensure there was no contamination between the soluble and insoluble fractions, the same samples were tested for GAPDH by Western analysis. Equal amounts of protein were loaded for each sample as determined by spectrometric absorbance at 280 nm. The graph illustrates the densitometric ratio of insoluble to soluble fibronectin determined using ImageJ software. Statistical significance was determined using a one-way ANOVA ($p < 0.05$) (**B**) Confocal microscopy was used to observe changes in the fibronectin morphology in Hs578T cells following treatment with the same doses of U1026. Fibronectin was detected using a mouse anti-fibronectin primary antibody and donkey anti-mouse Alexa-Fluor-488 secondary antibody. Nuclei were stained with 1 μg/ml Hoechst 33342. Images were captured using the Zeiss LSM 510 Meta laser scanning confocal microscope 40x oil objective and analysed using AxiovisionLE 4.7.1 (Zeiss, Germany). Three images were captured for each treatment in areas where similar cell numbers were observed. Scale bars represent 20 μm. Values (in white) at the bottom of each frame represent the mean gray values (± standard deviation) for each treatment. Data are representative of triplicate images of three independent experiments showing similar results.

The mean gray value can be defined as the proportion of gray/white pixels relative to the total number of pixels in each frame, essentially giving an indication of the signal detected for each treatment. In response to the U1026 treatment, the mean gray value decreased in a dose-dependent manner from 50.47 ± 9.78 to 36.68 ± 1.99, suggesting a decrease in the fibronectin signal observed and corroborating the results observed by Western analysis. The nuclei panel was included to show that the change in the fibronectin matrix was not a result of a change in the number of cells.

3.1.10 Effect of exogenous Hsp90β on the proportion of soluble and insoluble fibronectin in Hs578T cells

Next we investigated the effect of addition of exogenous purified Hsp90β (50 ng/ml, 100 ng/ml and 1000 ng/ml) on the proportion of soluble and insoluble fibronectin in Hs578T cells (Figure 14). Exogenous bovine serum albumin (BSA) and exogenous fibronectin were added to cells at the same concentrations and used as negative and positive controls respectively. Cells were treated for 16 hours before harvesting as per the DOC assay (Brenner *et al.*, 2000). Western analysis showed that BSA did not have any considerable or dose-dependent effect on the insoluble/soluble fibronectin ratio relative to untreated cells. While exogenous fibronectin appeared to show a random trend, the insoluble/soluble fibronectin ratio was still considerably higher in comparison to the untreated cells. The most significant increase in the insoluble/soluble fibronectin ratio was observed in a dose-dependent manner when cells were treated with increasing concentrations of Hsp90β (Figure 14). In particular, at 500 ng/ml and 1000 ng/ml, Hsp90β increased the insoluble/soluble fibronectin ratio significantly relative to exogenous BSA and fibronectin at the same concentrations (Figure 14). The effect of these treatments on the fibronectin morphology was analysed by confocal microscopy (Figure 15).

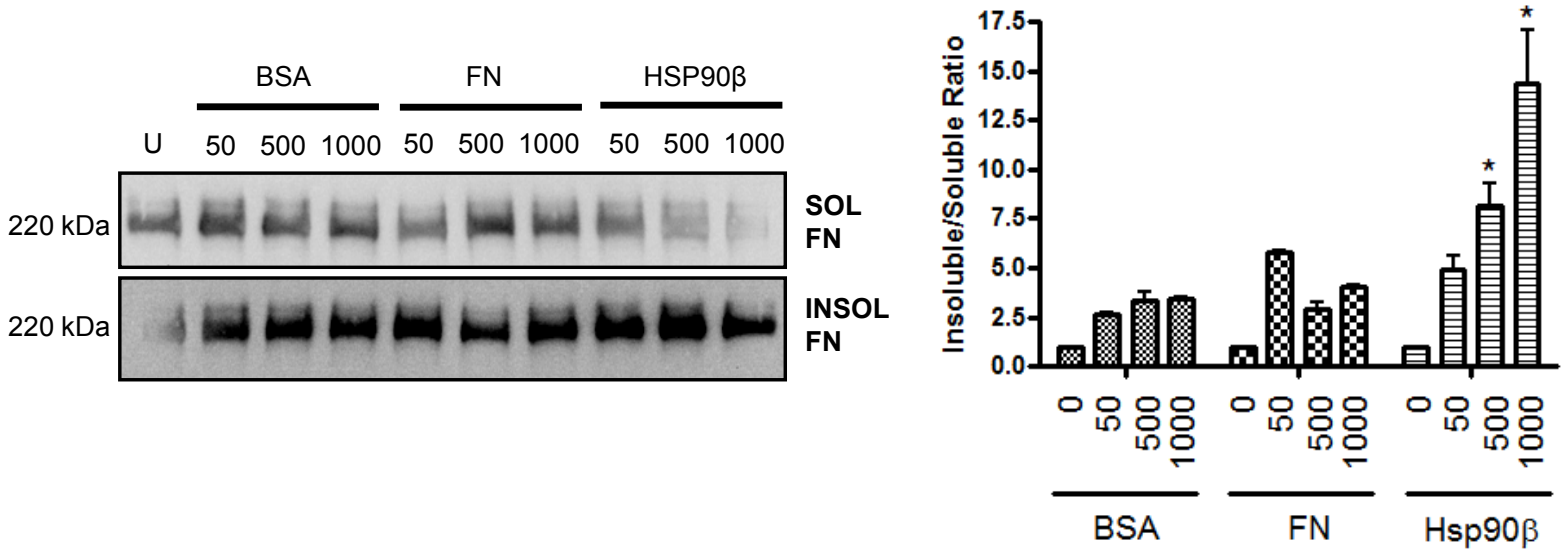

Figure 14: Exogenous Hsp90β increased the levels of insoluble fibronectin in Hs578T breast cancer cells.

Confluent Hs578T cells were incubated with bovine serum albumin (BSA), purified fibronectin or recombinant endotoxin-free Hsp90β at increasing concentrations of 50 ng/ml, 500 ng/ml and 1000 ng/ml. Following 16 hours incubation, cells were harvested using the DOC assay (Brenner *et al.*, 2000) and levels of soluble and insoluble fibronectin detected by Western analysis using an antibody against fibronectin. Equal amounts of protein were loaded for each sample as determined by spectrometric absorbance at 280 nm. The densitometry for each sample was determined using ImageJ and compared to the untreated (U) control. The graph illustrates the average relative proportion of insoluble to soluble fibronectin from triplicate experiments determined using ImageJ software. Statistical significance was determined using a one-way ANOVA ($p < 0.01$). Data are representative of three independent experiments with similar results.

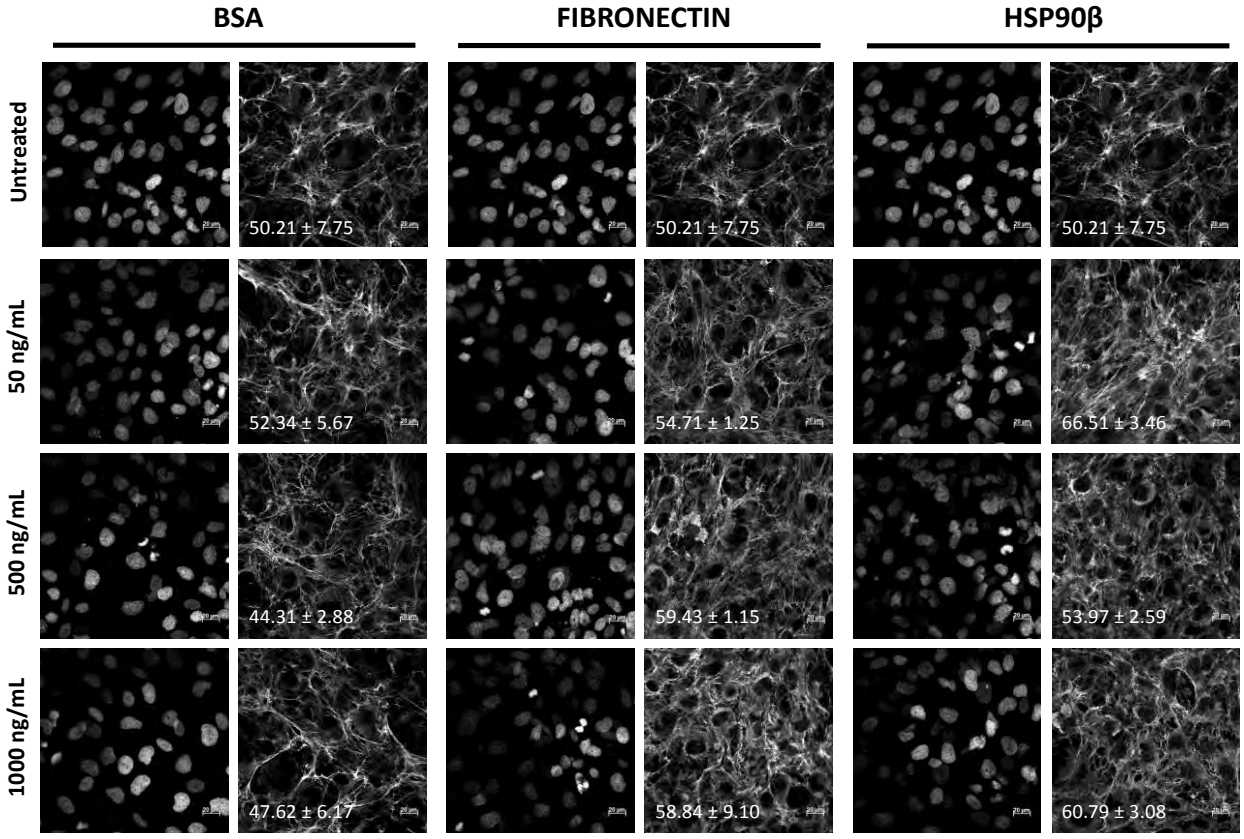

Figure 15: Exogenous Hsp90β increased the levels of extracellular fibronectin matrix in Hs578T breast cancer cells.

Hs578T cells were seeded onto sterile glass coverslips and incubated with bovine serum albumin (BSA), purified fibronectin or recombinant endotoxin-free Hsp90β for 16 hours at increasing concentrations of 50 ng/ml, 500 ng/ml and 1000 ng/ml. Fibronectin was detected using a mouse anti-fibronectin primary antibody followed by a donkey anti-mouse Alexa-Fluor-488 secondary antibody. Nuclei were stained with 1 µg/ml Hoechst 33342. Images were captured using the Zeiss LSM 510 Meta laser scanning confocal microscope 40x oil objective and analysed using AxiovisionLE 4.7.1 (Zeiss, Germany). Three images were captured for each treatment in areas where similar cell numbers were observed. Scale bars represent 20 µm. Values (in white) at the bottom of each frame represent the mean gray values (± standard deviation) for each treatment. Data are representative of triplicate images from three independent experiments showing similar results.

Exogenous BSA appeared to have no observable effect on the fibronectin matrix regardless of the concentration added to the cells. This was reflected by the mean gray values which showed no considerable increase or decrease in the fibronectin matrix (mean gray value of 47.62 ± 6.17 at the highest concentration compared to 50.21± 7.75 in untreated cells). In contrast, exogenous fibronectin and Hsp90β appeared to increase the proportion of extracellular fibronectin observed relative to untreated cells (Figure 15). This increase was quantified using the mean gray value which reported a change from 50.21 ± 7.75 in untreated cells to 58.84 ± 9.10 and 60.79 ± 3.08 for exogenous fibronectin (1000 ng/ml) and Hsp90β (1000 ng/ml) respectively. The nuclei panel was included to show that the increase in the fibronectin matrix was not as a result of a change in the cell number.

3.1.11 Effect of transient siRNA Hsp90 knockdown on the levels of soluble and insoluble fibronectin in Hs578T cells

Since the addition of purified Hsp90β increased the insoluble fibronectin matrix, we investigated whether the transient silencing of Hsp90α or Hsp90β using short interfering RNA (siRNA) would exhibit the opposite phenotype (Figure 16). Cells were transfected for 48 hours with a pool of 4 siRNA oligonucleotides targeted against unique sequences for either Hsp90α or Hsp90β. Cells transfected with a pool of scrambled, non-targeting siRNA oligonucleotides served as a negative control. Equal amounts of total protein from whole cell lysates of transfected cells were probed with antibodies against Hsp90α and Hsp90β by Western analysis. Approximately 30-40% knockdown was achieved for Hsp90α with little to no effect on the levels of Hsp90β. GAPDH was used as a control to ensure equal protein loading (Figure 16A). Soluble and insoluble fibronectin was harvested from transfected cells using the DOC assay (Brenner *et al.*, 2000) and DOC-soluble and DOC-insoluble lysates were probed with an antibody against fibronectin by Western analysis. When Hsp90α was transiently silenced, a decrease of approximately 40% and 80% was observed for soluble and insoluble fibronectin respectively (Figure 16A). Approximately 50% knockdown was achieved for Hsp90β with no observable effect on the levels of Hsp90α. Histone H3 was used as a control for equal protein

loading (Figure 16B). The effect of Hsp90β silencing on soluble and insoluble fibronectin was less pronounced in comparison to that achieved with Hsp90α knockdown. Nonetheless, Western analysis revealed a decrease of approximately 50% and 30% for soluble and insoluble fibronectin respectively as measured by the DOC assay (Figure 16B). To verify the Western analysis data and to determine the effect of Hsp90 knockdown on fibronectin morphology, transfected cells were analysed by confocal microscopy. Relative to cells transfected with the non-targeting control, a reduced fibronectin matrix was observed 48 hours after transfection with siRNA against Hsp90α or Hsp90β. This was confirmed by a decrease in the mean gray value which reported a change from 36.35 (± 3.26) to 26.66 (± 1.10) for Hsp90α knockdown and 29.09 (± 4.37) for Hsp90β knockdown. Interestingly, the decrease in the fibronectin matrix was more pronounced in cells where Hsp90α was transiently silenced (Figure 17). The nuclei panel was included to show that the knockdown treatments did not have a significant effect on cell viability or number.

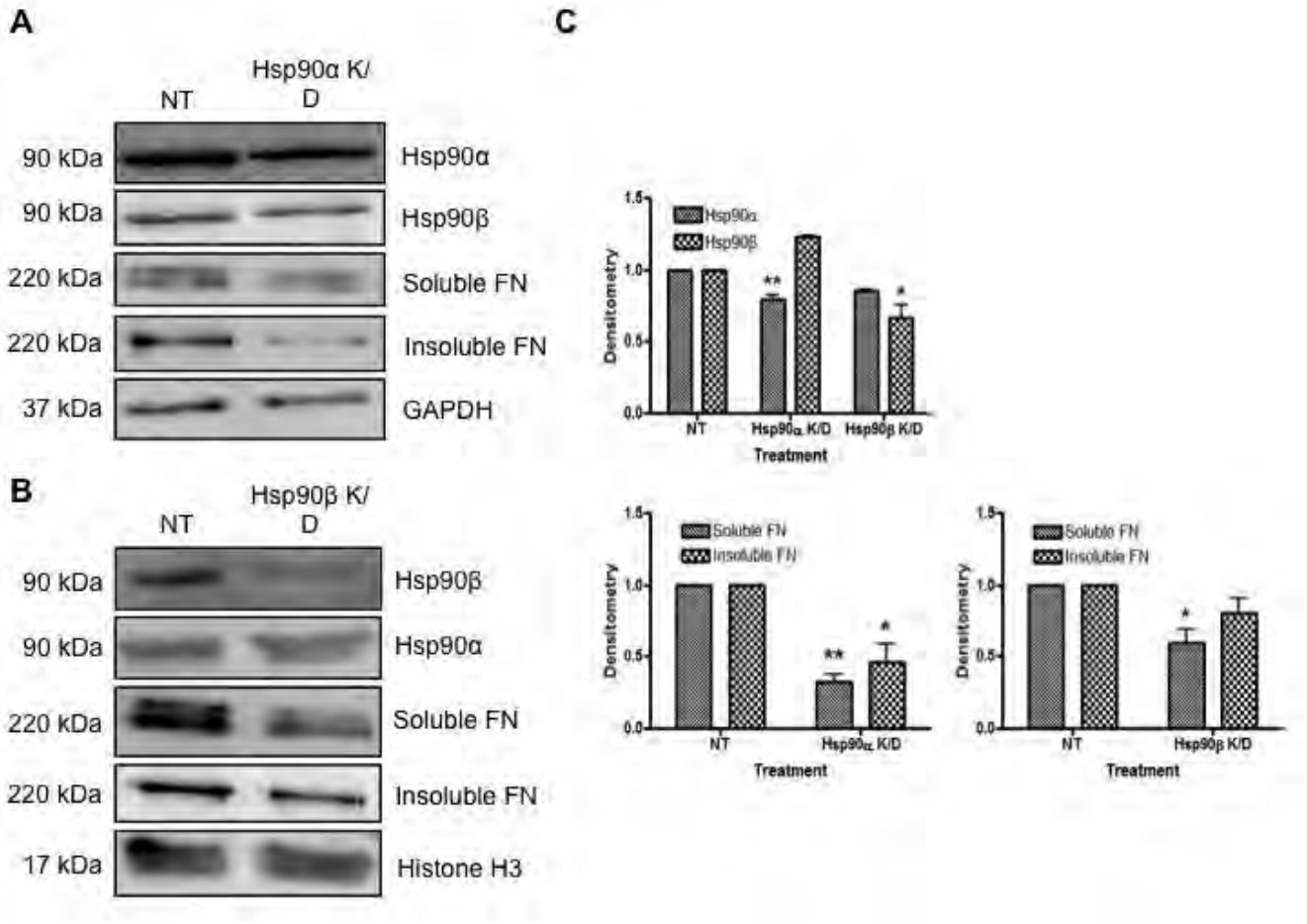

Figure 16: Knockdown (K/D) of Hsp90α or Hsp90β with siRNA decreased the proportion of soluble and insoluble fibronectin in Hs578T breast cancer cells.

(**A**) Hs578T cells were transfected with a pool of short interfering RNA (siRNA) oligonucleotides (25 nM) against Hsp90α. A scrambled non-targeting (NT) pool of siRNA oligonucleotides (25 nM) served as a negative control. After 48 hours, the level of Hsp90α was detected by Western analysis using primary antibodies against Hsp90α alone. DOC-soluble and DOC-insoluble lysates from transfected cells were created and equal amounts of protein loaded. The levels of soluble and insoluble fibronectin were determined by Western analysis using an antibody against fibronectin. To ensure equal sample loading, samples were probed with anti-GAPDH (1:1000). (**B**) Hs578T cells were transfected with a pool of siRNA oligonucleotides (25 nM) against Hsp90β. A scrambled non-targeting (NT) pool of siRNA oligonucleotides (25 nM) served as a negative control. Samples were harvested and analysed as described in (**A**) with the exception that an antibody against Histone H3 (1:1000) was used to ensure equal protein loading. (**C**) The graphs illustrate the densitometry that was determined using ImageJ software and was used to quantify the silencing of Hsp90α or Hsp90β normalized to the loading controls (upper panel) or the levels of soluble and insoluble fibronectin (lower panel). Data are representative of three independent experiments with similar results.

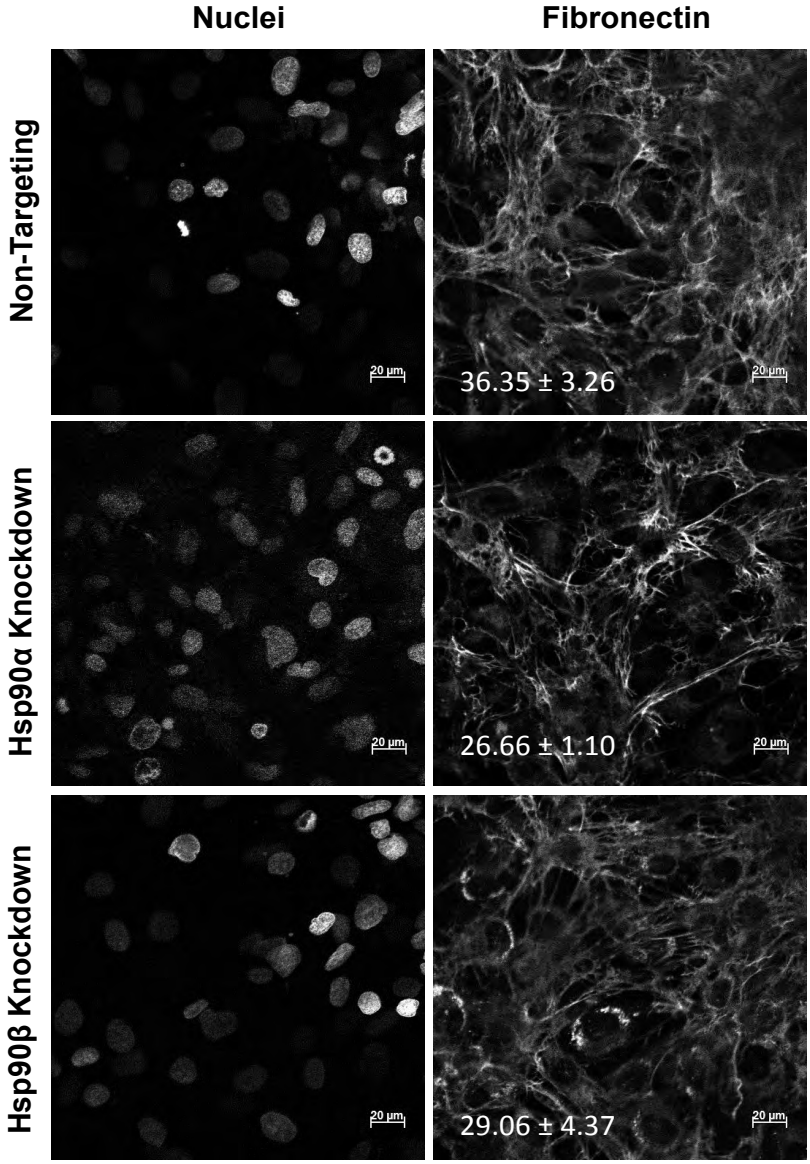

Figure 17: Knockdown of Hsp90α or Hsp90β resulted in a reduction in the extracellular fibronectin matrix of Hs578T breast cancer cells.

Hs578T cells transfected with siRNA against Hsp90α or Hsp90β were seeded onto sterile glass coverslips and allowed to adhere. After a 48 hour transfection period, the cells were fixed and incubated with a primary antibody against fibronectin (1:100), followed by a donkey anti-mouse Alexa-Fluor-488 secondary antibody. Transfection with a scrambled, non-targeting pool of siRNA served as a negative control. Nuclei were stained with 1 µg/ml Hoechst 33342. Images were captured using the Zeiss LSM 510 Meta laser scanning confocal microscope 40x oil objective and analysed using AxiovisionLE 4.7.1 (Zeiss, Germany). Three images were captured for each treatment in areas where similar cell numbers were observed. Scale bars represent 20 µm. Values (in white) at the bottom of each frame represent the mean gray values (± standard deviation) for each treatment. Data are representative of triplicate images of three independent experiments showing similar results.

3.1.12 Effect of pharmacological inhibition of Hsp90 on the levels of soluble and insoluble fibronectin in Hs578T cells

In an attempt to simultaneously inhibit Hsp90α and Hsp90β, we tested the effect of published Hsp90 inhibitors (geldanamycin and novobiocin) on the proportion of soluble and insoluble fibronectin (Figure 18). Hs578T cells were treated with increasing doses of either geldanamycin (500 nM, 2000 nM and 4000 nM) or novobiocin (250 μM, 750 μM and 1500 μM) for 16 hours before harvesting as per the DOC assay. Cells were also treated with an integrin-binding peptide (RGDS) and its mutant analogue (RADS) as controls for the DOC assay. The RGDS peptide is a ubiquitous integrin-binding motif found in extracellular matrix proteins, including fibronectin (Ruoslahti, 1996). Binding to the RGD motif should theoretically stimulate signaling pathways that regulate fibronectin matrix formation. In contrast, the RAD analogue should exhibit the opposite effect by competing with fibronectin for integrin binding (Verderio *et al.*, 2003). Western analysis to detect fibronectin showed that the RGDS peptide stimulated the expression of both soluble and insoluble fibronectin whereas the RADS mutant resulted in a reduction of the levels of both soluble and insoluble fibronectin. Geldanamycin treatments caused a dose-dependent increase in the proportion of insoluble fibronectin, but no change in the proportion of soluble fibronectin. In contrast, treatment with novobiocin showed a dose-dependent decrease in the levels of both soluble and insoluble fibronectin (Figure 18). The effect of each of the aforementioned treatments on fibronectin matrix morphology

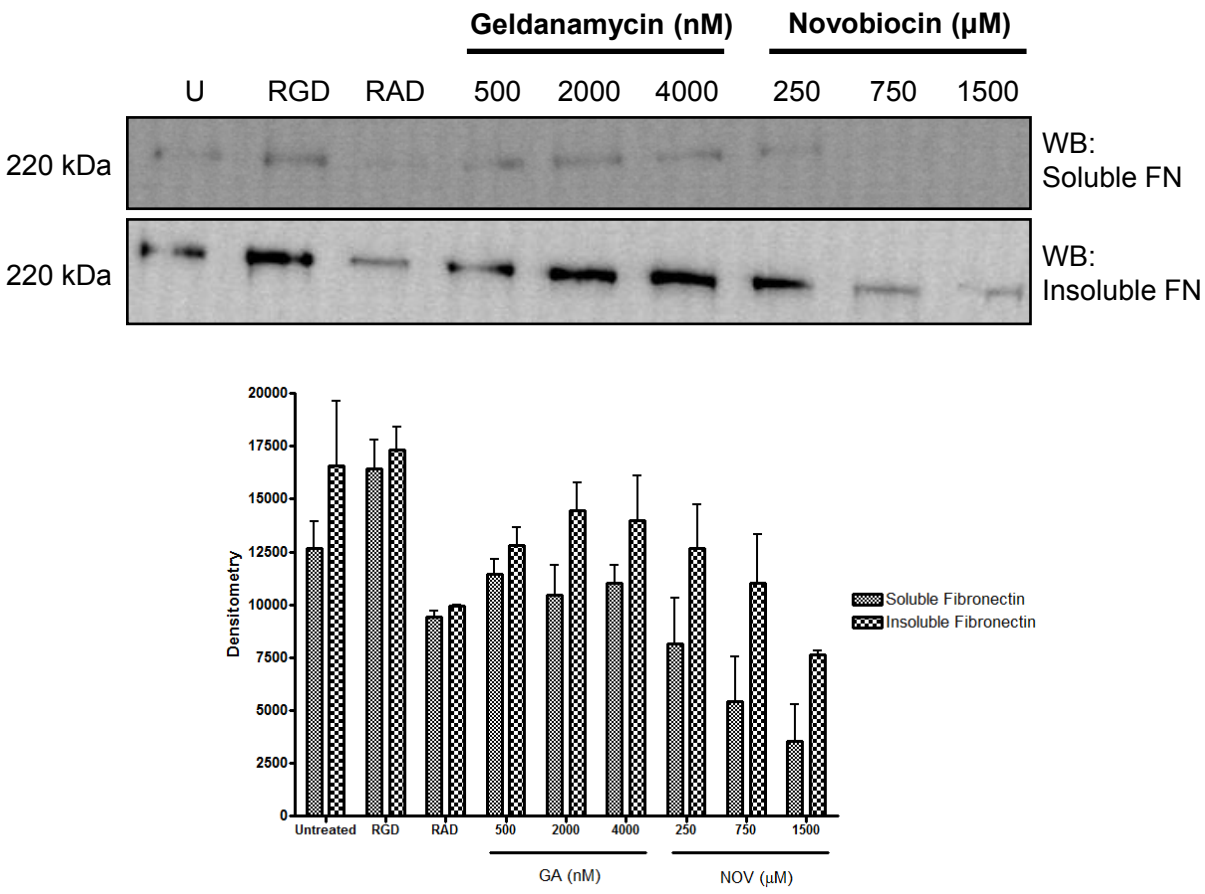

Figure 18: Inhibition of Hsp90 with the small molecule inhibitors, geldanamycin and novobiocin, resulted in differential effects on the levels of soluble and insoluble fibronectin in Hs578T breast cancer cells.

Confluent Hs578T cells were treated with either 5 μg/mL of an integrin-binding peptide (RGD) or its mutant analogue (RAD) as controls. Cells were treated with increasing doses of geldanamycin (GA: 500 nM, 2000 nM, 4000 nM) or novobiocin (NOV: 250 μM, 750 μM, 1500 μM); concentrations below the determined IC_{50} values (Figure 9). Cells were treated for 16 hours after which they were harvested according to the DOC assay (Brenner *et al.*, 2000). The effect of the treatments on the levels of soluble and insoluble fibronectin was determined by Western analysis. Equal amounts of total protein from the soluble and insoluble fractions were probed for the presence of fibronectin using a primary antibody against human fibronectin. The associated densitometry (below graph) was determined using ImageJ software. Statistical significance was determined using a one-way ANOVA and error bars represent data of three independent experiments with similar results.

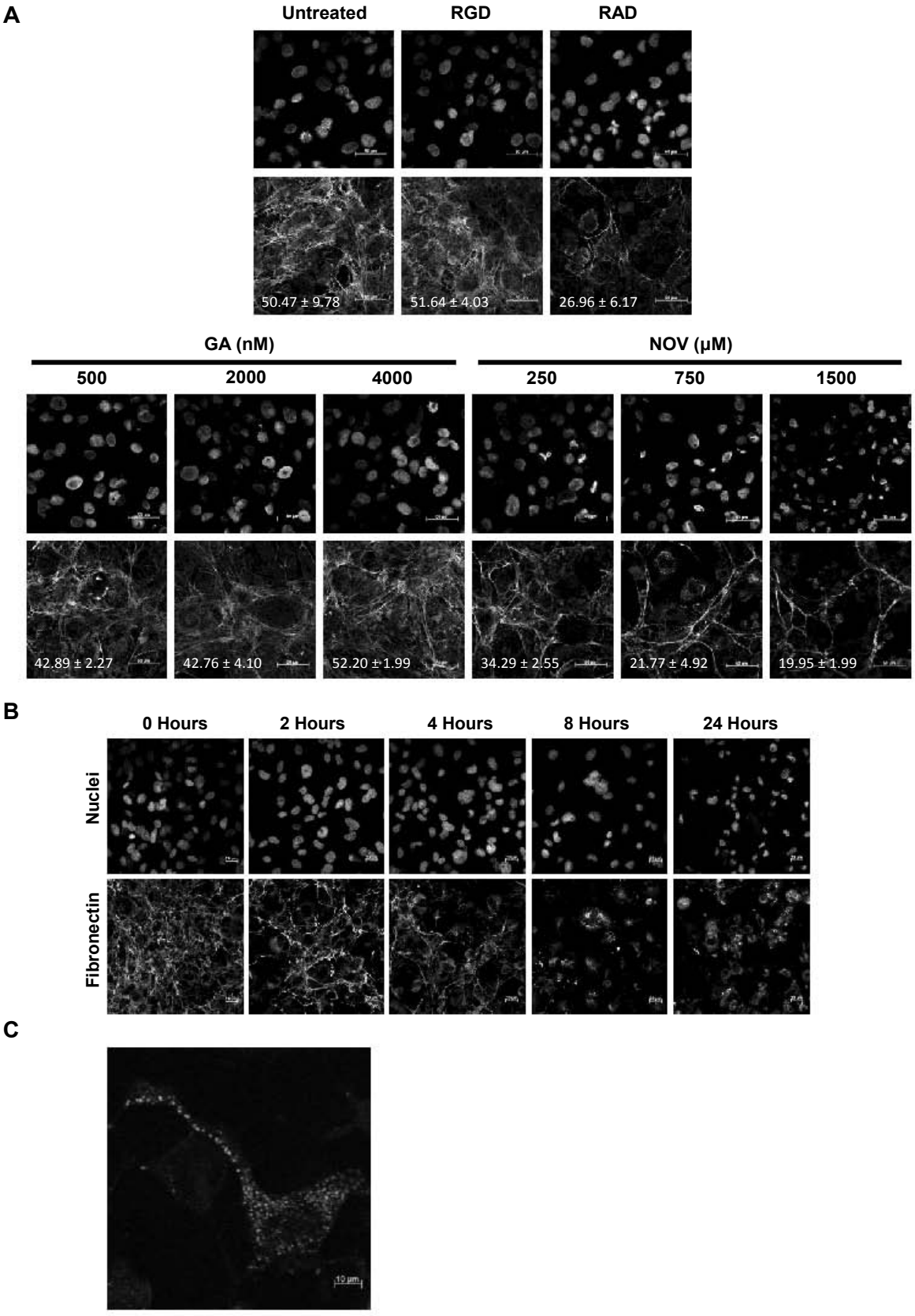

Figure 19: legend over page

Figure 19: Inhibition of Hsp90 with novobiocin resulted in a dose-dependent change in the fibronectin morphology in Hs578T breast cancer cells.

Hs578T cells (9 x 10^5 cells/ml) were seeded onto sterile glass coverslips and allowed to adhere overnight. The following day, cells were treated with an integrin-binding RGD peptide or the mutant RAD analogue (5 µg/ml) or increasing doses of geldanamycin (GA: 500 nM, 2000 nM, 4000 nM) or novobiocin (NOV: 250 µM, 750 µM, 1500 µM) for 16 hours. Cells were harvested, fixed and incubated with a mouse primary antibody against human fibronectin (1:100) followed by anti-mouse Alexa-Fluor-488 secondary antibody (1:500). Nuclei were stained with 1 µg/ml Hoechst 33342. Images were captured using the Zeiss LSM 510 Meta laser scanning confocal microscope 40x oil objective and analysed using AxiovisionLE 4.7.1 (Zeiss, Germany). Three images were captured for each treatment in areas where similar cell numbers were observed. Scale bars represent 20 µm. Values (in white) at the bottom of each frame represent the mean gray values (± standard deviation) for each treatment. Data are representative of three independent experiments with similar results. (**B**) Inhibition of Hsp90 with novobiocin resulted in a time-dependent decrease in the extracellular fibronectin matrix. Hs578T breast cancer cells were seeded onto sterile glass coverslips and allowed to adhere for 16 hours prior to treatment with novobiocin (NOV; 1 mM) over a time period of 24 hours. Cells were harvested at different time intervals (0, 2, 4, 8 and 24 hours), fixed and incubated with a mouse primary antibody against human fibronectin (1:100) followed by anti-mouse Alexa-Fluor-488 secondary antibody (1:500). Nuclei were stained with 1 µg/ml Hoechst 33342. Images were captured using the Zeiss LSM 510 Meta laser scanning confocal microscope 40x oil objective and analysed using AxiovisionLE 4.7.1 (Zeiss, Germany). Three images were captured for each treatment in areas where similar cell numbers were observed. Scale bars represent 20 µm. (**C**) Inhibition of Hsp90 with novobiocin caused the formation of small, vesicular-like structures in Hs578T cells. Cells were seeded onto sterile glass coverslips and allowed to adhere overnight at 37°C prior to treatment with novobiocin (1 mM) for a period of 16 hours. Cells were harvested, fixed and incubated with a mouse primary antibody against human fibronectin (1:100) followed by anti-mouse Alexa-Fluor-488 secondary antibody (1:500). Nuclei were stained with 1 µg/ml Hoechst 33342. Images were captured using the Zeiss LSM 510 Meta laser scanning confocal microscope 63x oil objective and analysed using AxiovisionLE 4.7.1 (Zeiss, Germany). Scale bars represent 20 µm.

was analysed by confocal microscopy (Figure 19A). Relative to the untreated cells, treatment with the RGDS peptide increased the proportion of insoluble fibronectin (mean gray value 51.64 ± 4.03) observed while the RADS mutant peptide showed a considerable decrease (mean gray value 26.96 ± 6.17), both corroborating the Western analysis data (Figure 18). Cells treated with geldanamycin showed an increase in the mean gray value from 42.89 ± 2.27 at 500 nM to 52.20 ± 1.99 at 4000 nM, supporting the results for Western analysis which showed an increase in the levels of insoluble fibronectin (Figure 18). Geldanamycin also appeared to affect the morphology of the matrix, demonstrating a more ordered fibrillar network compared to the untreated cells (Figure 19A). More interestingly, cells treated with novobiocin showed a dose-dependent decrease in the fibronectin fibrillar network with increasing doses of the Hsp90 inhibitor. A decrease from 50.47 ± 9.78 for untreated cells to 34.29 ± 2.55 at 250 μM novobiocin, 21.77 ± 4.92 at 750 μM novobiocin and 19.95 ± 1.99 at 1500 μM novobiocin was observed which was similar to the mean gray value of 26.96 ± 6.17 in cells treated with the RADS peptide. The nuclei panel was included for all treatments to illustrate that the change in the fibronectin matrix was not due to an increase or decrease in cell number.

Since inhibition of Hsp90 with novobiocin exhibited an interesting fibronectin phenotype, we decided to use this inhibitor for further studies to investigate the role of Hsp90 in fibronectin matrix assembly. To provide support for the dose-dependent decrease in fibronectin observed following novobiocin treatment, we next investigated whether this decrease in fibronectin was also time-dependent. Cells were treated with a fixed concentration of novobiocin (1 mM) and harvested over a range of time intervals (0, 2, 4, 8 and 24 hours) and prepared for confocal microscopy (Figure 19B). A time-dependent decrease in the fibronectin matrix was observed coupled with the appearance of small, vesicular-like structures within the cytoplasm of many cells. A high resolution image of these putative vesicular structures is shown (Figure 19C).

3.1.13 Investigation of the ability of exogenous Hsp90β to reverse the loss in the fibronectin matrix following Hsp90 knockdown or treatment with novobiocin

Next we investigated whether exogenous Hsp90β was capable of rescuing the phenotype associated with novobiocin-treated or Hsp90-knockdown cells (Figure 20). Hs578T cells were treated with a dose of novobiocin below the calculated IC_{50} value (1 mM) for 1 hour after which Hps90β (100 ng/ml) was added to the cell culture media for a period of 16 hours. Cells treated with Hsp90β (100 ng/ml) or novobiocin (1 mM) alone served as controls. Sterile coverslips were added to the wells of each treatment for analysis by confocal microscopy. After the treatment period, soluble and insoluble fibronectin were harvested from cells as per the DOC assay (Brenner *et al.*, 2000) and the coverslips processed for confocal microscopy. Relative to the untreated cells, exogenous Hsp90β alone increased the proportion of both soluble and insoluble fibronectin (Figure 20A). In cells treated with novobiocin, a reduction in both soluble and insoluble fibronectin was expected. While a decrease was observed for the soluble fibronectin fraction, a slight increase was seen in the proportion of insoluble fibronectin relative to the untreated control (Figure 20A). Cells treated with a combination of novobiocin (1 mM) and Hsp90β (100 ng/ml) revealed that exogenous Hsp90β was unable to induce the recovery of the insoluble fibronectin matrix following novobiocin treatment (Figure 20A). Confocal microscopy corroborated the Western analysis data and showed that cells treated with Hsp90β alone resulted in a greater, more pronounced fibronectin matrix in comparison to untreated cells. This was supported by an increase in the mean gray value from 33.28 ± 5.76 for untreated cells to 52.83 ± 0.80 in treated cells (Figure 20B). Novobiocin caused an almost complete loss in the extracellular fibronectin matrix and consistently exhibited small, vesicular-like structures as was observed in previous experiments. A decrease from 33.28 ± 5.76 to 8.67 ± 2.61 was observed in the mean gray value. Cells treated with novobiocin and Hsp90β together showed a decrease in the mean gray values from 33.28 ± 5.76 to 16.17 ± 1.05, which was more similar to the novobiocin treated sample than the Hsp90β or untreated sample.

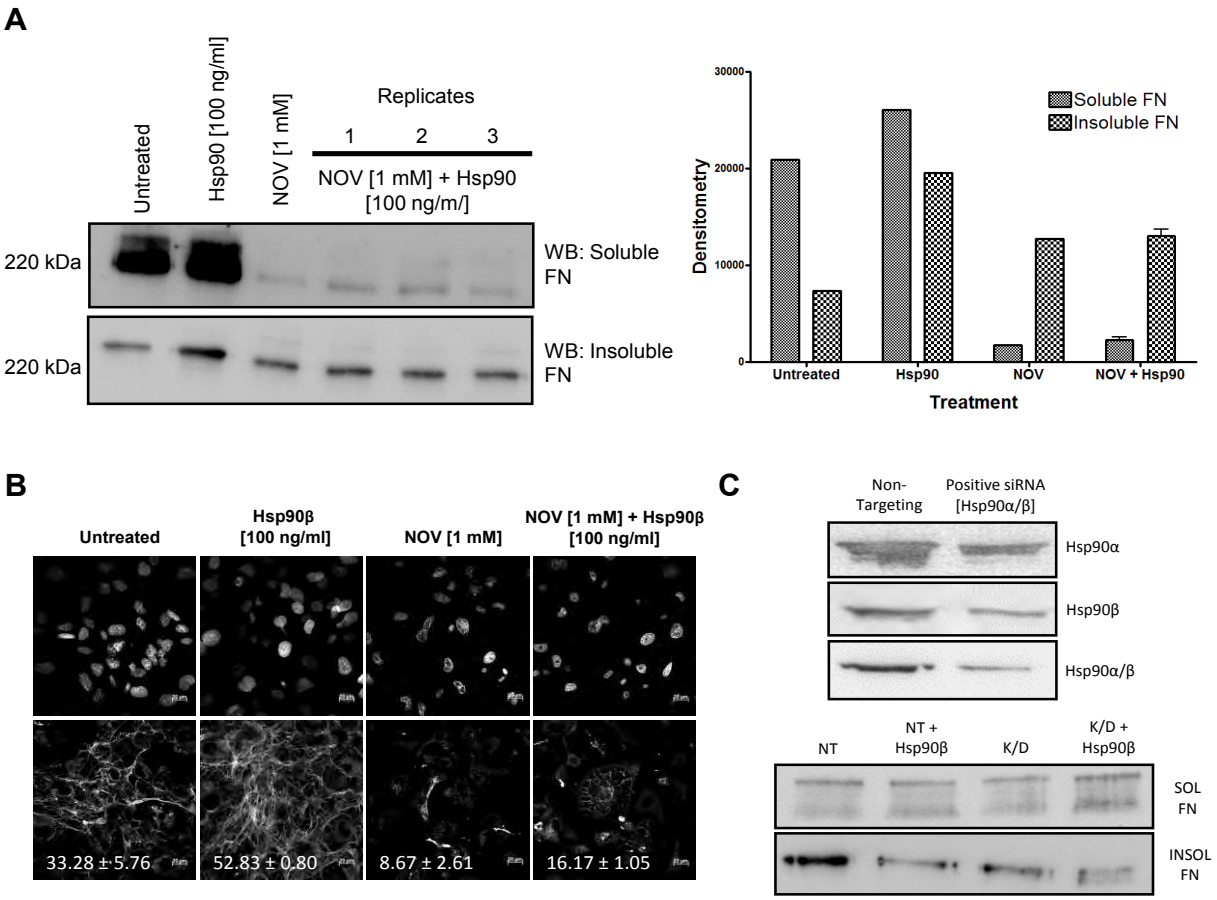

Figure 20: Exogenous Hsp90β was not able to reverse the reduction in the fibronectin matrix in Hs578T cells following treatment of cells with novobiocin.

(**A**) Confluent Hs578T cells were allowed to adhere overnight and then treated with novobiocin (1 mM). An hour later, Hsp90β (100 ng/mL) was added to the cells and incubated overnight at 37°C. Cells treated with Hsp90β (100 ng/ml) alone or novobiocin (1 mM) alone served as controls. The densitometry (right) was determined using ImageJ. Statistical significance was determined by a one-way ANOVA. (**B**) Confluent Hs578T cells were seeded onto sterile glass coverslips and treated as described in (**A**). Cells were harvested, fixed and incubated with a mouse primary antibody against human fibronectin (1:100) followed by anti-mouse Alexa-Fluor-488 secondary antibody (1:500). Nuclei were stained with 1 µg/ml Hoechst 33342. Images were captured using the Zeiss LSM 510 Meta laser scanning confocal microscope 40x oil objective and analysed using AxiovisionLE 4.7.1 (Zeiss, Germany). Three images were captured for each treatment in areas where similar cell numbers were observed. Scale bars represent 20 µm. Values (in white) at the bottom of each frame represent the mean gray values (± standard deviation) for each treatment. Data are representative of three independent experiments with similar results. (**C**) Hs578T cells (90% confluent) were allowed to adhere overnight at 37°C, 9% CO_2. The following day, the cells were simultaneously transfected with a pool of siRNA oligonucleotides (12 nM) against both Hsp90α and Hsp90β for 24 hours. Transfection with a pool of scrambled, non-targeting (NT) siRNA oligonucleotides was used as a negative control. The culture media was subsequently supplemented with Hsp90β (100 ng/ml) and treated for a further 24 hours prior to harvesting cells as per the DOC assay (Brenner *et al.*, 2000).

Addition of Hsp90β and novobiocin did not result in a recovery of the extracellular fibronectin matrix, but appeared to enhance the intracellular fibronectin phenotype observed with novobiocin treatment. The small, vesicular-like structures became more pronounced and the fibronectin displayed an unusual localization reminiscent of the endoplasmic reticulum or vacuolar staining (Figure 20B). We hypothesized that the reason no recovery was observed following the addition of Hsp90β may have been a result of inhibition by novobiocin of the soluble Hsp90β that was added to the culture media. To ensure this was not occurring, we repeated a similar experiment whereby cells were treated with novobiocin (1 mM) for 8 hours, the novobiocin was removed and media supplemented with Hsp90β (100 ng/ml) was replaced. Western analysis of DOC-soluble and DOC-insoluble fibronectin, however, showed that there was no change in the fibronectin levels after treatment with exogenous Hsp90β (*data not shown*).

Alongside pharmacological inhibition, we decided to ascertain whether exogenous Hsp90β had any effect on the recovery of the fibronectin matrix following the simultaneous knockdown of Hsp90α and Hsp90β. Cells were transfected with a pool of siRNA oligonucleotides (12 nM) against each Hsp90 isoform. The following day, the culture media was supplemented with Hsp90β (100 ng/ml) and treated for a further 24 hours prior to harvesting of soluble and insoluble fibronectin using the DOC assay (Brenner *et al.*, 2000). Approximately 70% knockdown was achieved for Hsp90α/β with little effect on cell viability. Following Hsp90 knockdown (K/D), there was a decrease in both soluble and insoluble fibronectin. This phenotype, however, was not recovered when soluble exogenous Hsp90β was added to the knockdown cells (Figure 20C). No observable change was noticed in the fibronectin morphology by confocal microscopy (*data not shown*).

3.1.14 Effect of novobiocin on a fluorescently-labeled extracellular fibronectin matrix

We next investigated whether the reduction in the extracellular fibronectin matrix was a result of degradation of the extracellular matrix or an inhibition of export of soluble

fibronectin. We designed an experiment that allowed us to study the dynamics of extracellular fibronectin only. Purified soluble fibronectin was labeled with a fluorescent dye (DyLight 550) by covalent binding of the NHS-moiety on the dye to primary amines on fibronectin. This labeled fibronectin could then be used by cells to build a fluorescent extracellular matrix that could be detected using excitation at a wavelength of 550 nm. Once labeled, the moles of dye per moles of protein was determined to be 1.355 moles dye/moles fibronectin, suggesting that proper labeling of fibronectin had occurred. To ensure that Hs578T cells could utilize this fibronectin to form the extracellular matrix, 50 nM of the labeled fibronectin was added to cells in suspension or under adherent conditions. A time period of 16 hours at 37°C was allowed for fibrillogenesis after which the cells were examined by confocal microscopy. Confocal microscopy revealed that when supplied with fluorescently labeled fibronectin under both suspension and adherent conditions, Hs578T cells successfully formed a fluorescent matrix (Figure 21A). This experiment was repeated and total fibronectin (including endogenously produced unlabelled fibronectin) was stained with a primary antibody against fibronectin followed by a species-specific Alexa-Fluor-488 secondary antibody. The rationale for this experiment was to determine what quantity of the total fibronectin matrix was derived from the exogenous fluorescent protein or the endogenous unlabelled fibronectin. Confocal microscopy showed that a large portion of the matrix was formed from the fluorescent exogenous fibronectin (red signal), but there were still regions where only endogenous fibronectin (green signal) was observed (Figure 21B). Collectively, these data demonstrated that cells could utilize the fluorescently labeled fibronectin to successfully form a large extracellular matrix that could be used in subsequent experiments to analyse the dynamics of extracellular fibronectin.

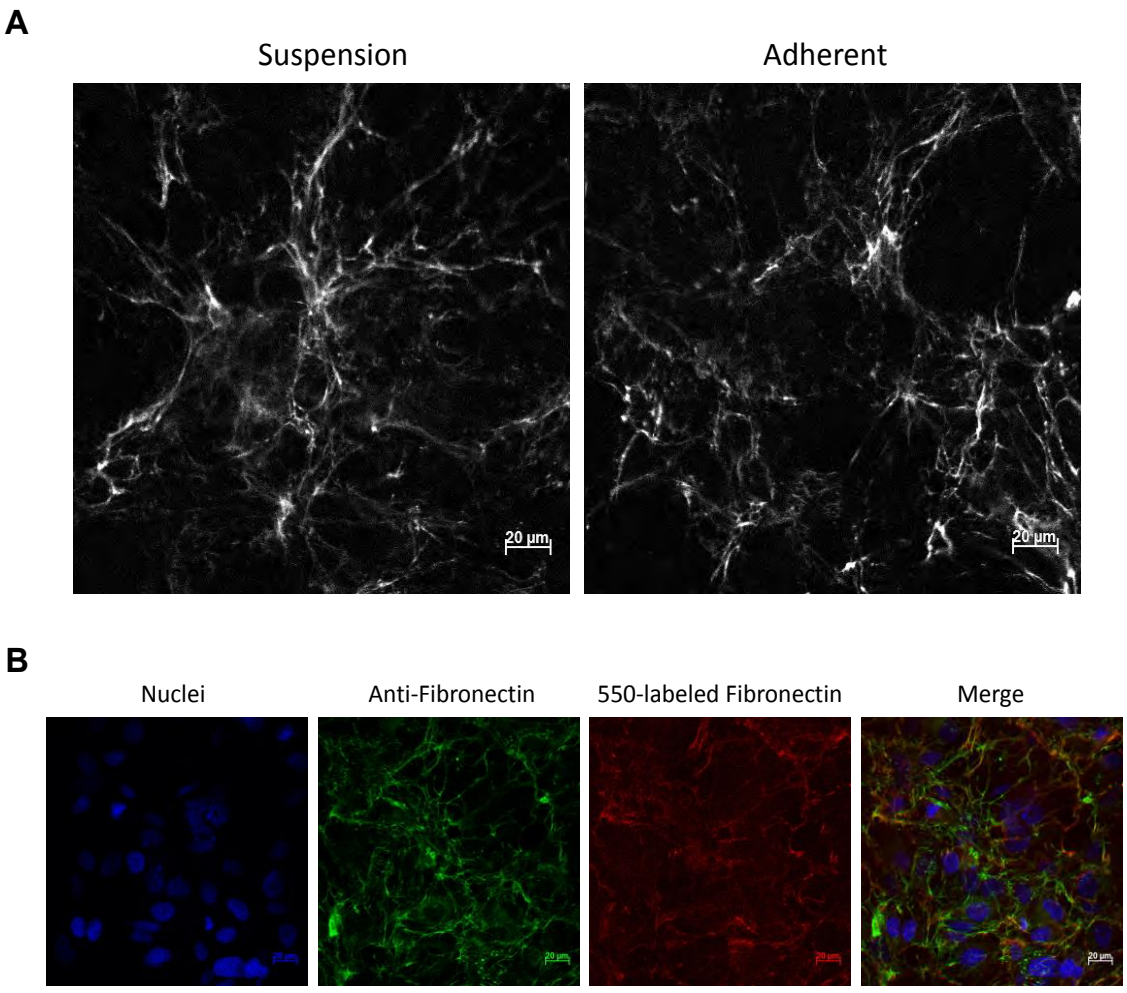

Figure 21: Human fibronectin was successfully labeled with the DyLight-550 dye and was incorporated into the extracellular fibronectin matrix of Hs578T breast cancer cells.

(**A**) Purified fibronectin was labeled using the DyLight-550 labeling kit according to manufacturers' instructions. The labeled fibronectin (50 nM) was added to the cell culture media of Hs578T cells in suspension (left) or that had been allowed to adhere overnight (right). The cells were subsequently incubated at 37°C for 24 hours to allow the fibronectin matrix to form prior to microscopy. (**B**) Fluorescently labeled fibronectin (50 nM) was added to the cell culture supernatant of adherent Hs578T cells and incubated for 24 hours. Cells were harvested, fixed and incubated with human anti-fibronectin primary antibody followed by a species specific Alexa Fluor-488 conjugated secondary antibody. Nuclei were stained with 1 µg/ml Hoechst 33342. Images were captured using the Zeiss LSM 510 Meta laser scanning confocal microscope 40x oil objective and analysed using AxiovisionLE 4.7.1 (Zeiss, Germany). Scale bars represent 20 µm.

Next we investigated the effect of Hsp90 inhibition with novobiocin on the extracellular fluorescent fibronectin matrix (Figure 22). Hs578T cells were treated with 50 nM labeled fibronectin, allowed to undergo fibrillogenesis for 16 hours and subsequently treated with novobiocin (1 mM) over a time course of 0, 2, 4, 8 and 24 hours. Cells were harvested and analysed by confocal microscopy. A time-dependent decrease in the fluorescent fibronectin matrix was observed upon novobiocin treatment. A considerable loss in the fibronectin matrix was observed after 2 hours with an almost complete loss in the matrix after 24 hours (Figure 22A). No distinct vesicular-like structures were observed, as was seen for endogenous fibronectin when stained with antibodies. However, after 24 hours a faint, diffuse cytoplasmic signal was observed (Figure 22A), which may have been due to the accumulation of the fluorescent fibronectin molecule inside the cell.

This novobiocin-induced effect was subsequently analysed using live cell imaging over a period of 9 hours (Figure 22B). Hs578T cells were seeded into a glass-bottomed cell culture dish and treated with 50 nM labeled fibronectin for 16 hours. The culture dish was placed in the Zeiss LSM 510 Meta laser scanning confocal microscope unit pre-conditioned to an atmospheric temperature of 37°C and maintained at CO_2 levels of 10%. Novobiocin (1 mM) was added to the cells after the presence of the fluorescent matrix was confirmed by excitation at 550 nm. AxiovisionLE 4.7.1 software was used to set up the parameters of the experiment such that images were captured at 15 minute intervals over a 9-hour time period. This time period was deemed suitable since a considerable loss in the fluorescent matrix was seen at 8 hours in the previous time-course experiment (Figure 22A). As a control, this experiment was repeated for cells that were not treated with novobiocin. Five individual frames for each experiment (at 0, 3, 5, 7 and 9 hours) suggested that changes in the matrix in untreated cells occurred due to fibronectin matrix turnover and assembly, but no considerable change in the matrix density was observed. Upon treatment with novobiocin, a time-dependent decrease in the fluorescent fibronectin matrix was observed. A live cell video clip was generated from the images obtained to illustrate this reduction in the fibronectin matrix in more detail (LIVE CELL MOVIE 1 - see compact disc attached).

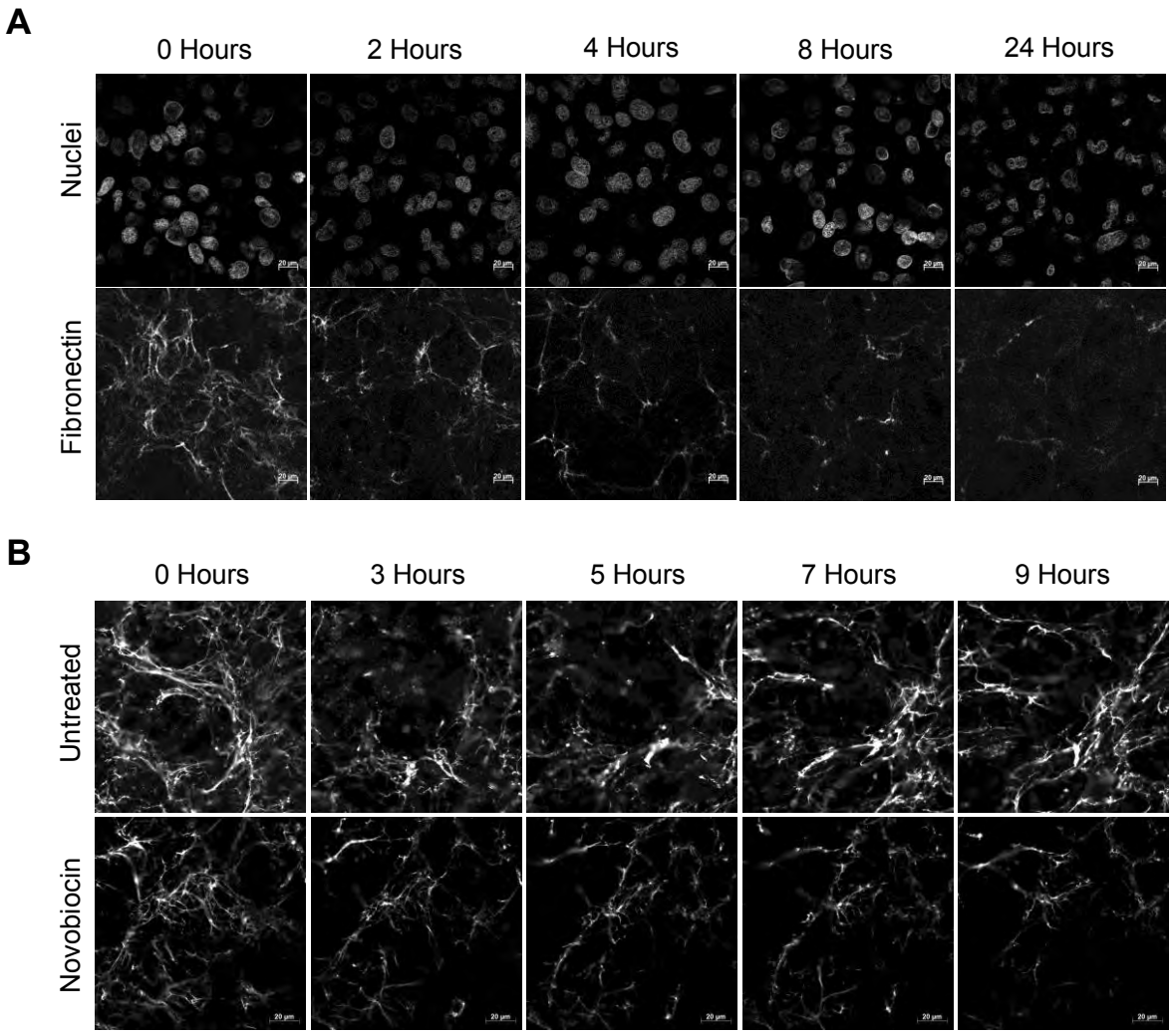

Figure 22: Novobiocin induced a time-dependent decrease in fluorescently labeled fibronectin in Hs578T breast cancer cells.

(**A**) Confluent Hs578T cells were allowed to undergo fibrillogenesis in media supplemented with fibronectin (50 nM) covalently conjugated to the fluorescent DyLight-550 dye overnight at 37°C. The following day, cells were treated with novobiocin (1 mM) for a period of 2, 4, 8 or 24 hours. After each time interval, the cells were harvested, fixed and the nuclei stained with 1 µg/ml Hoechst 33342. Images were captured using the Zeiss LSM 510 Meta laser scanning confocal microscope 40x oil objective and analysed using AxiovisionLE 4.7.1 (Zeiss, Germany). Three images were captured for each treatment in areas where similar cell numbers were observed. Scale bars represent 20 µm. Data are representative of three independent experiments with similar results. (**B**) Hs578T cells were seeded in a sterile glass-bottomed culture dish in phenol-red free media supplemented with fluorescently labeled fibronectin (50 nM) and incubated overnight at 37°C. The following day, cells either remained untreated or the media was supplemented with novobiocin (1 mM) and live cell images were captured every 15 minutes over a period of 9 hours using the Zeiss LSM 510 Meta laser scanning confocal microscope. Scale bars represent 20 µm. All images were captured using the 63x oil objective and analysed using AxiovisionLE 4.7.1 (Zeiss, Germany) and Windows Movie Maker software.

A video clip was also generated from the images captured for the untreated control and showed the dynamic turnover and formation of the matrix that occurred naturally within the cells (LIVE CELL MOVIE 2 – see compact disc attached). In these experiments, small vesicular-like structures were observed, similar to those seen for endogenous fibronectin stained with antibodies. These data collectively suggest that extracellular fibronectin was being internalized upon inhibition of Hsp90 with novobiocin.

3.1.15 Effect of novobiocin on the uptake of CFDA-SE-labeled fibronectin in Hs578T cells

To confirm whether the reduction in the fibronectin matrix upon novobiocin treatment was a result of the internalization of fibronectin, we evaluated the uptake of fibronectin labeled with the carboxyfluorescein diacetate succinimidyl ester (CFDA-SE). CFDA-SE is non-fluorescent until the acetate groups of the dye have been cleaved by intracellular esterases, after which the dye fluoresces when excited at a wavelength of 488 nm (Wang *et al.*, 2005). Similar to the DyLight-550 dye, CFDA-SE contains a succinimidyl moiety that is capable of binding to the primary amines of any protein within interacting range. As a consequence, only CFDA-SE-labeled fibronectin that has been internalized should become fluorescent due to the action of intracellular esterases. As a means to analyse the effect of novobiocin on CFDA-SE-labeled fibronectin (CFDA-SE-FN), the change in the fluorescence of CFDA-SE was assessed using flow cytometry (Figure 23) and confocal microscopy (Figure 24). Flow cytometry showed that cells treated with CFDA-SE-FN alone (Figure 23A, red dotted line) exhibited some fluorescence (mean fluorescence = 9144) in the FITC channel in comparison to untreated cells (mean fluorescence = 296) (Figure 23A, grey shaded peak), suggesting that Hs578T cells internalized the extracellular fibronectin. Upon treatment with novobiocin, the FITC-H peak (Figure 23A, blue solid line) shifted to the right of the red line by one log scale and the mean fluorescence increased to 50 000 in comparison to cells treated with CFDA-SE-FN alone (Figure 23A, red dotted line). Hs578T cells were also treated with two different doses of novobiocin (250 μM and 750 μM) and the CFDA-SE fluorescence was monitored by flow cytometry. At the lowest concentration of novobiocin (250 μM), the

FITC-H peak (Figure 23B, blue solid line) shifted approximately one log scale to the right in comparison to cells treated with CFDA-SE-FN alone (Figure 23B, red dotted line). An increase in mean fluorescence from approximately 500 to 2200 was reported (Figure 23B). With an increase in novobiocin concentration, the FITC-H peak (Figure 22B, green solid line) appeared to shift to the left, suggesting the CFDA-SE fluorescence was decreasing. At 750 μM novobiocin, the mean fluorescence decreased to approximately 1600 compared to the mean fluorescence of 2200 associated with 250 μM novobiocin.

Confocal microscopy was used to visualize the fluorescence associated with the CFDA-SE-labeled fibronectin in untreated and novobiocin-treated cells (Figure 24). Henceforth, untreated cells refer to cells that were treated with CFDA-SE-FN alone, but not with novobiocin. A small subset of the total number of untreated cells (28.13 ± 6.82%) showed green fluorescence, an indication that CFDA-SE-FN had been internalized and cleaved by intracellular esterases. Upon treatment with 250 μM novobiocin, every cell observed displayed green fluorescence (100% CFDA-SE positive cells). This data supported the observations made by flow cytometry where a log scale increase in mean fluorescence was detected (Figure 23B, blue solid line). At a concentration of 750 μM novobiocin, the number of cells exhibiting green fluorescence decreased considerably compared to the lowest concentration of novobiocin (250 μM). However, the number of cells that had internalized the CFDA-SE-FN was still higher compared to the untreated cells (53.34 ± 5.39%) (Figure 24).

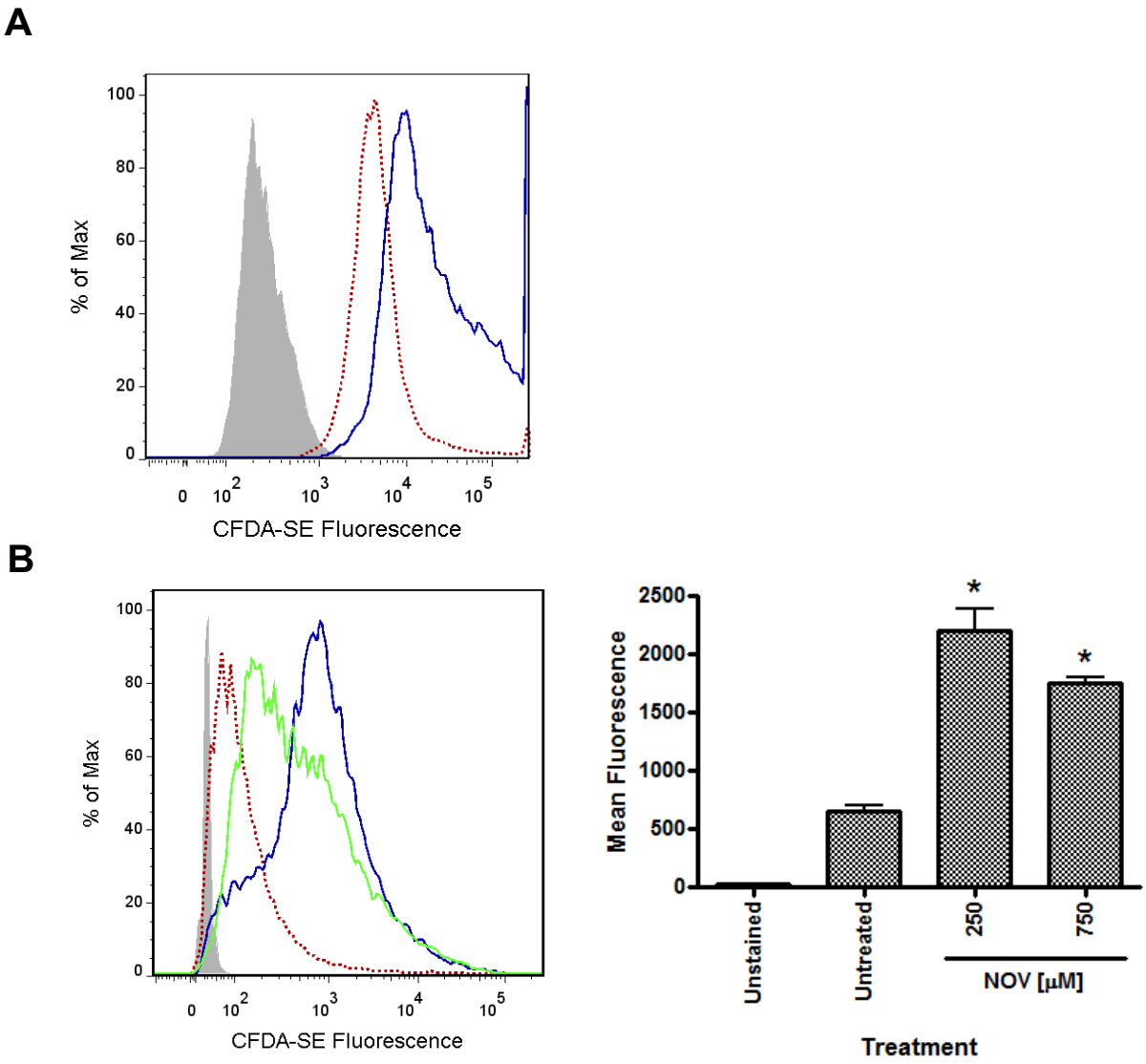

Figure 23: Novobiocin treatment resulted in an increase in the uptake of fibronectin labeled with carboxyfluorescein diacetate succinimidyl ester (CFDA-SE) in Hs578T breast cancer cells.

(**A**) Confluent Hs578T cells were allowed to adhere for 8 hours after which the cell culture media was supplemented with either 500 nM CFDA-SE-labeled fibronectin (red dotted line) alone or a combination of 500 nM CFDA-SE-FN and 1 mM novobiocin (blue solid line) and incubated for a period of 16 hours. Cells were lifted with trypsin/EDTA, washed and analysed by flow cytometry in the FITC channel. Cells not provided with CFDA-SE-FN (grey shaded peak) were analysed as a reference for each treatment. (**B**) Cells were treated in the same manner as described in (**A**) with the exception that cells were treated with a low (250 μM; blue solid line) or medium (750 μM; green solid line) dose of novobiocin (NOV). The change in the mean fluorescence was determined using FlowJo 7.6.5 software as illustrated in the histogram. Statistical significance relative to the untreated cells was determined using a one-way ANOVA ($p < 0.01$). Data are representative of two independent experiments with similar results.

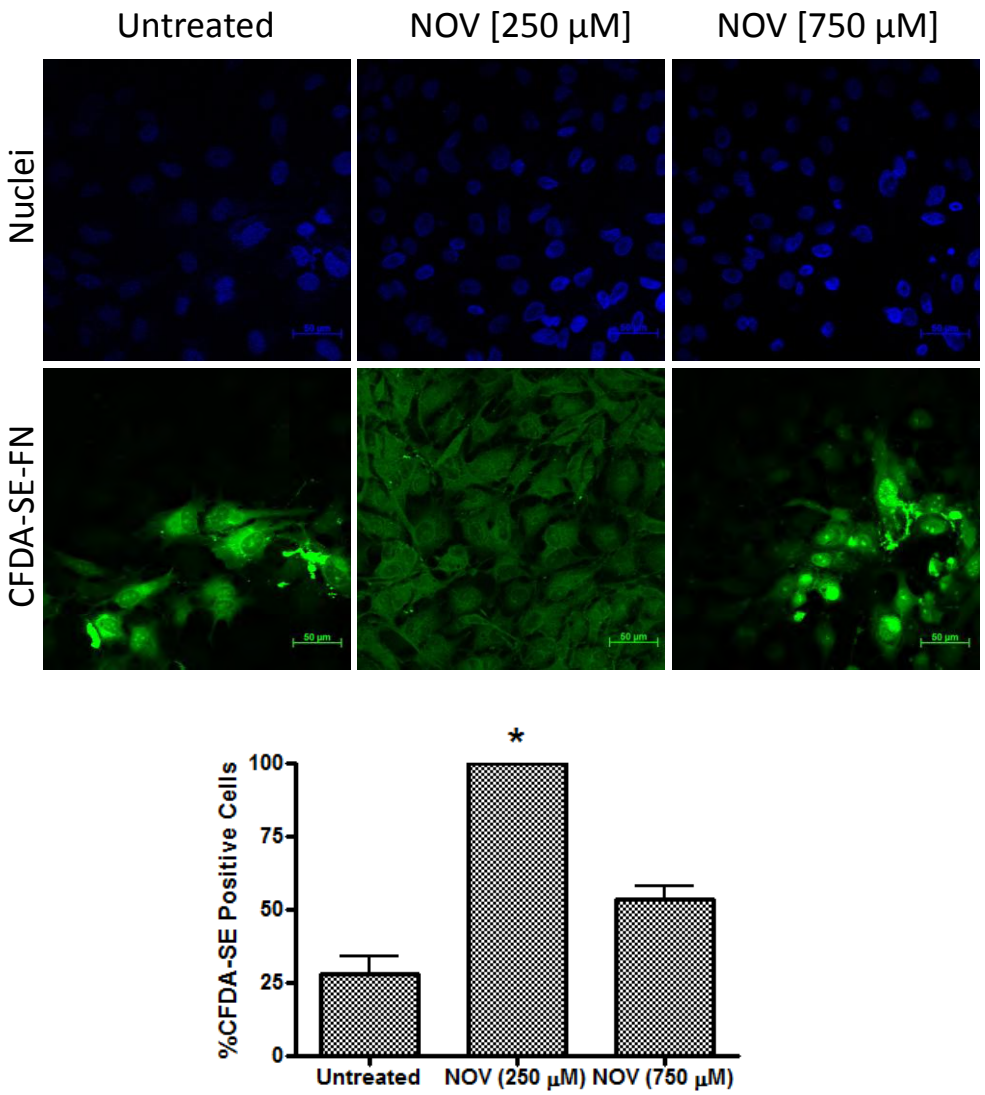

Figure 24: Novobiocin treatment increased the uptake of CFDA-SE-FN in Hs578T breast cancer cells.

Cells were seeded onto sterile, glass coverslips and allowed to adhere for 8 hours prior to treating cells with either CFDA-SE-FN alone (500 nM) or a combination of CFDA-SE-FN (500 nM) and novobiocin at either a low or medium dose (NOV: 250 µM and 750 µM respectively). Cells were incubated for 16 hours prior to analysis by microscopy. Nuclei were stained with 1 µg/ml Hoechst 33342. Images were captured using the Zeiss LSM 510 Meta laser scanning confocal microscope 40x oil objective and analysed using AxiovisionLE 4.7.1 (Zeiss, Germany). Three images were captured for each treatment in areas where similar cell numbers were observed. Scale bars represent 50 µm. The graph illustrates the percentage of CFDA-SE positive cells determined for the two replicate experiments. This was calculated by dividing the total number of cells positive for fluorescence by the total number of cells (nuclei) in each frame. Statistical significance was determined using a one-way ANOVA ($p < 0.01$). Data are representative of two independent experiments with similar results.

3.1.16 Effect of vesicular trafficking inhibitors on novobiocin-treated Hs578T cells

We investigated whether the novobiocin-induced reduction in the fibronectin matrix could be reversed in cells treated with different inhibitors of vesicular trafficking. A panel of four inhibitors was screened including colchicine, methyl-β-cyclodextrin (MβC), Exo 1, and genistein. An initial screening of the four trafficking inhibitors at a single concentration was done in the absence and presence of novobiocin (1 mM) for a period of 8 hours (Figure 25), an incubation period previously determined to be optimal to observe a considerable reduction in the fibronectin matrix (Figure 19B). Treating cells with the trafficking inhibitors alone served as a control to ensure there was no considerable effect on cell viability or fibronectin morphology. Untreated cells formed a dense, extracellular fibronectin matrix that was considerably reduced following treatment with novobiocin. An identical phenotype was observed in cells treated with 0.01% DMSO (a solvent used to resuspend certain of the trafficking inhibitors). Cells treated with colchicine alone showed a reduced extracellular fibronectin matrix coupled with an increase in cytoplasmic fibronectin staining. This phenotype, however, was lost in cells treated with a combination of colchicine and novobiocin, and showed a dense extracellular fibronectin network (Figure 25). This phenotype was similar to that observed for Exo 1 where a loss in the extracellular matrix was observed with the exocytosis inhibitor alone, but a recovery was seen when cells were treated with a combination of Exo 1 and novobiocin. Methyl-β-cyclodextrin (MβC) alone did not seem to have any considerable effect on cell viability or fibronectin morphology compared to untreated cells. Interestingly, a combination of MβC and novobiocin showed an almost full recovery of the extracellular fibronectin matrix when directly compared to cells treated with novobiocin alone. Genistein showed a similar phenotype to MβC, but the fibronectin matrix recovery was considerably lower in cells treated with a combination of genistein and novobiocin (Figure 25).

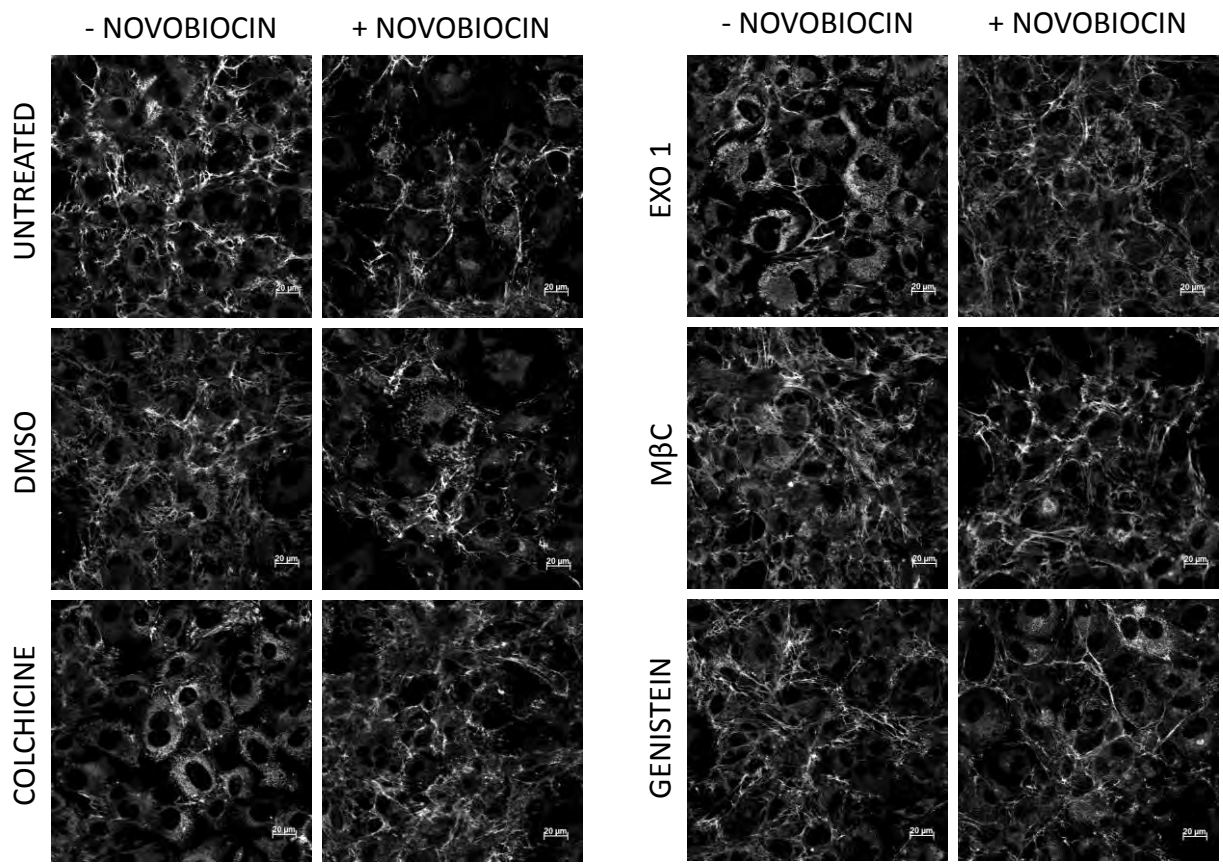

Figure 25: Screening of endocytosis and exocytosis inhibitors for the ability to reverse the loss of the fibronectin matrix following inhibition of Hsp90 with novobiocin.

Confluent Hs578T cells were allowed to adhere overnight at 37°C. The following day, cells were treated with inhibitors of vesicular trafficking (Colchicine, Exo 1, Methyl-β-Cyclodextrin and Genistein), either alone (- NOVOBIOCIN) or in combination with novobiocin (+ NOVOBIOCIN; 1 mM) and incubated for 7 hours at 37°C. Cells treated with the vesicular trafficking inhibitors alone served as a control. Cells were fixed and incubated with mouse primary anti-fibronectin (1:100) followed by anti-mouse Alexa-Fluor-488 secondary antibody (1:500). Images were captured using the Zeiss LSM 510 Meta laser scanning confocal microscope 40x oil objective and analysed using AxiovisionLE 4.7.1 (Zeiss, Germany). Three images were captured for each treatment in areas where similar cell numbers were observed. Scale bars represent 20 µm.

These data suggested that MβC showed the most promising results for reversing the fibronectin phenotype associated with novobiocin treatment. Cells were treated with a low (50 μM), medium (500 μM) or high (5 mM) dose of MβC in the absence or presence of novobiocin (1 mM) and the effect on the fibronectin morphology was observed via confocal microscopy (Figure 26). Untreated cells showed the typical dense fibronectin matrix in the absence of novobiocin (mean gray value of 37.63 ± 1.11), which was subsequently lost when cells were treated with novobiocin (mean gray value of 25.46 ± 5.70). With an increasing dose of MβC alone, very little effect was seen on the fibronectin morphology when compared to untreated cells. In cells treated with MβC and novobiocin, a dose-dependent increase in the extracellular fibronectin matrix was observed with increasing doses of MβC at a fixed concentration of novobiocin. This effect was made evident when the mean gray value for each frame was determined. When cells were treated with novobiocin and the lowest concentration of MβC (0.05 mM), the mean gray value (19.54 ± 2.88) was similar to cells treated with novobiocin alone (25.46 ± 5.70). However, when cells were treated with novobiocin and increasing doses MβC (0.5 m and 5 mM), the mean gray values increased to 28.39 ± 4.63 and 33.60 ± 4.24 respectively, with the highest concentration reporting a value similar to that reported for untreated cells (37.63 ± 1.11).

3.1.17 Colocalization analysis between endosomal/lysosomal marker proteins and fibronectin in novobiocin-treated Hs578T cells

We decided to investigate using confocal microscopy whether fibronectin within the vesicle-like structures described previously colocalized with certain endocytic markers. The markers used included an early endosome (Rab-5), a late endosome (Rab-7) and a lysosomal protein (LAMP-1) (Burgdorf *et al.*, 2007). For all three marker proteins, there was no colocalization with fibronectin in untreated cells as measured by the Pearson's correlation coefficient (R). This value has a range from -1 to +1, where -1 represents absolute exclusion or perfect negative correlation, +1 represents a perfect positive correlation and 0 represents random overlap (Adler and Parmryd, 2010).

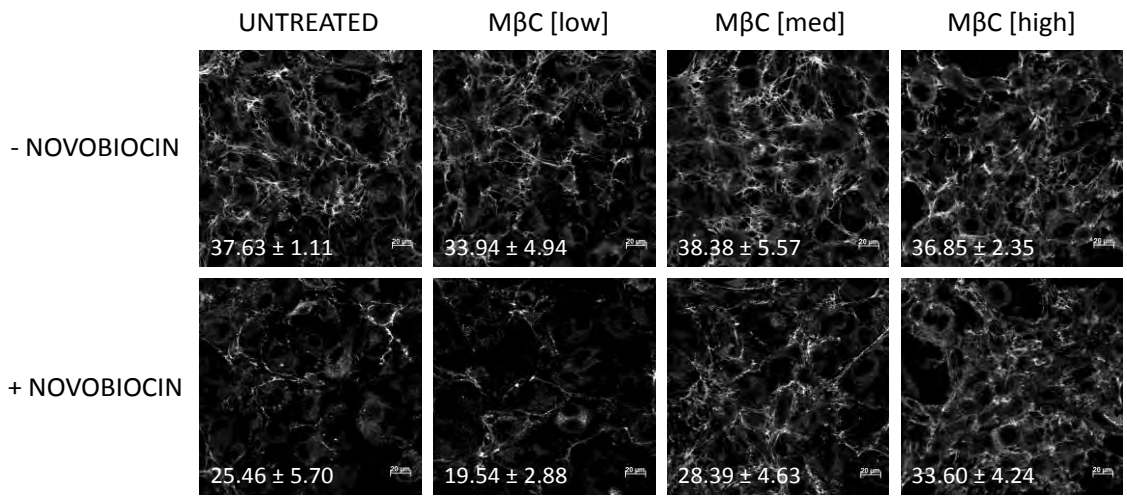

Figure 26: Methyl-β-Cyclodextrin (MβC) was able to reverse the reduced fibronectin matrix following inhibition of Hsp90 with novobiocin.

Confluent Hs578T cells were allowed to adhere and form the fibronectin matrix overnight at 37°C. The following day, cells were treated with an increasing dose of methyl-β-cyclodextrin (MβC; 50 μM, 500 μM, 5 mM) and incubated for 1 hour prior to treating the cells with novobiocin (+ NOVOBIOCIN; 1 mM) for 7 hours at 37°C. Cells treated with the endocytosis inhibitor alone (- NOVOBIOCIN) served as a control. Cells were harvested, fixed and incubated with mouse primary anti-fibronectin (1:100) followed by anti-mouse Alexa-Fluor-488 secondary antibody (1:500). Images were captured using the Zeiss LSM 510 Meta laser scanning confocal microscope 40x oil objective and analysed using AxiovisionLE 4.7.1 (Zeiss, Germany). Three images were captured for each treatment in areas where similar cell numbers were observed. Scale bars represent 20 μm. Values (in white) at the bottom of each frame represent the mean gray values (± standard deviation) for each treatment. Data are representative of three independent experiments with similar results.

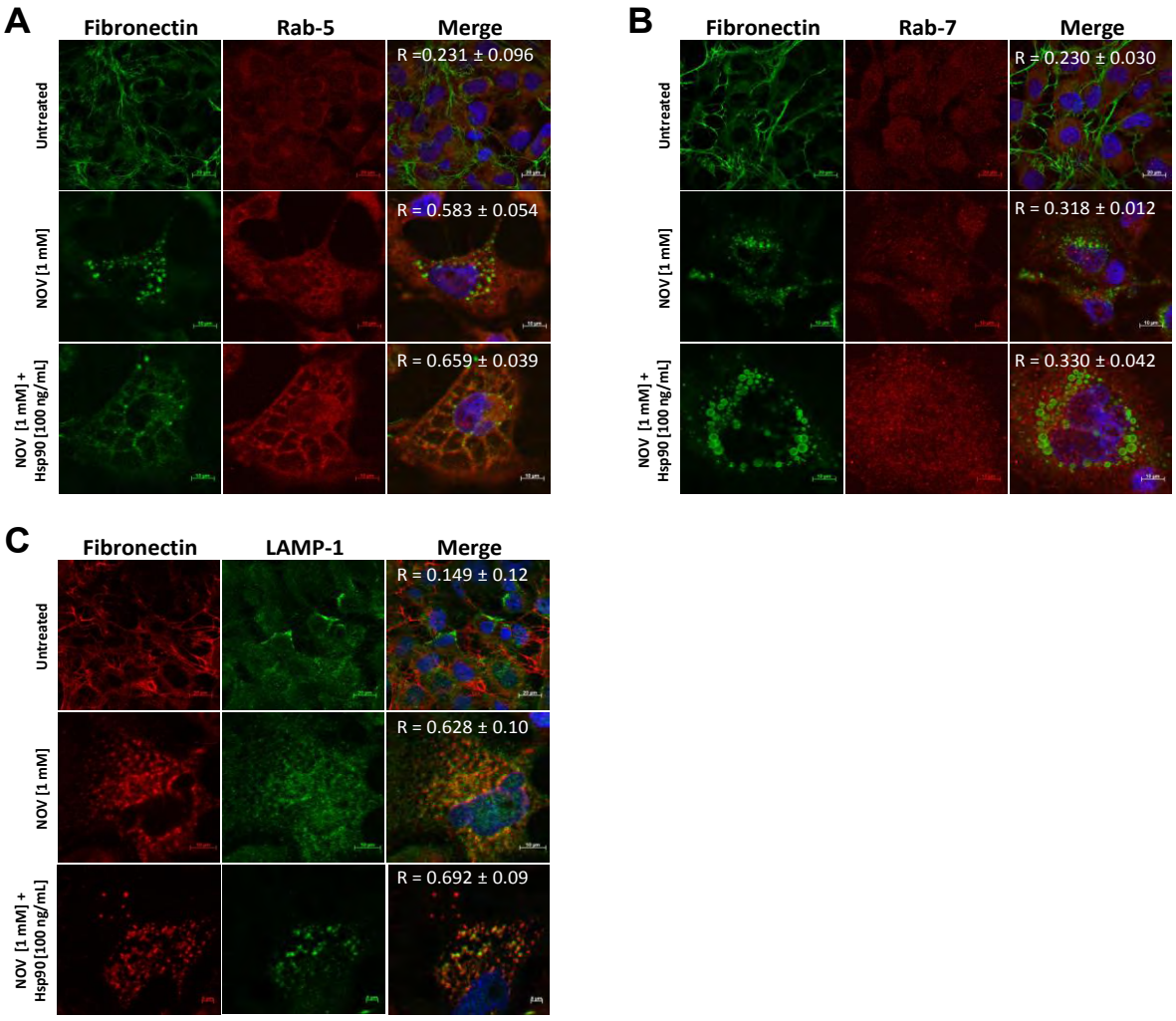

Figure 27: Fibronectin co-localized with the early endosomal marker (Rab-5) and the lysosomal marker (LAMP-1), but not with a late endosomal marker (Rab-7) following novobiocin treatment.

Hs578T breast cancer cells were seeded onto sterile, glass coverslips and were treated either with novobiocin (NOV; 1 mM) alone or with a combination of novobiocin and Hsp90β (100 ng/ml) for 16 hours at 37°C. Cells were harvested, fixed and incubated with primary antibodies against (**A**) Rab-5, (**B**) Rab-7 and (**C**) LAMP-1 followed by anti-mouse Alexa-Fluor-488 (green) and anti-rabbit Alexa-Fluor-555 (red) secondary antibodies. Nuclei were stained with 1 µg/ml Hoechst 33342. Images were captured using the Zeiss LSM 510 Meta laser scanning confocal microscope and analysed using AxiovisionLE 4.7.1 (Zeiss, Germany). Scale bars are represented on each image frame. Data are representative of two independent experiments with similar results. Co-localization analysis was achieved using ImageJ software. Values (in white) represent the Pearson's correlation coefficient (R) for each treatment.

The Pearson's correlation coefficients for untreated cells were 0.231 ± 0.096, 0.230 ± 0.030 and 0.149 ± 0.12 for Rab-5, Rab-7 and LAMP-1 with fibronectin respectively, which are within a range considered to represent random overlap and suggested that there was no colocalization between these signals (Figure 27). In cells treated with novobiocin, there was a partial colocalization between fibronectin and Rab-5 (R = 0.583 ± 0.054) which became more pronounced when exogenous Hsp90β was added to the cells (R = 0.659 ± 0.039). Interestingly, treatment with both Hsp90β and novobiocin induced a similar morphology to previous experiments whereby fibronectin was localized in reticular structures. Colocalization was observed between fibronectin and Rab-5 within these structures (Figure 27A). While colocalization was established with the early endosomal marker, Rab-5, fibronectin did not appear to colocalize with the late endosome marker, Rab-7, regardless of whether cells were treated with novobiocin or a combination of novobiocin and Hsp90β. The Pearson's correlation coefficients for all three treatments were below 0.5 and tended towards random as opposed to a strong linear correlation (Figure 27B). Fibronectin, however, showed a positive colocalization signal with LAMP-1 with a Pearson's correlation coefficient of 0.628 ± 0.10 for novobiocin-treated cells and 0.692 ± 0.09 for cells treated with novobiocin and exogenous Hsp90β (Figure 27C).

Chapter 4 :

Discussion

4.1 A novel role for Hsp90 in extracellular fibronectin matrix dynamics

According to our knowledge, this was the first study to provide several pieces of evidence that linked Hsp90 chaperone function to extracellular fibronectin matrix assembly. Broadly, our data showed that Hsp90 was found extracellularly in breast cancer and could be isolated in complex with fibronectin both *ex vivo* and *in vitro*. Furthermore, the extracellular fibronectin matrix was shown to be regulated by Hsp90. Exogenous Hsp90 demonstrated an ability to increase the insoluble fibronectin matrix while, in contrast, Hsp90 knockdown or inhibition with novobiocin resulted in the internalization and proposed turnover of the fibronectin matrix. Based on these data and together with published information on Hsp90 function and fibronectin dynamics, we propose a model that described the putative role of Hsp90 in fibronectin matrix dynamics (Figure 28).

Intracellular Hsp90 may be important for the stability and/or export of soluble fibronectin to the cell exterior (Stage 1). Upon secretion, we proposed that extracellular Hsp90 was required for either the stability of the insoluble fibronectin matrix or played an active role in facilitating the unfolding and maturation of fibronectin fibrils (Stage 2). When Hsp90 was transiently silenced or activity was inhibited with novobiocin (Stage 3), we proposed that fibronectin matrix instability resulted and the matrix was targeted for degradation through an endocytic pathway. Stage 4 illustrates the potential pathway used for the endocytic internalization of extracellular fibronectin. We proposed that fibronectin was incorporated into endosomes that were trafficked to lysosomes (LAMP-1) via Rab-5 and an unknown intermediary Rab protein (potentially Rab-9). Each of these stages is discussed and critiqued in more detail throughout this section.

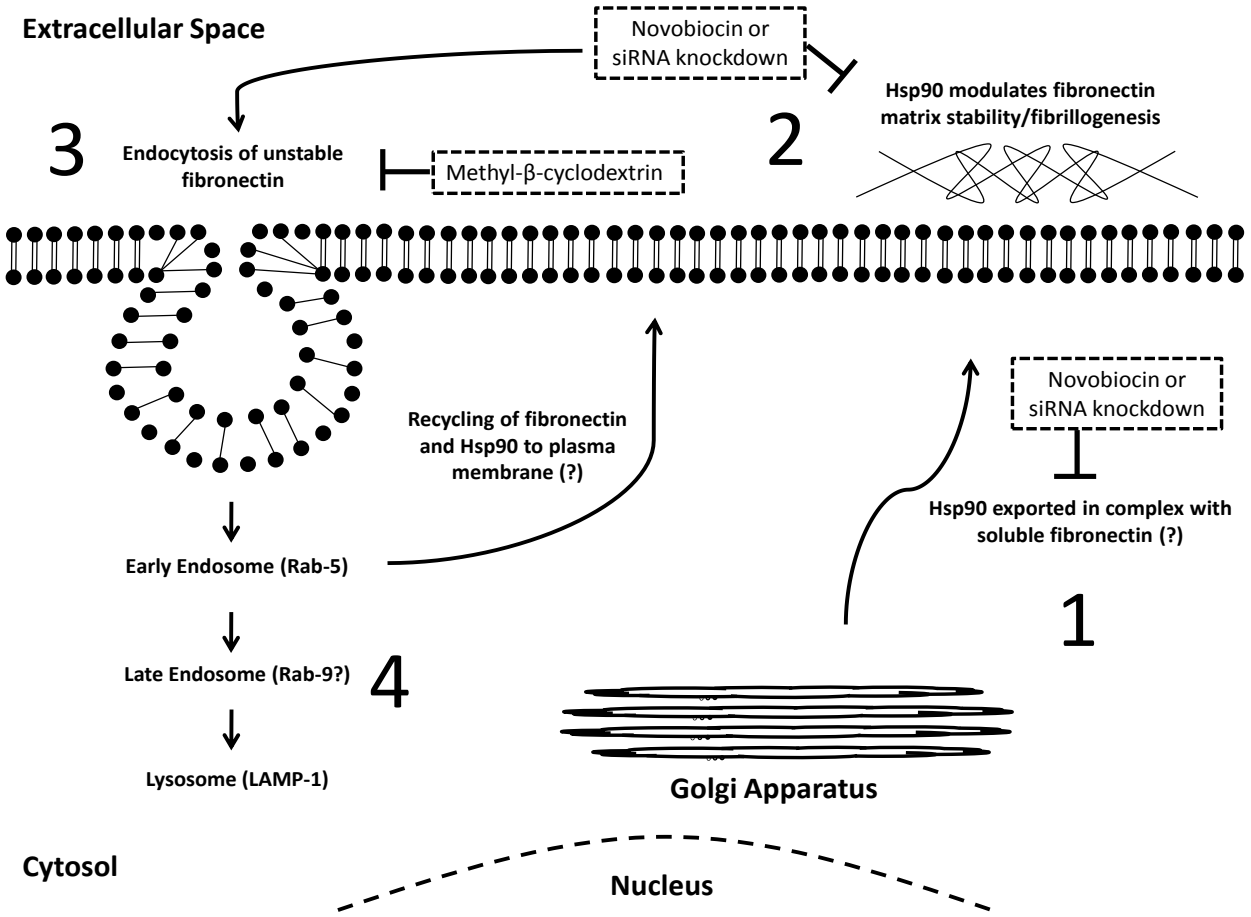

Figure 28: Schematic model of the putative role of intracellular and extracellular Hsp90 in fibronectin matrix assembly.

(1) Intracellular Hsp90 may be required to maintain soluble fibronectin in a stable, inactivated state and chaperones the matrix protein to the cell exterior for assembly. (2) Upon secretion, the β_1-integrin binds the RGD motif on the fibronectin molecule, initiating the unfolding and aggregation of insoluble fibronectin fibres. Extracellular Hsp90 may be required to assist in this unfolding process or to maintain the stability of the insoluble fibronectin matrix. Hsp90 knockdown or inhibition with novobiocin interrupts the interaction between Hsp90 and fibronectin, causing fibronectin matrix instability. (3) The unstable fibronectin matrix is then targeted for degradation via receptor-mediated endocytosis, which can be blocked by the presence of endocytosis inhibitors such as methyl-β-cyclodextrin. (4) Internalized fibronectin is trafficked to lysosomes (LAMP-1) for degradation via the intermediary vesicles expressing Rab-5 and possibly Rab-9, but not via Rab-7. It is possible that endocytosed Hsp90 may also mediate the recycling of itself and fibronectin in complex with Rab11a.

4.1.1 Hsp90 was found extracellularly in breast cancer cells

With the aim of characterizing new clients of extracellular Hsp90, we screened a panel of 5 cancer cell lines to determine whether Hsp90 was expressed extracellularly. We showed that Hsp90α and Hsp90β were highly expressed in cancer cell lines of different origin, cell type and malignancy. Furthermore, immunofluorescence supported that Hsp90α/β were abundant intracellular proteins that localized diffusely throughout the cytoplasm and nucleus and extended to the membrane periphery of some cells. Literature has claimed that high Hsp90 expression was associated with poor prognoses and was proportional to its metastatic potential of cancer cells (Banerji, 2008; Pick *et al.*, 2007). In addition, some have reported differential expression of the individual cytosolic Hsp90 isoforms, with greater inducibility of Hsp90α observed in laryngeal (Shi *et al.*, 1998), rat gliosarcoma (Chang *et al.*, 2006) and breast cancer cells (Perotti *et al.*, 2008; Yano *et al.*, 1996). Our data were consistent with these claims and suggested that cells characterized as highly aggressive (MDA-MB-231, Hs578T and SW620 cells) expressed higher levels of Hsp90α/β relative to the non-metastatic counterparts (MCF-7 and SW480 cells). This trend was reproduced when the relative expression of Hsp90α or Hsp90β were compared. This is the first report to have compared the levels of Hsp90α or Hsp90β expressed within these particular cell lines. This may suggest that cancers of different origin and cell type exhibit different chaperone expression profiles.

Interestingly, Hsp90β exhibited a unique localization as punctate structures within the nucleus. These structures may represent areas of gene transcription regulation by Hsp90 and its associated transcription factor, heat shock factor-1 (HSF-1) (Jolly *et al.*, 1997). Alternatively, Hsp90 has also been shown to interact with RNA-binding proteins to facilitate ribonuclear protein (RNP) assembly (Holt *et al.*, 1999). In addition to nuclear punctate structures, the Hsp90β staining pattern in Hs578T breast cancer cells was reminiscent of cytoskeletal actin stress fibers (Pellegrin and Mellor, 2007). From as early as the 1980s, it has been established that Hsp90 was an actin-binding protein and facilitated actin dynamics through interacting with key regulatory proteins, such as N-WASP (Koyasu *et al.*, 1986; Park *et al.*, 2005; Taiyab and Rao, 2010). These data would suggest that Hsp90α and Hsp90β may possess roles specific to its location.

While immunofluorescence suggested that a portion of Hsp90α/β was localized at the periphery of some cancer cells, there was no evidence to discriminate whether Hsp90 was localized intracellularly or extracellularly. Studies would suggest that at least a portion of Hsp90 resided extracellularly (Tsutsumi *et al.*, 2008), but whether Hsp90 fulfills its function as an integral membrane protein or a secreted soluble protein that associates with the membrane is still under scrutiny. Using surface biotinylation of extracellular-facing proteins, we provided evidence to support that at least a portion of the Hsp90α/β observed at the cell periphery was extracellular. This was further supported by the almost complete loss in the affinity purified Hsp90 fraction following digestion with the extracellular protease, trypsin. In addition to these data, an ELISA against Hsp90α showed that a portion of extracellular Hsp90α was found in a soluble form in the cell culture supernatant of all the cancer cell lines studied. Collectively, these data were consistent with literature which has demonstrated that two distinct pools of extracellular Hsp90 may exist (Eustace *et al.*, 2004). Whether the extracellular membrane-associated pool of Hsp90 was derived from the extracellular soluble pool (or vice versa) or whether the two pools of extracellular Hsp90 had fundamentally distinct origins has yet to be determined. It has been proposed that cytosolic Hsp90 was secreted via a non-conventional pathway, potentially trafficked by exosomes (Hegmans *et al.*, 2004; McCready *et al.*, 2010). However, it still remains possible that extracellular Hsp90 existed as a membrane-bound protein that became an extracellular soluble protein after cleavage from the membrane surface, as has been demonstrated for other ectodomain proteins such as tumor necrosis factor-α (Black *et al.*, 1997). The limitation of our study was that the data was incomplete in describing the specific Hsp90 isoforms found extracellularly. While the surface biotinylation assay identified extracellular Hsp90α/β, the ELISA was limited to identifying extracellular soluble Hsp90α. Futhermore, the surface biotinylation assay was limited in that it did not describe whether both isoforms were expressed on the cell surface or whether a preference was assigned for either Hsp90α or Hsp90β. Currently, there is a considerable amount of controversy surrounding whether Hsp90α or Hsp90β (or both) are found extracellularly (Eustace *et al.*, 2004; Hegmans *et al.*, 2004). In addition to this, the discovery of a

truncated Hsp90 isoform, known as Hsp90N, suggested that the extracellular, membrane-bound Hsp90 isoform was a distinct gene (Grammatikakis *et al.*, 2002). Our data did not show the presence of a 75 kDa Hsp90 isoform, as has been described for Hsp90N, suggesting that either Hsp90N expression was limited to specific cancer cell types (such as the pancreatic cancer from which it was isolated) or that Zurawska and colleagues (2008) were correct in their assumption that Hsp90N was an artifact and not representative of a classical Hsp90 isoform (Zurawska *et al.*, 2008). Nonetheless, consistent with literature, we were able to show that cytosolic Hsp90α and/or Hsp90β were found extracellularly. As a consequence, we selected MDA-MB-231 breast cancer cells as the model cell line to characterize the client proteome of extracellular Hsp90. The rationale for this decision was based on the high expression of total cytosolic Hsp90 and the dominant putative membrane staining pattern for Hsp90 observed by confocal microscopy within this cell line.

4.1.2 Fibronectin may be a putative client protein for extracellular Hsp90 in breast cancer

It is well established that Hsp90 is able to interact with a diverse range of protein substrates to promote correct protein folding and proper function. These substrates have been termed Hsp90 'client proteins' (Taipale *et al.*, 2012). This study aimed at better elucidating the extracellular Hsp90 client proteome in breast cancer cells. Using a cell-impermeable crosslinker with a spacer arm of 12Å, we were able to immunoprecipitate a complex from MDA-MB-231 breast cancer cells that suggested a putative direct interaction between Hsp90β and the extracellular matrix protein, fibronectin. The mass spectrometry data showed the presence of both Hsp90α and Hsp90β in the list of hits, but reported a higher number of query matches and higher relative protein abundance for Hsp90β. This may be due to the fact that the anti-Hsp90α/β antibody used to immunoprecipitate the complex preferentially bound the β-isoform. Furthermore, *in vitro* pull down assays and surface plasmon resonance (SPR) spectroscopy suggested that Hsp90β interacted with soluble fibronectin both in solution and on a solid surface respectively. While the SPR data represented an incomplete

study, it provided preliminary evidence to suggest an interaction with weak affinity indicated by a slow, gradual association and rapid dissociation. Fibronectin is an important extracellular regulator of cell migration, morphology and adhesion and may rely on weak, transient binding of associated proteins as opposed to more permanent, higher affinity binding. As a consequence, covalent crosslinking of proteins that interact with fibronectin (as was done here) may be required to successfully pull down the complex by immunoprecipitation. This type of weak binding has been described for numerous interactions associated with cell migration and adhesion (Anton *et al.*, 1994; Dustin *et al.*, 1997; Friedl *et al.*, 1998; Loskutoff *et al.*, 1999; Palecek *et al.*, 1999); roles that are consistent with those alluded for extracellular Hsp90. Additional support for a putative interaction between Hsp90 and fibronectin was shown following inhibition of Hsp90 with the published inhibitors, geldanamycin and novobiocin. Numerous authors have reported that Hsp90 client proteins become ubiquitinated and subsequently degraded by proteasomes following inhibition of Hsp90 with either of the aforementioned inhibitors (Blagg and Kerr, 2005; Donnelly and Blagg, 2008; Parsell and Lindquist, 1993; Qing *et al.*, 2006; Theodoraki and Caplan, 2012). We observed a dose-dependent decrease in total fibronectin levels upon Hsp90 inhibition in Hs578T breast cancer cells, suggesting that fibronectin may be a putative Hsp90 client in MDA-MB-231 cells (as originally isolated) because it acted as canonical client in Hs578T cells. To ensure that the decrease in total fibronectin was not a result of cell death, it would be necessary to test the cells for apoptosis by flow cytometry staining for apoptotic markers, such as propidium iodide or annexin V.

Fibronectin is a protein that exists in two conformations: an inactive, soluble conformation that, upon secretion from the cell, is unfolded by numerous cell processes that allow the formation of an active, insoluble matrix (Wierzbicka-Patynowski and Schwarzbauer, 2003). Given the characteristic model for folding of client proteins achieved by Hsp90, it is not uncommon for Hsp90 to hold a protein in one conformation, allow maturation/activation and subsequently release the substrate when the secondary, active conformation has been acquired (Buchner, 1999). This has represented a model for the folding of numerous client proteins, such as steroid

hormone receptors, and might reflect an accurate model for the unfolding of fibronectin from a soluble to an insoluble conformation. The role of chaperones in facilitating the unfolding of proteins has been described in the formation of prion precursor proteins (PrP) (Jones and Tuite, 2005). Prion proteins initially exist as a cellular PrP (PrP^{c}) isoform that consists mostly of α-helical regions that remain soluble. Upon unfolding of the PrP^{c} isoform, the α-helices are converted to insoluble β-sheets that form the disease-causing scrapie isoform (PrP^{Sc}) (Harrison *et al.*, 1997). Hsp104, an ATP-dependent yeast chaperone, has been proposed to facilitate this disassembly and unfolding of prion amyloid aggregates (α-helical structures) into smaller, fragmented "seeds" that allow the nucleation and formation of these higher molecular weight β-sheet products (Jones and Tuite, 2005). Therefore, prion proteins represent an example of a protein that contains the same amino acid sequence, but are able to adopt two functional conformations with the assistance of chaperone-mediated folding/unfolding. Hsp90 has also demonstrated an ability to regulate the folding of numerous different major classes of proteins which do not share similar sequence motifs. Consequently, it has been proposed that the three-dimensional conformation of a protein, as opposed to its peptide sequence, may be more essential for chaperone-substrate interactions (Buchner, 1999). If this concept applies for the majority of Hsp90 client proteins, Hsp90 may be able to bind fibronectin in both its soluble and insoluble conformations to modulate fibronectin folding.

It has been established that other chaperones (or proteins with chaperone-like activity) bind extracellular matrix proteins and regulate their stability or conformation. Hsp47 (also known as colligin), initially discovered on the surface of murine parietal endoderm cells, has been reported to bind type IV collagen where it is important for the post-translational processing of procollagen into mature collagen fibrils. Although the mechanism is not well defined, it was shown that Hsp47 was secreted along the biosynthetic secretory pathway in complex with collagen to the cell surface where it was also proposed to act as a receptor for collagen fibrillogenesis (Sauk *et al.*, 2005). Similarly, a protein termed SPARC (Secreted Protein Acidic and Rich in Cysteine), which exhibited chaperone-like properties, has been reported to directly modulate the

extracellular collagen matrix, with SPARC-null cells producing defective fibrils of significantly smaller size (Emerson *et al.*, 2006; Martinek *et al.*, 2007). While it has been established that SPARC is not required for the fusion of collagen fibrils to form a dense matrix, it has been proposed that the chaperone-like protein is essential for the maturation of collagen fibrils that are capable of fusion in later stages of fibrillogenesis, similar to the model described for infectious prion proteins (Bradshaw, 2009). The ER chaperone, calreticulin, has been shown to bind the extracellular matrix proteins, fibrinogen (B-β chain) and laminin on the surface of human fetal lung fibroblast and B16 mouse melanoma cells respectively (Gray *et al.*, 1995; White *et al.*, 1995). Furthermore, the ER Hsp90 isoform (GRP94) has also shown to be closely associated with the processing and transport of cartilage oligomeric matrix protein (COMP), a component of the extracellular matrix surrounding chondrocytes (Hecht *et al.*, 2001). Collectively, these data (combined with our own) suggest that chaperones are capable of binding extracellular matrix proteins and may possess novel, yet undefined roles in extracellular matrix dynamics. In particular, we proposed that fibronectin acted as a novel extracellular Hsp90 client protein and that Hsp90 may directly modulate fibronectin matrix assembly. While we predicted that the use of a cell-impermeable crosslinker would allow us to isolate extracellular complexes only, there is still the possibility that the crosslinker was internalized by the cell (possibly through endocytosis or phagocytosis), allowing the crosslinking of intracellular proteins. Nonetheless, whether Hsp90 and fibronectin were crosslinked intracellularly or extracellularly, to the best of our knowledge, this is the first study to suggest a direct interaction between the two proteins.

4.1.3 Hsp90 was involved in fibronectin matrix dynamics

Given that Hsp90 is a known regulator of protein folding, its putative interaction with fibronectin may provide novel insight into fibronectin matrix dynamics. We showed that the addition of exogenous Hsp90β to Hs578T cells increased the proportion of insoluble fibronectin in a dose-dependent manner relative to the exogenous BSA control, suggestive of a role for extracellular Hsp90 in fibronectin fibrillogenesis (Figure 25, Stage 2). Furthermore, the knockdown or pharmacological inhibition of Hsp90α/β

proved to be detrimental to the extracellular fibronectin matrix, with decreased levels of soluble and insoluble fibronectin and the appearance of intracellular vesicular-like structures reminiscent of exosomes or endosomes. This reduction in the fibronectin matrix following these treatments, however, could not be recovered by the addition of exogenous Hsp90β alone. These data collectively suggested a function for Hsp90 in fibronectin matrix assembly and/or stability at both an intracellular and extracellular level (Figure 25, Stage 1 and Stage 2). Interestingly, while soluble and insoluble fibronectin were sensitive to the siRNA knockdown of both Hsp90α and Hsp90β, fibronectin stability appeared to be more sensitive to the knockdown of Hsp90α. This was surprising since the complex isolated from MDA-MB-231 cells alluded to an interaction with Hsp90β. These data might be a result of the increased cell death associated with Hsp90α knockdown as opposed to the levels of cell death observed following Hsp90β knockdown. Alternatively, these results might have suggested that the interaction between fibronectin and Hsp90 may not be isoform specific. This was consistent with literature which has reported that, regardless of the distinct roles for each Hsp90 isoform, the list of protein clients was largely redundant (Kurokawa *et al.*, 2008). However, there has been evidence to suggest that Hsp90α and Hsp90β are able to bind the same client proteins to varying degrees, suggestive that each isoform may have unique chaperoning activities depending on the client protein involved. This preferential binding has been described specifically for Hsp90β and the apoptotic proteins, Apaf-1 and Bcl-2 (Kuo *et al.*, 2012; Kurokawa *et al.*, 2008; Voss *et al.*, 2000). If true, this might reflect that binding of fibronectin to Hsp90 was preferentially assigned to Hsp90α. To test this, however, a detailed binding kinetics study between fibronectin and each Hsp90 isoform would be required. Furthermore, as endotoxin free commercial preparations were only available for the Hsp90β protein, we would still need to test the effect of exogenous Hsp90α on the recovery of the fibronectin matrix following novobiocin treatment. This would be particularly relevant given the possible greater sensitivity of fibronectin stability to Hsp90α. In support of this, the studying of individual Hsp90 isoforms has become increasingly important based on evidence that Hsp90β was essential for placental development in mice, with homozygous knockout transgenic lines exhibiting lethal phenotypes a few days into embryogenesis even in the presence of

fully functional Hsp90α (Voss *et al.*, 2000). This may suggest that while Hsp90α and Hsp90β might have a level of redundancy in the client proteins that they bind, it may not be feasible to extend this redundancy to the level of Hsp90 function.

Pharmacological inhibition of Hsp90 with geldanamycin or novobiocin also exhibited an interesting phenotype whereby each inhibitor elicited a unique and differential effect on soluble and insoluble fibronectin. Novobiocin induced a dose-dependent decrease in both the soluble and insoluble levels of fibronectin coupled with an increase in intracellular fibronectin staining within small, vesicular structures. In contrast, geldanamycin did not have any effect on fibronectin levels, but appeared to induce the formation of a more ordered, fibrillar network. The difference between the effects of each inhibitor might be explained by the sites at which they bind Hsp90. Geldanamycin is known to bind the N-terminal ATPase domain of intracellular Hsp90 and prevents its ability to establish an active conformation (Schnaider *et al.*, 2000; Stebbins *et al.*, 1997). Consequently, intracellular Hsp90 has been well characterized as an ATP-dependent chaperone. Some have, however, claimed that this Hsp90 ATPase function may not be required extracellularly and that the middle and charged linker regions of the protein are more actively involved in its extracellular function (Cheng *et al.*, 2008). Furthermore, it is well established that ATP exists in micromolar concentrations in the extracellular space (Gordon, 1986), possibly below an appropriate concentration for regulating extracellular Hsp90 function. This might explain why geldanamycin had no observable effect on the fibronectin matrix. In contrast, novobiocin binds the C-terminal pocket of Hsp90 and is a competitive binder of numerous co-chaperones (Hop, p23, immunophilins and Cdc37) essential for intracellular Hsp90 client transfer and *in vivo* function (Donnelly and Blagg, 2008). While the specificity of novobiocin has been questioned, to date reports have indicated that the only other target of inhibition was bacterial gyrase II (Donnelly and Blagg (2008), suggesting a degree of selectivity against Hsp90. Yun *et al.* (2004) reported that treatment with novobiocin led to a reduced interaction between Hsp90 and the co-chaperones: p23 and FKBP52. Interestingly, Hsp90 has been shown to be highly complexed with p23 and Hop in Hs578T breast cancer cells when compared to the paired, non-cancerous Hs578BsT equivalent, suggestive of the importance of these co-

chaperones in our cell line (Kamal *et al.*, 2003). Given that Hsp90 has been shown to form extracellular multi-chaperone complexes in association with client proteins (Sims *et al.*, 2011), our data might have suggested that extracellular Hsp90 may be dependent on these or other co-chaperones for binding and chaperoning fibronectin. Recent studies have identified an extracellular Hsp90 multi-chaperone complex in the conditioned media of breast cancer cells composed of many of the major components of the intracellular complex, including Hsp70, Hsp40, Hop and p23 (Sims *et al.*, 2011). Furthermore, addition of these chaperones and co-chaperones was able to enhance the activation of matrix metalloproteinase-2 (MMP-2), an extracellular protease responsible for collagen breakdown (Sims *et al.*, 2011; Walsh *et al.*, 2011). While we were able to show that fibronectin immunoprecipitated with Hsp90β in the absence of these accessory proteins, one cannot ignore the limitations of an *in vitro* system for studying dynamic protein-protein interactions.

It is also highly probable that post-translational modifications of extracellular Hsp90 might render a change in the ability of the chaperone to bind or act on extracellular substrates. Scroggins and colleagues (2006) demonstrated that acetylation of a single residue (K294) on the Hsp90 molecule determined the outcome of many functional properties including the ability of Hsp90 to bind substrates and co-chaperones. Given that the Hsp90β protein used in these assays was purified in a baculovirus system, it is probable that the protein was post-translationally modified in a different manner to a mammalian system.

However, one cannot ignore the possibility that the effect of novobiocin may be indirect as opposed to an effect at the level of the Hsp90-fibronectin interaction. For example, it is possible that the effect observed was via the degradation of key Hsp90 signaling client proteins such as extracellular regulated kinase 1/2 (ERK1/2); similar to the effect seen when MEK1/2 was inhibited with U1026. However, the phospho-ERK/ERK ratio increased relative to untreated cells (*data not shown*), suggesting that the mitogen activated protein kinase (MAPK) pathway was not inhibited. Another explanation might be provided by the actin-binding properties of Hsp90. It has been established in

literature that Hsp90 interacted with actin filaments and was directly involved in regulating cytoskeletal changes (Koyasu *et al.*, 1986; Park *et al.*, 2005; Taiyab *et al.*, 2010). Some have reported that chemical agents that interrupted the nucleation and polymerization of actin also disrupted fibronectin matrix assembly (Pelkmans *et al.*, 2002; Sottile and Hocking, 2002).

It is possible that Hsp90 may not regulate fibronectin polymerization directly, but serves a role in chaperoning fibronectin to the cell surface where polymerization can be initiated by integrin-binding. A similar mechanism has been described for fibulin-5, a protein with chaperone-like properties, and tropoelastin during the process of elastic fibre assembly (Midwood and Schwarzbauer, 2002). The authors proposed that fibulin-5 chaperones tropoelastin to the cell surface by binding to integrins via the RGD motif present within the epidermal growth factor-like repeat. Once secured at the plasma membrane, tropoelastin can then be released and translocated to a microfibril scaffold that allows the assembly of elastic fibres (Midwood and Schwarzbauer, 2002). In a similar manner, upon secretion from the cell, Hsp90 may be responsible for chaperoning fibronectin to specific focal adhesion points on the plasma membrane. Once secured at the cell surface, binding of the β1-integrin to the RGD motif on fibronectin may then initiate fibronectin polymerization. If this represented a similar model, interruption of the Hsp90-fibronectin interaction by novobiocin might compromise fibronectin matrix assembly.

While we initially isolated an extracellular complex containing Hsp90β and fibronectin, the inability of exogenous Hsp90β to recover the fibronectin matrix following Hsp90 knockdown or inhibition with novobiocin would suggest that fibronectin stability and/or transport was regulated at both an intracellular and extracellular level (Figure 25; Stage 1 and Stage 2). A concomitant dependency on both intra- and extracellular chaperone pools has been demonstrated for collagen stability by Hsp47 (Nagai *et al.*, 2000). Studies showed that knockdown of the chaperone resulted in aberrant pro-collagen maturation along the biosynthetic secretory pathway as well as detrimental effects on the insoluble extracellular collagen matrix (Nagai *et al.*, 2000). This might reflect an

accurate model for the role of Hsp90 in fibronectin stability or transport. For example, intracellular Hsp90 may be required for the stability and/or transport of soluble fibronectin to the cell exterior (Figure 25, Stage 1) where extracellular Hsp90 was then required for the stability and/or unfolding of fibronectin into an insoluble matrix (Figure 25, Stage 2).

4.1.4 Inhibition of Hsp90 with novobiocin led to fibronectin internalization via a receptor-mediated endocytic pathway

Fibronectin matrix turnover is a major regulator of numerous important processes including cell migration, differentiation and tissue repair. Mechanistic insight into how this turnover occurs, however, has only recently been investigated. Sottile and Hocking (2002) have reported that the stability and maintenance of the extracellular fibronectin matrix was dependent on its continual polymerization into an insoluble matrix. Upon inhibition of this process, depolymerization of the fibronectin matrix was observed coupled with an increase in the degradation of fibronectin within lysosomes (Sottile and Hocking, 2002). Furthermore, evidence was provided to suggest that the deposition of other extracellular matrix (ECM) proteins, including collagen-I and thrombospondin-1, was dependent on an existing fibronectin network (Sottile and Hocking, 2002). These data alluded to a major role for fibronectin in the organization and assembly of the ECM. While ECM remodeling can occur extracellularly with the help of proteases such as plasmin and matrix metalloproteinases, it was recently shown that fibronectin turnover can occur intracellularly via a caveolin-1 dependent endocytic pathway to the lysosomes (Sottile and Chandler, 2005). While some have indicated that fibronectin endocytosis occurred in conjunction with the recycling of integrins, others have provided evidence that fibronectin catabolism was regulated by receptor-mediated endocytosis (Salicioni *et al.*, 2002), particularly via low density lipoprotein receptor-related protein (LRP-1). We have provided several supporting pieces of evidence to suggest that inhibition of Hsp90 with novobiocin induced the uptake and reduction of the extracellular fibronectin matrix, proposed to occur via receptor-mediated endocytosis (Figure 25, Stage 3 and Stage 4).

Some might argue that the reduction in the fibronectin matrix observed may have resulted from interference in the secretion of soluble fibronectin to the cell exterior. A loss in its secretion coupled with the natural turnover of the fibronectin matrix (as a result of changes in cell migration, morphology and adhesion) could have provided a feasible alternative explanation for our data. This is particularly relevant since other common Hsp90 inhibitors have been reported to have detrimental effects on the vesicular trafficking of proteins out of the cell (Lotz *et al.*, 2007). These authors showed that the intra-Golgi transport of the Vesicular Stomatitis Virus Glycoprotein (VSVG) in a cell-free system was sensitive to the Hsp90 inhibitors: geldanamycin, radicicol and macbecin (Lotz *et al.*, 2007). They proposed that the mechanism by which Hsp90 was involved in intracellular transport was through the docking and tethering of transport vesicles through the ATPase-dependent chaperoning of Rab proteins (Lotz *et al.*, 2007). Another study reported that both ER-to-Golgi and intra-Golgi transport were blocked in cells treated with the geldanamycin analogues, 17-(dimethylaminoethylamino)-17-demethoxygeldanamcyin (17-DMAG) and 17-AAG (Chen and Balch, 2006). However, the limitation of the aforementioned studies was the use of Hsp90 inhibitors that bound the N-terminal ATPase domain only. According to our knowledge, this is the first study to have investigated the effect of a C-terminal Hsp90 inhibitor on the trafficking of proteins. Our data would suggest that the site at which the Hsp90 inhibitors bind were critical for the phenotype observed. This was in agreement with the observations that the N-terminal and C-terminal Hsp90 inhibitors exhibited differential effects on the levels of soluble and insoluble fibronectin. Studies have reported that geldanamycin and novobiocin have differential effects on the activity of HSF-1, suggesting that our observations were not uncommon. Novobiocin was shown to decrease both DNA-binding and transcription of heat shock genes in the early stages of heat shock treatment whereas geldanamycin increased the stability of HSF-1 trimers and delayed their disassembly when the heat shock treatment was ceased (Conde *et al.*, 2009). Collectively, these data suggested that novobiocin might possess a novel effect on vesicular transport. It may be possible to assume that novobiocin, instead of affecting the export of intracellular proteins, may affect alternate trafficking pathways that could include the internalization of extracellular proteins. While our data would suggest this for

fibronectin, we did not investigate whether novobiocin blocked the export of intracellular proteins. This could be tested using a cell-free system transport assay, as was done for geldanamycin in studies by Lotz and colleagues (2007).

To support that novobiocin was indeed having an effect on transport of fibronectin into the cell as opposed to interfering with its secretion, we designed a set of experiments that would allow us to observe the effect of novobiocin on the levels of extracellular fibronectin only as well as to show whether novobiocin induced fibronectin uptake. To monitor the levels of extracellular fibronectin, we labeled purified soluble fibronectin with a fluorescent dye and added the labeled protein to cells. This experiment allowed us to observe the changes associated with an extracellular fluorescent matrix as opposed to total fibronectin observed when detected with fluorescent antibodies against fibronectin. Both a time-course inhibition study and live cell imaging showed evidence that novobiocin caused a time-dependent decrease in the extracellular fluorescent fibronectin matrix. This reduction in extracellular fibronectin was confirmed to occur via internalization by the cell based on the uptake of CFDA-SE-labeled fibronectin added to Hs578T cells. The conclusions reached for this study were based on the fluorescent dye, CFDA-SE, which remained non-fluorescent until the acetate groups had been cleaved by intracellular esterases (Wang *et al.*, 2005). In this manner, any fluorescence detected gave an indication of the level of internalized fibronectin. These data collectively provided evidence to support that novobiocin caused a decrease in the extracellular fibronectin matrix coupled with an increase in its uptake. Furthermore, we were able to show that the potential mechanism by which this occurred was through receptor-mediated endocytosis. We tested the effect of different inhibitors of vesicular trafficking on their ability to restore the fibronectin matrix following treatment with novobiocin. A panel of four inhibitors was screened including colchicine, methyl-β-cyclodextrin (MβC), Exo 1 and genistein. Colchicine is an inhibitor of microtubule-based transport through interference with the microtubule organizing centre (Hastie, 1991). MβC is a specific inhibitor of endocytosis associated with caveolae (particularly caveolin-1 mediated endocytosis), but has also shown activity against clathrin-dependent endocytosis. The mechanism of action involves the complexing of MβC with

cholesterol molecules in lipid rafts on the surface of the membrane. The cholesterol is subsequently removed from the membrane, compromising proper formation of endocytic vesicles (Marsh and Pelchen-Matthews, 2000). Exo 1 is a specific inhibitor of exocytosis through activating the Golgi ADP-ribosylation factor-1 GTPase (Feng *et al.*, 2003). Finally, genistein has been shown to inhibit certain tyrosine protein kinases that regulate signaling pathways related to vesicular trafficking (Ghazizadeh and Fleit, 1994). Genistein has also, however, shown activity against caveolae-mediated endocytosis (Rejman *et al.*, 2004). Our data showed that MβC exhibited the most promising results in reversing the fibronectin phenotype associated with the novobiocin treatment. MβC is a specific inhibitor of endocytosis and possesses few off-target effects on cells (Rodal *et al.*, 1999), which made it an attractive inhibitor with which to conduct further mechanistic studies. We showed that after blocking endocytosis with MβC, novobiocin was no longer able to induce the loss of the extracellular fibronectin matrix and the phenotype was reversed in a dose-dependent manner to levels similar to those observed for untreated cells (Figure 25, Stage 3).

To further support our hypothesis, we showed that fibronectin, within the small vesicular-like structures observed, colocalized with the early endosomal marker, Rab-5, and the lysosomal marker, LAMP-1, but not the late endosomal marker, Rab-7. These data agree with Sottile and Chandler (2002) and suggested that the final destination for the internalized fibronectin was most likely the lysosomes, but the pathway used excluded the intermediary protein, Rab-7. It is possible that a different intermediary Rab protein was used during fibronectin matrix turnover, such as Rab-9 (Ganley *et al.*, 2004) (Figure 25, Stage 4). Furthermore, a higher degree of colocalization and a change in fibronectin distribution was observed in cells treated with a combination of novobiocin and exogenous Hsp90β. Given that Hsp90 has been implicated in Rab recycling and intracellular vesicular transport (Chen and Balch, 2006; Lotz *et al.*, 2008), it may be possible that the exogenous Hsp90 was internalized in complex with fibronectin and involved in shuttling the fibronectin to different subcellular compartments (such as lysosomes or the endoplasmic reticulum) or alternatively back to the plasma membrane. Hsp90 has been reported to bind Rab11a which facilitated both the recycling of

extracellular α-synuclein to the plasma membrane as well as its degradation via an endosomal pathway to the lysosomes (Liu *et al.*, 2009). Consequently, Hsp90 may be serving a dual role in recycling the fibronectin matrix while also promoting its degradation via an endosomal-lysosomal pathway (Figure 25, Stage 4).

4.2 Implications of this study for drug development

Given this novel insight into the putative role of Hsp90 in fibronectin matrix dynamics, it is important to consider the therapeutic implications that this study might have for cancer and cancer metastasis. Hsp90 is a *bone fide* cancer drug target and a number of specific Hsp90 inhibitors are currently in clinical trial. It is possible that these compounds may be used to inhibit the interaction with fibronectin in relevant cancers. Current literature regarding the expression of fibronectin within different cancers is contradictory. Zheng and colleagues (2007) showed that nicotine induced the expression of fibronectin within non-small cell lung carcinoma (NSCLC) which resulted in the proliferation of the cancer cells. Hanamura and colleagues (1997) screened 29 adenocarcinomas and 5 non-neoplastic mucosa samples for the levels of fibronectin mRNA. Results suggested that the adenocarcinomas, particularly myofibroblasts, produced fibronectin mRNA in 96% of cells in comparison to zero mRNA detected in the non-neoplastic samples. The authors therefore proposed that fibronectin was a critical component for neoplastic transformation and cancer progression. Lastly, Yang and colleagues (2007) showed that fibronectin expression, regulated by the *Twist* transcription factor, was increased in gastric cancer and was associated with increased cancer cell invasion. In contrast to these findings, some have shown that normal cells demonstrate an ability to build a substantial extracellular fibronectin matrix which is subsequently lost upon oncogenic transformation. However, these authors suggested that the loss in fibronectin was not due to a decrease in fibronectin expression, but rather an inability for cells to deposit the matrix protein at the cell surface (Hayman *et al.*, 1981). Alongside these contradictory findings, others have argued over the role that fibronectin may serve in cancer progression and metastasis. Some have argued that the breakdown of the fibronectin matrix allowed cells to detach from their microenvironment and migrate to secondary locations (Duffy *et al.*, 1992). Others have argued that the

fibronectin matrix provided a scaffold to which cells can attach and subsequently migrate (McCarthy and Furcht, 1984). It is clear from this controversy that the role of fibronectin in cancer is more complex than originally thought and may need to be characterized before therapies are designed against this extracellular matrix protein or against proteins, such as Hsp90, that might regulate its assembly.

4.3 Conclusions

The biochemistry of intracellular Hsp90 has been well elucidated partly due to extensive research on its clientele and interacting partners. The biological function of extracellular Hsp90, however, remains largely uncharacterized. The limited research available has alluded to a role for extracellular Hsp90 in cell migration and invasion, potentially contributing to the metastatic process of cancer cells. However, the mechanism by which this is achieved is still under scrutiny. Eustace *et al.* (2004) have proposed that cancer cell invasion is facilitated by extracellular Hsp90 activating matrix metalloproteinase-2 (MMP-2). Others have proposed that extracellular Hsp90 activates tissue plasminogen activator (tPA) which converts plasminogen to plasmin, subsequently increasing cell motility and invasion. Our data suggests that Hsp90 may possess a more direct role in modulating extracellular matrix dynamics through a direct interaction with fibronectin.

Our data suggested that both intracellular and extracellular Hsp90 were involved in extracellular fibronectin matrix assembly, either through stabilizing the fibronectin molecule or through facilitating the folding of the fibrils into an insoluble fibronectin network. Furthermore, a reduction in Hsp90 levels or activity led to a reduced insoluble matrix, proposed to be mediated by receptor-mediated endocytosis and degradation of fibronectin in lysosomes. Interestingly, Salicioni and colleagues (2002) have reported that fibronectin catabolism can be facilitated through endocytosis involving the low density lipoprotein-like receptor-1 (LRP-1). Interestingly, LRP-1 has been shown to interact with Hsp90 resulting in the uptake and recycling of Hsp90 in macrophage and dendritic cells (Basu *et al.*, 2001). It would be interesting to investigate whether

fibronectin was endocytosed in complex with LRP-1 and Hsp90 following inhibition with novobiocin.

Chapter 5 :

References

Adler, J. and Parmryd, I. (2010). Quantifying Colocalization by Correlation: The Pearson Correlation Coefficient is Superior to the Mander's Overlap Coefficient. *Cytometry*, 77A: 733-742.

Aligue, R., Akhavan-Niak, J. and Russell, P. (1994). A role for Hsp90 in cell cycle control: Wee1 tyrosine kinase activity requires interaction with Hsp90. *EMBO J.*, 13(24): 6099-6106.

Allan, R.K., Mok, D., Ward, B.K. and Ratajczak, T. (2006). Modulation of Chaperone Function and Cochaperone Interaction by Novobiocin in the C-terminal Domain of Hsp90. *J. Biol. Chem.*, 281(11): 7161-7171.

Althoff, K., Müllberg, J., Aasland, D., Voltz, N., Kallen, K-J., Grötzinger, J. and Rose-John, S. (2001). Recognition sequences and structural elements contribute to shedding susceptibility of membrane proteins. *Biochem. J.*, 353: 663-672.

Annamalai, B., Liu, X., Gopal, U. and Isaacs, J.S. (2009). Hsp90 Is an Essential Regulator of EphA2 Receptor Stability and Signaling: Implications for Cancer Cell Migration and Metastasis. *Mol. Cancer. Res.*, 7: 1021-1032.

Anton, E.S., Weskamp, G., Reichhardt, L.F. and Matthew, W.D. (1994). Nerve growth factor and its low-affinity receptor promote Schwann cell migration. *Proc. Natl. Acad. Sci. USA*, 91: 2795-2799.

Argon, Y. and Simen, B.B. (1999). GRP94, an ER chaperone with protein and peptide binding properties. *Sem. Cell Develop. Biol.*, 10(5): 495-505.

Bagatell, R. and Whitesell, L. (2004). Altered Hsp90 function in cancer: A unique therapeutic opportunity. *Mol. Cancer Ther.*, 3: 1021-1030.

Banerji, U. (2008). Heat Shock Protein 90 as a Drug Target: Some Like It Hot. *Clin Cancer Res*, 15: 9-14.

Baneyx, G., Baugh, L. and Vogel, V. (2001). Fibronectin extension and unfolding within cell matrix fibrils controlled by cytoskeletal tension. *Proc. Natl. Acad. Sci.*, 99(8): 5139-5143.

Banz, V.M., Medová, M., Keogh, A., Furer, C., Zimmer, Y., Candinas, D. and Stroka, D. (2009). Hsp90 transcriptionally and post-translationally regulates the expression of NDRG1 and maintains the stability of its modifying kinase GSK3β. *Biochim. Biophys. Acta*, 1793: 1597-1603.

Basso, A.D., Solit, D.B., Chiosis, G., Giri, B., Tsichlis, B. and Rosen, N. (2002). Akt Forms an Intracellular Complex with Heat Shock Protein 90 (Hsp90) and Cdc37 and Is Destabilized by Inhibitors of Hsp90 Function. *J. Biol. Chem.*, 277(42): 39858-39866.

Basu, S., Binder, R.J., Ramalingam, T., and Srivastava, P.K. 2001. CD91 Is a Common Receptor for Heat Shock Proteins gp96, hsp90, hsp70, and Calreticulin. *Immunity* 14: 303-313

Becker, B., Multhoff, G., Farkas, B., Wild, P-J., Landthaler, M., Stolz, W. and Vogt, T. (2004). Induction of Hsp90 protein expression in malignant melanomas and melanoma metastases. *Exp. Dermatol.*, 13: 27-32.

Black, R.A., Rauch, C.T., Kozlosky, C.J., Peschon, J.J., Slack, J.L., Wolfson, M.F., Castner, B.J., Stocking, K.L., Reddy, R., Srinivasan, S., Nelson, N., Boiani, N., Schooley, K.A., Gerhart, M., Davis, R., Fitzner, J.N., Johnson, R.S., Paxton, R.J., March, C.J. and Cerretti, D.P. (1997). A metalloproteinase disintegrin that releases tumor-necrosis factor-α from cells. *Nature*, 385: 729-733.

Blagg, B.S.J. and Kerr, T.D. (2005). Hsp90 Inhibitors: Small Molecules That Transform the Hsp90 Protein Folding Machinery into a Catalyst for Protein Degradation. *Med. Res. Rev.*, 26(3): 310-338.

Blagosklonny, M.V., Toretsky, J., Bohen, S. and Neckers, L. (1996). Mutant conformation of p53 translated in vitro or in vivo requires functional HSP90. *Proc. Natl. Acad. Sci. USA*, 93: 8379-8383.

Bradshaw, A.D. (2009). The role of SPARC in extracellular matrix assembly. *J. Cell Commun. Signal.*, 3: 239-246.

Brenner, K.A., Corbett, S.A. and Schwarzbauer, J.E. (2000). Regulation of fibronectin matrix assembly by activated Ras in transformed cells. *Oncogene*, 19: 3156-3163.

Brychzy, A., Rein, T., Winklhofer, K.F., Hartl, F.U., Young, J.C. and Obermann, W.M.J. (2003). Cofactor Tpr2 combines two TPR domains and a J domain to regulate the Hsp70/Hsp90 chaperone system. *EMBO J.*, 22: 3613-3623.

Buchner, J. (1999). Hsp90 & Co. – a holding for folding. *TIBS*, 24: 136-141.

Bukau, B., Weissman, J. and Horwich, A. (2006). Molecular Chaperones and Protein Quality Control. *Cell*, 125: 443-451.

Burgdorf, S., Kautz, A., Böhnert, V., Knolle, P.A. and Kurts, C. (2007). Distinct Pathways of Antigen Uptake and Intracellular Routing in CD4 and CD8 T Cell Activation. *Science*, 316: 612-616.

Calderwood, S.K., Khaleque, M.A., Sawyer, D.B. and Ciocca, D.R. (2006). Heat shock proteins in cancer: chaperones of tumorigenesis. *TRENDS Biochem. Sci.*, 31(3): 164-172.

Candiano, G., Bruschi, M., Musante, L., Santucci, L., Ghiggeri, G.M., Carnemolla, B., Orecchia, P., Zardi, L. and Righetti, P.G. (2004). Blue silver: A very sensitive colloidal Coomassie G-250 staining for proteome analysis. *Electrophoresis*, 25: 1327-1333.

Cerchietti, L.C., Lopes, E.C., Yang, S.N., Hatzi, K., Bunting, K.L., Tsikitas, L.A., Mallik, A., Robles, A.I., Walling, J., Varticovski, L., Shaknovich, R., Bhalla, K.N., Chiosis, G. and Melnick, A. (2009). A purine

scaffold Hsp90 inhibitor destabilizes BCL-6 and has specific antitumor activity in BCL-6-dependent B cell lymphomas. *Nat. Med.*, 15: 1369-1376.

Chang, Y-S., Lo, C-W., Sun, F-C., Chang, M.D. and Lai, Y-K. (2006). Differential expression of Hsp90 isoforms in geldanamycin-treated 9L cells. *Biochem. Biophys. Res. Comm.*, 344: 37-44.

Chen, B., Piel, W.H., Gui, L., Bruford, E. and Monteiro, A. (2005). The HSP90 family of genes in the human genome: Insights into their divergence and evolution. *Genomics*, 86: 627-637.

Chen, C.Y. and Balch, W.E. (2006). The Hsp90 Chaperone Complex Regulates GDI-dependent Rab Recycling. *Mol. Biol. Cell*, 17: 3494-3507.

Chen, J-S., Hsu, Y-M., Chen, C-C., Chen, L-L., Lee, C-C. and Huang, T-S. (2010). Secreted Heat Shock Protein 90α Induces Colorectal Cancer Cell Invasion through CD91/LRP-1 and NF-κB-mediated Integrin α_v Expression. *J. Biol. Chem.*, 285(33): 25458-25466.

Cheng, C-F. and Li, W. (2008). Secretion of Heat Shock Protein-90 (Hsp90) by Normal Cells Under Stress or by Tumor Cells During Invasion: Why? *Cancer Ther.*, 6: 765-772.

Cheng, C-F., Fan, J., Fedesco, M., Guan, S., Li, Y., Bandyopadhyay, B., Bright, A.M., Yerushalmi, D., Liang, M., Chen, M., Han, Y-P., Woodley, D.T. and Li, W. (2008). Transforming Growth Factor α (TGFα)-Stimulated Secretion of HSP90α: Using the Receptor LRP-1/CD91 To Promote Human Skin Cell Migration against a TGFβ-Rich Environment during Wound Healing. *Mol. and Cell Biol.*, 28(10): 3344-3358.

Christopher, R.A., Kowalczyk, A.P. and McKeown-Longo, P.J. (1997). Localization of fibronectin matrix assembly sites on fibroblasts and endothelial cells. *J. Cell Sci.*, 110: 569-581.

Citri, A., Harari, D., Shohat, G., Ramakrishnan, P., Gan, J., Lavi, S., Eisenstein, M., Kimchi, A., Wallach, D., Pietrokovski, S. and Yarden, Y. (2006). Hsp90 Recognizes a Common Surface on Client Kinases. *J. Biol. Chem.*, 281(20): 14361-14369.

Conde, R., Belak, Z.R., Nair, M., O'Carroll, R.F. and Ovsenek, N. (2009). Modulation of Hsf1 activity by novobiocin and geldanamycin. *Biochem. Cell. Biol.*, 87(6): 845-851.

Crawford, D.C., Chobanian, A.V. and Brecher, P. (1994). Angiotensin II induces fibronectin expression associated with cardiac fibrosis in the rat. *Circ. Res.*, 74: 727-739.

Csermely, P., Schnaider, T., Söti, C., Prohászka, Z. and Nardai, G. (1998). The 90-kDa Molecular Chaperone Family: Structure, Function, and Clinical Applications. A Comprehensive Review. *Pharmacol Ther.*, 79(2): 129-168.

Dittmar, K.D., Demady, D.R., Stancato, L.F., Krishna, P. and Pratt, W.B. (1997). Folding of the Glucocorticoid Receptor by the Heat Shock Protein (hsp) 90-based Chaperone Machinery. *J. Biol. Chem.*, 272(34): 21213-21220.

Donnelly, A. and Blagg, B.S.J. (2008). Novobiocin and Additional Inhibitors of the Hsp90 C-Terminal Nucleotide-binding Pocket. *Curr. Med. Chem.*, 15(26): 2702-2717.

Dowling, P., Walsh, N. and Clynes, M. (2008). Membrane and membrane-associated proteins involved in the aggressive phenotype displayed by highly invasive cancer cells. *Proteomics*, 8: 4054-4065.

Duffy, M.J. (1992). The role of proteolytic enzymes in cancer invasion and metastasis. *Clin. Exp. Metastasis*, 10: 145-155.

Dustin, M.L., Golan, D.E., Zhu, D-M., Miller, J.M., Meier, W., Davies, E.A. and van der Merwe, P.A. (1997). Low Affinity Interaction of Human or Rat T Cell Adhesion Molecule CD2 with Its Ligand Aligns Adhering Membranes to Achieve High Physiological Activity. *J. Biol. Chem.*, 272(49): 30889-30898.

Eletto, D., Dersh, D. and Argon, Y. (2010). GRP94 in ER quality control and stress responses. *Sem. Cell Develop. Biol*., 21(5): 479-485.

Emerson, R.O., Sage, E.H., Ghosh, J.G. and Clark, J.I. (2006). Chaperone-Like Activity Revealed in the Matricellular Protein SPARC. *J. Cell. Biochem.*, 98: 701-705.

Eustace, B.K. and Jay, D.G. (2004). Extracellular Roles for the Molecular Chaperone, hsp90. *Cell Cycle*, 3(9): 1098-1100.

Eustace, B.K., Sakurai, T., Stewart, J.K., Yimlamai, D., Unger, C., Zehetmeier, C., Lain, B., Torella, C., Henning, S.W., Beste, G., Scroggins, B.T., Neckers, L., Ilag, L.L. and Jay, D.G. (2004). Functional proteome screens reveal an essential extracellular role for hsp90 alpha in cancer cell invasiveness. *Nat. Cell Biol.*, 6: 507-514.

Felts, S.J., Owen, B.A.L., Nguyen, P., Trepel, J., Donner, D.B. and Toft, D.O. (2000). The hsp90-related Protein TRAP1 Is a Mitochondrial Protein with Distinct Functional Properties. *J. Biol. Chem*., 275(5): 3305-3312.

Feng, Y., Yu, S., Lasell, T.K.R., Jadhav, A.P., Macia, E., Chardin, P., Melancon, P., Roth, M., Mitchison, T. and Kirchhausen, T. (2003). Exo1: A new chemical inhibitor of the exocytic pathway. *Proc. Natl. Acad. Sci.*, 100(11): 6469-6474.

Fernandis, A.Z., Prasad, A., Band, H., Klösel, R. and Ganju, R.K. (2004). Regulation of CXCR4-mediated chemotaxis and chemoinvasion of breast cancer cells. *Oncogene*, 23: 157-167.

Friedl, P., Zänker, K.S. and Bröcker, E-B. (1998). Cell Migration Strategies in 3-D Extracellular Matrix: Differences in Morphology, Cell Matrix Interactions, and Integrin Function. *Micro. and Res. Tech*., 43: 369-378.

Ganley, I.G., Carroll, K., Bittova, L. and Pfeffer, S. (2004). Rab9 GTPase Regulates Late Endosome Size and Requires Effector Interaction for Its Stability. *Mol. Biol. Cell*, 15: 5420-5430.

George, E.L., Georges-Labouesse, E.N., Patel-King, R.S., Rayburn, H. and Hynes, R.O. (1993). Defects in mesoderm, neural tube and vascular development in mouse embryos lacking fibronectin. *Development*, 119: 1079-1091.

Ghazizadeh, S. and Fleit, H.B. (1994). Tyrosine phosphorylation provides an obligatory early signal for Fc gamma RII-mediated endocytosis in the monocytic cell line THP-1. *J. Immunol.*, 152(1): 30-41.

Goes, F.S. and Martin, J. (2001). Hsp90 chaperone complexes are required for the activity and stability of yeast protein kinases Mik1, Wee1 and Swe1. *Eur. J. Biochem.*, 268: 2281-2289.

Gopal, U., Bohonowych, J.E., Lema-Tome, C., Liu, A., Garrett-Mayer, E., Wang, B. and Isaacs, J. (2011). A Novel Extracellular Hsp90 Mediated Co-Receptor Function for LRP1 Regulates EphA2 Dependent Glioblastoma Cell Invasion. PLoS ONE, 6(3): e17649. doi:10.1371/journal.pone.0017649.

Gordon, J.L. (1986). Extracellular ATP: effects, sources and fate. *Biochem. J.*, 233: 309-319.

Grammatikakis, N., Lin, J., Grammatikakis, A., Tsichlis, P. and Cochran, B. (1999). $P50^{cdc37}$ Acting in Concert with Hsp90 is Required for Raf-1 Function. *Mol. Cell. Biol*., 19(3): 1661-1672.

Grammatikakis, N., Vultur, A., Ramana, C.V., Siganou, A., Schweinfest, C.W., Watson, D.K. and Raptis, L. (2002). The Role of Hsp90N, a New Member of the Hsp90 Family, in Signal Transduction and Neoplastic Transformation. *J. Biol. Chem.*, 277(10): 8312-8320.

Gray, A.J., Park, P.W., Broekelmann, T.J., Laurent, G.F., Reeves, J.T., Stenmark, K.R. and Mecham, R.P. (1995). The Mitogenic Effects of the Bβ Chain of Fibrinogen Are Mediated through Cell Surface Calreticulin. *J. Biol. Chem.*, 270(44): 26602-26606.

Gupta, G.P. and Massagué, J. (2006). Cancer Metastasis: Building a Framework. *Cell*, 127: 679-695.

Hanahan, D. and Weinberg, R.A. (2000). The Hallmarks of Cancer. *Cell*, 100: 57-70.

Hanamura, N., Yoshida, T., Matsumoto, E., Kawarada, Y. and Sakakura, T. (1997). Expression of fibronectin and tenascin-C mRNA by myofibroblasts, vascular cells and epithelial cells in human colon adenomas and carcinomas. *Int. J. Cancer*, 73: 10-15.

Harris, S.F., Shiau, A.K. and Agard, D.A. (2004). The Crystal Structure of the Carboxyl-Terminal Dimerization Domain of htpG, the *Escherichia coli* Hsp90, Reveals a Potential Substrate Binding Site. *Structure*., 12: 1087-1097.

Harrison, P.M., Bamborough, P., Daggett, V., Prusiner, S.B. and Cohen, F.E. (1997). The prion folding problem. *Curr. Opin. Struct. Biol.*, 7: 53-59.

Hartl, F., Hlodan, R. and Langer, T. (1994). Molecular chaperones in protein folding: the art of avoiding sticky situations. *TIBS*. 19: 20-25.

Hartl, F.U. and Hartl, M.H. (2002). Molecular Chaperones in the Cytosol: from Nascent Chain to Folded Protein. *Science*, 295: 1852-1858.

Hastie, S.B. (1991). Interactions of colchicine with tubulin. *Pharmacol. & Ther.*, 51(3): 377-401.

Hayman, E.G., Engvall, E. and Ruoslahti, E. (1981). Concomitant Loss of Cell Surface Fibronectin and Laminin from Transformed Rat Kidney Cells. *J. Cell. Biol.*, 88: 352-357.

Hecht., J.T., Hayes, E., Snuggs, M., Decker, G., Montufar-Solis, D., Doege, K., Mwalle, F., Poole, R., Stevens, J. and Duke, P.J., (2001). Calreticulin, PDI, Grp94 and BiP chaperone proteins are associated with retained COMP in pseudoachondroplasia chondrocytes. Matrix Biol., 20: 251-262.

Hegmans, J.P., Bard, M.P., Hemmes, A., Luider, T.M., Kleijmeer, M.J., Prins, J.B., Zitvogel, L., Burgers, S.A., Hoogsteden, H.C. and Lambrecht, B.N. (2004). Proteomic analysis of exosomes secreted by human mesothelioma cells. *Am. J. Pathol.*, 164: 1807-1815.

Holt, S.E., Aisner, D.L., Baur, J., Tesmer, V.M., Dy, M., Ouellette, M., Trager, J.B., Morin, G.B., Toft, D.O., Shay, J.W., Wright, W.E. and White, M.A. (1999). Functional requirement of p23 and Hsp90 in telomerase complexes. *Genes Dev.*, 13: 817-826.

Holzbeierlein, J.M., Windsperger, A. and Vielhauer, G. (2010). Hsp90: A Drug Target? *Curr. Oncol. Rep.*, 12: 95-101.

Hu, Y. and Mivechi, N.F. (2003). HSF-1 Interacts with Ral-binding Protein 1 in a Stress-responsive, Multiprotein Complex with HSP90 in vivo. *J. Biol. Chem.*, 278(19): 17299-17306.

Huber, R. and Bode, W. (1978). Structural basis of the activation and action of trypsin. *Acc. Chem. Res.*, 11(3): 114-122.

Jackson, S.E., Queitsch, C. and Toft, D. (2004). Hsp90: from structure to phenotype. *Nat. Struct. Mol. Biol*., 11(12): 1152-1155.

Johnson, S., Michalak, M., Opas, M. and Eggleton, P. (2001). *TRENDS in Cell Biol.*, 11(3): 122-129.

Jones, G.W. and Tuite, M.F. (2005). Chaperoining prions: the cellular machinery for propagating an infectious protein? *BioEssays*, 27: 823-832.

Jolly, C., Morimoto, R.I., Robert-Nicoud, M. and Vourc'h C. (1997). HSF1 transcription factor concentrates in nuclear foci during heat shock: relationship with transcription sites. *J. Cell Sci.*, 110: 2935-2941.

Kamal, A., Thao, L., Sensintaffar, J., Zhang, L., Boehm, M. F., Fritz, L. C., Burrows, F. G. (2003). A high-affinity conformation of Hsp90 confers tumour selectivity on Hsp90 inhibitors. *Nature*, 425: 407- 410.

Keselowsky, B.G. and García, A.J. (2004). Quantitative methods for analysis of integrin binding and focal adhesion formation on biomaterial surfaces. *Biomaterials*, 26: 413-418.

Koyasu, S., Nishida, E., Kadowaki, T., Matsuzaki, F., Iida, K., Harada, F., Kasuga, M., Sakai, H. and Yahara, I. (1986). Two mammalian heat shock proteins, HSP90 and HSP100, are actin-binding proteins. *Proc. Natl. Acad. Sci. USA*, 83: 8054-8058.

Kretsinger, R.H. (1976). Calcium-Binding Proteins. *Ann. Rev. Biochem.*, 45: 239-266.

Kuo, C-C., Liang, C-M., Lai, C-Y. and Liang, S-M. (2012). Involvement of Heat Shock Protein (Hsp)90β but not Hsp90α in Antiapoptotic Effect of CpG-B Oligodeoxynucleotide. *J. Immunol.*, 178: 6100-6108.

Kurokawa, M., Zhao, C., Reya, T. and Kornbluth, S. (2008). Inhibition of Apoptosome Formation by Suppression of Hsp90β Phosphorylation in Tyrosine Kinase-Induced Leukemias. *Mol. Cell. Biol.*, 28(17): 5494-5506.

Laemlli, U.K. (1970). Cleavage of Structural Proteins during the Assembly of the Head of Bacteriophage T4. *Nature*, 227: 680-685.

Lei, H., Romeo, G. and Kazlauskas, A. (2004). Heat Shock Protein 90α-Dependent Translocation of Annexin II to the Surface of Endothelial Cells Modulates Plasmin Activity in the Diabetic Rat Aorta. *Circ. Res.*, 94: 902-909.

Li, W., Li, Y., Guan, S., Fan, J., Cheng, C.F., Bright, A.M., Chinn, C., Chen, M. and Woodley, D.T. (2007). Extracellular heat shock protein-90alpha: linking hypoxia to skin cell motility and wound healing. *EMBO J.*, 26: 1221-1233.

Liao, D.F., Jin, Z.G., Baas, A.S., Daum, G., Gygi, S.P., Aebersold, R. and Berk, B.C. (2000). Purification and Identification of Secreted Oxidative Stress-induced Factors from Vascular Smooth Muscle Cells. *J. Biol. Chem.*, 275: 189-196.

Liu, X., Yan, Z., Huang, L., Guo, M., Zhang, Z., and Guo, C. (2011). Cell surface heat shock protein 90 modulates prostate cancer cell adhesion and invasion through the integrin-β1/focal adhesion kinase/c-Src signaling pathway. *Oncol. Rep.,* 25: 1343-1351.

Loskutoff, D.J., Curriden, S.A., Hu, G. and Deng, G. (1999). Regulation of cell adhesion by PAI-1. *APMIS*, 107: 54-61.

Lotz, G.P., Brychzy, A., Heinz, S. and Obermann, W.M.J. (2007). A novel HSP90 chaperone complex regulates intracellular vesicle transport. *J. Cell Sci.*, 121: 717-723.

Lui, J., Zhang, J-P., Shi, M., Quinn, T., Bradner, J., Beyer, R., Chen, S. and Zhang, J. (2009). Rab11a and HSP90 Regulate Recycling of Extracellular α-Synuclein. *J. Neurosci.*, 29(5): 1480-1485.

Maity, G., Fahreen, S., Banerji, A., Choudhury, P.R., Sen, T., Dutta, A. and Chatterjee, A. (2010). Fibronectin-integrin mediated signaling in human cervical cancer cells (HeLa). *Mol. Cell. Biochem.*, 336: 65-74.

Mao, Y. and Schwarzbauer, J.E. (2005). Fibronectin fibrillogenesis, a cell-mediated matrix assembly process. *Matrix Biol.*, 24: 389-399.

Marsh, M. and Pelchen-Matthews, A. (2000). Endocytosis in Viral Replication. *Traffic*, 1: 525-532.

Martinek, N., Shahab, J., Sodek, J. and Ringuette, M. (2007). Is SPARC an Evolutionarily Conserved Collagen Chaperone? *J. Dent. Res.*, 86: 296-305.

Mayer, M.P. and Bukau, B. (2004). Hsp70 chaperones: Cellular functions and molecular mechanism. *Cell Mol. Life Sci.*, 62: 670-684.

McCarthy, J.B. and Furcht, L.T. (1984). Laminin and Fibronectin Promote the Haptotactic Migration of B16 Mouse Melanoma Cells In Vitro. *J. Cell. Biol.*, 98: 1474-1480.

McCready, J., Sims, J.D., Chan, D. and Jay, D.G. (2010). Secretion of extracellular hsp90alpha via exosomes increases cancer cell motility: a role for plasminogen activation. *BMC Cancer*, 10(294).

Meyer, P., Prodromou, C., Hu, B., Vaughan, C., Roe, M., Panaretou, B., Piper, P.W. and Pearl, L.H. (2003). Structural and Functional Analysis of the Middle Segment of Hsp90: Implications for ATP Hydrolysis and Client Protein and Cochaperone Interactions. *Mol. Cell*, 11: 647-658.

Michels, A.A., Kanon, B., Konings, A.W.T., Ohtsuka, K., Bensaude, O. and Kampinga, H.H. (1997). Hsp70 and Hsp40 Chaperone Activities in the Cytoplasm and the Nucleus of Mammalian Cells. *J. Biol. Chem.*, 272(52): 33283-33289.

Midwood, K.S. and Schwarzbauer, J.E. (2002). Elastic Fibers: Building Bridges Between Cells and Their Matrix. *Curr. Biol.*, 12: R279-R281.

Miller, A.B., Hogestraeten, B., Staquet, M. and Winkler, A. (1981). Reporting results of cancer treatment. *Cancer*, 47: 207-214.

Minet, E., Mottet, D., Michel, G., Roland, I., Raes, M., Remacle, J. and Michiels, C. (1999). Hypoxia-induced activation of HIF-1: a role of HIF-1α-Hsp90 interaction. *FEBS Lett.*, 460: 251-256.

Mizejewski, G.J. (1999). Role of Integrins in Cancer: Survey of Expression Patterns. *Proc. Soc. Exp. Biol. Med.*, 222: 124-138.

Multhoff, G. and Hightower, L.E. (1996). Cell surface expression of heat shock proteins and the immune response. *Cell Stress & Chap.*, 1(3): 167-176.

Nagai, N., Hosokawa, M., Itohara, S., Adachi, E., Matsushita, T., Hosokawa, N. and Nagata, K. (2000). Embryonic Lethality of Molecular Chaperone Hsp47 Knockout Mice Is Associated with Defects in Collagen Biosynthesis. *J. Cell Biol.*, 150(6): 1499-1505.

Nardai, G., Schnaider, T., SŐti, C., Ryan, M.T., Hoj, P.B., Somogyi, J. and Csermely, P. (1996). Characterization of the 90 kDa heat shock protein (hsp90)-associated ATP/GTP-ase. J. Biosci., 21: 179-190.

Ngubo, M., Kemp, G., and Patterton, H.G. 2011. Nano-electrospray tandem mass spectrometric analysis of the acetylation state of histones H3 and H4 in stationary phase in *Saccharomyces cerevisiae. BMC Biochem.* 12: 34-43

Palecek, S.P., Horwitz, A.F. and Lauffenburger, D.A. (1999). Kinetic Model for Integrin-mediated Adhesion Release During Cell Migration. *Ann. Biomed. Eng.*, 27: 219-235.

Palermo, C.M., Westlake, C.A. and Gasiewicz, T.A. (2005). Epigallocatechin gallate inhibits aryl hydrocarbon receptor gene transcription through an indirect mechanism involving binding to a 90 kDa heat shock protein. *Biochem.*, 44: 5041-5052.

Panaretou, B., Prodromou, C., Roe, S.M., O'Brien, R., Ladbury, J.E., Piper, P.W. and Pearl, L.H. (1998). ATP binding and hydrolysis are essential to the function of the Hsp90 molecular chaperone *in vivo*. *EMBO J.*, 17(16): 4829-4836.

Panaretou, B., Siligardi, G., Meyer, P., Maloney, A., Sullivan, J.K., Singh, S., Millson, S.H., Clarke, P.A., Naaby-Hansen, S., Stein, R., Cramer, R., Mollapour, M., Workman, P., Piper, P.W., Pearl, L.H. and Prodromou, C. (2002). Activation of the ATPase Activity of Hsp90 by the Stress-Regulated Cocahperone Aha1. *Mol. Cell*, 10: 1307-1318.

Park, S.J., Suetsugu, S. and Takenawa, T. (2005). Interaction of HSP90 to N-WASP leads to activation and protection from proteasome-dependent degradation. *The EMBO J.*, 24: 1557-1570.

Parsell, D.A. and Lindquist, S. (1993). The Function of Heat-Shock Proteins in Stress Tolerance: Degradation and Reactivation of Damaged Proteins. *Annu. Rev. Genet.*, 27: 437-496.

Pearl, L.H. (2005). Hsp90 and Cdc37 – a chaperone cancer conspiracy. *Curr. Opin. Genetics Develop.*, 15(1): 55-61.

Pearl, L.H. and Prodromou, C. (2000). Structure and *in vivo* function of Hsp90. *Curr. Opin. Struct. Biol.*, 10: 46-51.

Pelkmans, L., Kartenbeck, J. and Helenius, A. (2002). Local actin polymerization and dynamin recruitment in SV40-induced internalization of caveolae. *Science*, 296: 535-539.

Pellegrin, S. and Mellor, H. (2007). Actin stress fibres. *J. Cell Sci.*, 120: 3491-3499.

Perotti, C., Liu, R., Parusel, C.T., Böchner, N., Schultz, J., Bork, P, Pfitzner, E., Groner, B. and Shemanko, C.S. (2008). Heat shock protein-90-alpha, a prolactin-STAT5 target gene identified in breast cancer cells, is involved in apoptosis regulation. Breast Can. Res., 10: R94 (doi:10.1186/bcr2193)

Pick, E., Kluger, Y., Giltnane, J.M., Moeder, C., Camp, R.I., Rimm, D.I. and Kluger, H.M. (2007). High HSP90 Expression Is Associated with Decreased Survival in Breast Cancer. Cancer Res., 67(7): 2932-2937.

Pratt, W.B. (1998). The hsp90-based Chaperone System: Involvement in Signal Transduction from a Variety of Hormone and Growth Factor Receptors. *Soc. Exp. Biol. Med.*, 217: 420-434.

Pratt, W.B. and Toft, D.O. (2003). Regulation of Signaling Protein Function and Trafficking by the hsp90/hsp70-Based Chaperone Machinery. *Exp. Biol. Med.*, 228: 111-133.

Pratt, W.B., Galigniana, M.D., Harrell, J.M. and DeFranco, D.B. (2004). Role of hsp90 and the hsp90-binding immunophilins in signaling protein movement. *Cell. Signal.*, 16: 857-872.

Pratt, W.B., Morishima, Y., Peng, H-M. and Osawa, Y. (2010). Proposal for a role of the Hsp90/Hsp70-based chaperone machinery in making triage decisions when proteins undergo oxidative and toxic damage. *Exp. Biol. Med.*, 235: 278-289.

Prescott, M.F., Sawyer, W.K., Von Linden-Reed, J., Jeune, M., Chou, M., Caplan, S.L. and Jeng, A.Y. (1999). Effect of matrix metalloproteinase inhibition on progression of atherosclerosis and aneurysm in LDL receptor-deficient mice overexpression MMP-3, MMP-12, and MMP-13 and on restenosis in rats after balloon injury. *Ann. NY Acad. Sci.*, 878: 179-190.

Prince, T. and Matts, R.L. (2004). Definition of Protein Kinase Sequence Motifs That Trigger High Affinity Binding of Hsp90 and Cdc37. *J. Biol. Chem.*, 279(38): 39975-39981.

Qing, G., Yan, P. and Xiao, G. (2006). Hsp90 inhibition results in autophagy-mediated proteasome-independent degradation of IκB kinase (IKK). *Cell Res.*, 16: 895-901.

Rejman, J., Oberle, V., Zuhorn, I.S. and Hoekstra, D. (2004). Size-dependent internalization of particles via the pathways of clathrin- and caveolae-mediated endocytosis. *Biochem. J.*, 377: 159-169.

Reyes-del Valle, J., Chávez-Salinas, S., Medina, F. and del Angel, R.M. (2005). Heat Shock Protein 90 and Heat Shock Protein 70 Are Components of Dengue Virus Receptor Complex in Human Cells. *J. Virol.*, 79(8): 4557-4567.

Richter, K. and Buchner, J. (2001). Hsp90: Chaperoning Signal Transduction. *J. Cell. Phys.*, 188: 281-290.

Ridley, A.J., Schwartz, M.A., Burridge, K., Firtel, R.A., Ginsberg, M.H., Borisy, G., Parsons, J.T. and Horwitz, A.R. (2003). Cell Migration: Integrating Signals from Front to Back. *Science*, 302: 1704-1709.

Rodal, S.K., Skretting, G., Garred, Ø., Vilhardt, F., van Deurs, B. and Sandvig, K. (1999). Extraction of Cholesterol with Methyl-β-Cyclodextrin Perturbs Formation of Clathrin-coated Endocytic Vesicles. *Mol. Biol. Cell*, 10: 961-974.

Ruoslahti, E. (1996). RGD and other recognition sequences for integrins. *Ann. Rev. Cell Develop. Biol.*, 12: 697-715.

Salicioni, A.M., Mizelle, K.S., Loukinova, E., Mikhailenko, I., Strickland, D.K. and Gonias, S.L. (2002). The Low Density Lipoprotein Receptor-related Protein Mediates Fibronectin Catabolism and Inhibits Fibronectin Accumulation on Cell Surfaces. *J. Biol. Chem.*, 277(18): 16160-16166.

Sato, S., Fujita, N. and Tsuruo, T. (2000). Modulation of Akt kinase activity by binding to Hsp90. *Proc. Natl. Acad. Sci*., 97(20): 10832-10837.

Sato, N., Yamamoto, T., Sekine, Y., Yumioka, T., Junicho, A., Fuse, H. and Matsuda, T. (2003). Involvement of heat-shock protein 90 in the interleukin-6-mediated signaling pathway through STAT3. *Biochem. Biophys. Res. Comm*., 300: 847-852.

Sauk, J.J., Nikitakis, N., and Siavash, H. 2005. Hsp47 a novel collagen binding serpin chaperone, autoantigen and therapeutic target. *Front Biosci.* 10: 107-118

Schlesinger, M.J. (1990). Heat Shock Proteins. *J. Biol. Chem.*, 265(21): 12111-12114.

Schmitt, E., Gehrmann, M., Brunet, M., Multhoff, G. and Garrido, C. (2006). Intracellular and extracellular functions of heat shock proteins: repercussions in cancer therapy. *J. Leuk. Biol*., 81:15-27.

Schnaider, T., Somogyi, J., Csermely, P. and Szamel, M. (2000). The Hsp90-specific inhibitor geldanamycin selectively disrupts kinase-mediated signaling events of T-lymphocyte activation. *Cell Stress & Chap.*, 5(1): 52-61.

Schwarzbauer, J.E. and Sechler, J.L. (1999). Fibronectin fibrillogenesis: a paradigm for extracellular matrix assembly. *Curr. Opin. Cell Biol.*, 11: 622-627.

Scroggins, B.T., Robzyk, K., Wang, D., Marcu, M.G., Tsutsumi, S., Beebe, K., Cotter, R.J., Felts, S., Toft, D., Kamitz, L., Rosen, N. and Neckers, L. (2007). An Acetylation Site in the Middle Domain of Hsp90 Regulates Chaperone Function. *Mol. Cell*, 25: 151-159.

Seger, R. and Krebs, E.G. (1995). The MAPK signaling cascade. *FASEB J.*, 9: 726-735.

Shi, Y., Zhao, M. and Xu, X. (1998). Comparative study of expression levels of the major human heat shock proteins in cancer and normal tissues. *Zhonghua Zhong Liu Za Zhi*, 20(4): 277-279.

Sidera, K., Samiotaki, M., Yfanti, E., Panayotou, G. and Patsavoudi, E. (2004). Involvement of Cell Surface HSP90 in Cell Migration Reveals a Novel Role in the Developing Nervous System. *J. Biol. Chem.*, 279(44): 45379-45388.

Sidera, K., Gaitanou, M., Stellas, D., Matsas, R. and Patsavoudi, E. (2008). A Critical Role for HSP90 in Cancer Cell Invasion Involves Interaction with the Extracellular Domain of HER-2. *J. Biol. Chem.*, 283(4): 2031-2041.

Sims, J.D., McCready, J. and Jay, D.G. (2011). Extracellular Heat Shock Protein (Hsp)70 and Hsp90α Assist in Matrix Metalloproteinase-2 Activation and Breast Cancer Cell Migration and Invasion. PLoS ONE, 6(4): e18848. doi:10.1371/journal.pone.0018848.

Smith, J.R. and Workman, P. (2007). Targeting the cancer chaperone HSP90. *Drug Disc. Today Ther. Strat.*, 4(4): 219-227.

Soldano, K.L., Jivan, A., Nicchitta, V. and Gewirth, D.T. (2003). Structure of the N-terminal Domain of GRP94. *J. Biol. Chem*., 279(48): 48330-48338.

Sørlie, T., Perou, C.M., Tibshirani, R., Aas, T., Geisler, S., Johnsen, H., Hastie, T., Eisen, M.B., van de Rijn, M., Jeffrey, S.S., Thorson, T., Quist, H., Matese, J.C., Brown, P.O., Botstein, D., Lønning, P.E. and Børresen-Dale, A-L. (2001). Gene expression patterns of breast carcinomas distinguish tumor subclasses with clinical implications. *Proc. Natl. Acad. Sci.*, 98(19): 10869-10874.

Sottile, J. and Chandler, J. (2005). Fibronectin Matrix Turnover Occurs through a Caveolin-1-dependent Process. *Mol. Biol. Cell*, 16: 757-768.

Sottile, J. and Hocking, D.C. (2002). Fibronectin Polymerization Regulates the Composition and Stability of Extracellular Matrix Fibrils and Cell-Matrix Adhesions. *Mol. Biol. Cell*, 13: 3546-3559.

Sreedhar, A.S., Kalmár, É., Csermely, P. and Shen, Y-F. (2004). Hsp90 isoforms: functions, expression and clinical importance. *FEBS Lett.*, 562: 11-15.

Stebbins, C.E., Russo, A.A., Schneider, C., Rosen, N., Hartl, F.U. and Pavletich, N.P. (1997). Crystal Structure of an Hsp90-Geldanamycin Complex: Targeting of a Protein Chaperone by an Antitumor Agent. *Cell*, 89: 239-250.

Steeg, P. (2006). Tumor metastasis: mechanistic insights and clinical challenges. *Nat. Med. Rev.*, 12(8): 895-904.

Stellas, D., Karameris, A. and Patsavoudi, E. (2008). Monoclonal Antibody 4C5 Immunostains Human Melanomas and Inhibits Melanoma Cell Invasion and Metastasis. *Clin. Cancer Res.*, 13: 1831-1838.

Suzuki, S. and Kulkarni, A.B. (2010). Extracellular heat shock protein HSP90beta secreted by MG63 osteosarcoma cells inhibits activation of latent TGF-beta1. *Biochem. Biophys. Res. Commun.*, 389(3): 525-531.

Szántó, I., Schnaider, T. and Csermely, P. (1996). Topoisomerase activity of the 90 kDa heat shock protein, hsp90. *Cell Biol. Int.*, 20: 246-247.

Taipale, M., Krykbaeva, I., Koeva, M., Kayatekin, C., Westover, K.D., Karras, G.I. and Lindquist, S. (2012). Quantitative Analysis of Hsp90-Client Interactions Reveals Principles of Substrate Recognition. *Cell*, 987-1001.

Taiyab, A. and Rao, C.M. (2010). HSP90 modulates actin dynamics: Inhibition of HSP90 leads to decreased cell motility and impairs invasion. *Biochim. Biophys. Acta*, 1813: 213-221.

Takada, Y., Ye, X. and Simon, S. (2007). The integrins. Gen. Biol., 8(215): doi:10.1186/gb-2007-8-5-215.

Terasawa, K., Minami, M. and Minami, Y. (2005). Constantly Updated Knowledge of Hsp90. *J. Biochem.*, 137: 443-447.

Theodoraki, M.A. and Caplan, A.J. (2012). Quality control and fate determination of Hsp90 client proteins. *Biochim. Biophys. Acta*, 1823: 683-688.

Thiery, J.P. (2002). Epithelial-mesenchymal transitions in tumour progression. *Nat. Rev. Cancer*, 2: 442-454.

Thuringer, D., Hammann, A., Benikhlef, N., Fourmaux, E., Bouchot, A., Wettstein, G., Solary, E. and Garrido, C. (2010). Transactivation of the Epidermal Growth Factor Receptor by heat shock protein 90 via Toll-like Receptor 4 contributes to the migration of glioblastoma cells. J. Biol. Chem., doi/10.1074/jbc.M110.154823.

Tissiéres, A., Mitchell, H.K. and Tracy, U. (1974). Protein synthesis in salivary glands of *Drosophila melanogaster*: relation to chromosome puffs. J. Mol. Biol., 84: 389.

Towbin, H., Staehelin, T. and Gordon, J. (1979). Electrophoretic transfer of proteins from polyacrylamide gels to nitrocellulose sheets: Procedure and some applications. Proc. Natl. Acad. Sci. USA, 76(9): 4350-4354.

Triantafilou, M. and Triantafilou, K. (2004). Heat-shock protein 70 and heat-shock protein 90 associate with Toll-like receptor 4 in response to bacterial lipopolysaccharide. *Biochem. Soc. Transact.*, 32(4): 636-639.

Tsutsumi, A. and Neckers, L. (2007). Extracellular heat shock protein 90: A role for a molecular chaperone in cell motility and cancer metastasis. *Cancer Sci.*, 98(10): 1536-1539.

Tsutsumi, S., Scroggins, B., Koga, F., Lee, M-J., Trepel, J., Felts, S., Carreras, C. and Neckers, L. (2008). A small molecule cell-impermeant Hsp90 antagonist inhibits tumor cell motility and invasion. *Oncogene*, 27: 2478-2487.

Tsutsumi, S., Beebe, K. and Neckers, L. (2009). Impact of Heat-shock Protein 90 on Cancer Metastasis. *Future Oncol.*, 5(5): 679-688.

Verderio, E.A.M., Telci, D., Okoye, A., Melino, G. and Griffin, M. (2003). A Novel RGD-independent Cell Adhesion Pathway Mediated by Fibronectin-bound Tissue Transglutaminase Rescues Cells from Anoikis. *J. Cell. Biol.*, 278(43): 42604-42614.

Voss, A.K., Thomas, T. and Gruss, P. (2000). Mice lacking HSP90β fail to develop a placental labyrinth. *Develop.*, 127: 1-11.

Walsh, N., Larkin, A., Swan, N., Conlon, K., Dowling, P., McDermott, R. and Clynes, M. (2011). RNAi knockdown of Hop (Hsp70/Hsp90 organising protein) decreases invasion via MMP-2 down regulation. *Cancer Lett.*, 306: 180-189.

Wang, X-Q., Duan, X-M., Liu, L-H., Fang, Y-Q. and Tan, Y. (2005). Carboxyfluorescein Diacetate Succinimidyl Ester Fluorescent Dye for Cell Labeling. *Acta Biochim. Biophys. Sin.*, 37(6): 379-385.

Wang, X., Song, X., Zhuo, W., Fu, Y., Shi, H., Liang, Y., Tong, M., Chang, G. and Luo, Y. (2009). The regulatory mechanism of Hsp90α secretion and its function in tumor malignancy. *Proc. Natl. Acad. Sci.*, Early Edition: 1-6 (doi_10.1073_pnas.0908151106).

Weber, P.C., Ohlendorf, D.H., Wendoloski, J.J. and Salemme, F.R. (1989). Structural origins of high-affinity biotin binding to streptavidin. *Science*, 243(4887): 85-88.

Weikl, T., Abelmann, K. and Buchner, J. (1999). An Unstructured C-Terminal Region of the Hsp90 Co-chaperone p23 is Important for its Chaperone Function. *J. Mol. Biol.*, 293: 685-691.

White, T.K., Zhu, Q. and Tanzer, M.L. (1995). Cell Surface Calreticulin Is a Putative Mannoside Lectin Which Triggers Mouse Melanoma Cell Spreading. *J. Biol. Chem.*, 270: 15926-15929.

Wierzbicka-Patynowski, I. and Schwarzbauer, J.E. (2003). The ins and outs of fibronectin matrix assembly. *J. Cell Sci.*, 116: 3269-3276.

Xu, W., Mimnaugh, E.G., Kim, J-S., Trepel, J.B. and Neckers, L.M. (2002). Hsp90, not Grp94, regulates the intracellular trafficking and stability of nascent ErbB2. *Cell Stress & Chaperones*, 7(1): 91-96.

Xu, W. and Neckers, L. (2007). Targeting the Molecular Chaperone Heat Shock Protein 90 Provides a Multifaceted Effect on Diverse Cell Signaling Pathways of Cancer Cells. *Clin. Cancer Res.*, 13: 1625-1629.

Yang, Z., Zhang, X., Gang, H., Li, X., Li, Z., Wang, T., Han, J., Luo, T., Wen F. and Wu, X. (2007). Up-regulation of gastric cancer cell invasion by *Twist* is accompanied by N-cadherin and fibronectin expression. *Biochem. Biophys. Res. Comm.*, 358: 925-930.

Yano, M., Naito, Z., Tanaka, S. and Asano, G. (1996). Expression and roles of heat shock proteins in human breast cancer. *Jpn. J. Cancer. Res.*, 87(9): 908-915.

Yfanti, E., Sidera, K., Margaritas, L.H. and Patsavoudi, E. (2004). The 4C5 Antigen Is Associated With Schwann Cell Migration During Development and Regeneration of the Rat Peripheral Nervous System. *Glia*, 45: 39-53.

Yu, X.M., Shen, G., Neckers, L., Blake, H., Holzbeierlein, J., Cronk, B. and Blagg, B.S.J. (2005). Hsp90 inhibitors identified from a library of novobiocin analogues. *J. Am. Chem. Soc.*, 127: 12778-12779.

Yun, B-G., Huang, W., Leach, N., Hartson, S.D. and Matts, R.L. (2004). Novobiocin Induces a Distinct Conformation of Hsp90 and Alters Hsp90-Cochaperone-Client Interactions. *Biochem.*, 43: 8217-8229.

Zhang, H. and Burrows, F. (2004). Targeting multiple signal transduction pathways through inhibition of Hsp90. *J. Mol. Med.*, 82: 488-499.

Zheng, Y., Ritzenthaler, J.D., Roman, J. and Han, S. (2007). Nicotine Stimulates Human Lung Cancer Cell Growth by Inducing Fibronectin Expression. *Am. J. Respir. Cell Mol. Biol.*, 37: 681-690.

Zurawska, A., Urbanski, J. and Bieganowski, P. (2008). Hsp90N – An accidental product of a fortuitous chromosomal translocation rather than a regular Hsp90 family member of human proteome. *Biochim. Biophys. Acta*., 1784: 1844-1846.